Proceedings of the

4th Oxford Tidal Energy Workshop

23-24 March 2015, Oxford, UK

Proceedings of the 4th Oxford Tidal Energy Workshop (OTE 2015)

23-24 March 2015, Oxford, UK

Monday 23rd March

Session 1: Devices and Turbulence

Poster Presentations (1)

Session 2: Basin Modelling (1)

Poster Presentations (2)

Session 3: Devices and Arrays

Tuesday 24th March

Session 4: Field Scale Turbulence

Session 5: Basin Modelling (2)

Poster Presentations (3)

Session 6: Devices and Control

Workshop Organisers:

Richard H. J. Willden	(Chairman)	University of Oxford
Christopher R. Vogel	(Co-Chairman)	University of Oxford

Scientific Committee Members:

T. A. A. Adcock	(University of Oxford)	T. Stallard	(University of Manchester)
G. T. Houlsby	(University of Oxford)	C. Stock-Williams	(E.ON)
I. Masters	(Swansea University)	C. R. Vogel	(University of Oxford)
T. Nishino	(Cranfield University)	R. H. J. Willden	(University of Oxford)

Sponsor:

Oxford Martin School (University of Oxford)

Measuring Turbulent Structures in Tidal Channels

Anna Young, Romain Guion
Whittle Laboratory, University of Cambridge, UK

Luca Camosi, Michael Corsar
School of Engineering, Cranfield University, UK

Summary: The lifespan of a tidal turbine is strongly affected by the unsteady loading it experiences, so the inflow unsteadiness must be known at the design stage. The favoured flow measurement device in the marine environment is the Acoustic Doppler Current Profiler (ADCP). The variance of steady velocity measurements from ADCPs has been studied in detail, but very little attention has been given to the fundamental limits of ADCPs in terms of the frequencies and lengthscales that they can capture. In this work, it is shown that a conventional (4-beam, bottom-mounted) ADCP acts as a low-pass filter to eddies, such that wavelengths below 3-4 m are attenuated by 90% or more. Furthermore, eddies that are captured are can be either amplified or attenuated depending on the precise turbulence characteristics of the site in question. This low-pass filtering is most damaging when data are extracted for particular frequencies, as a turbine designer may do when assessing fatigue life. It is therefore recommended that high-resolution data is captured over part of the water column and that this is used to calibrate ADCP data. In the second part of the work, the use of a five-hole fast-response pressure probe for this purpose is discussed, and the results from comparative tests at IFREMER are shown.

Introduction

In order to predict the fatigue life of a tidal turbine, the level of unsteadiness in the incoming flow must be quantified, right from the largest scales of turbulence down to fractions of the blade chord. Acoustic Doppler Current Profilers (ADCPs) have long been used to provide steady flow measurement profiles, and their reliability in this respect is well-known. However, they are now being used to provide tidal turbine designers with turbulent flow data, and very little attention has been given to the intrinsic limitations of ADCPs in terms of the frequencies and lengthscales that they can capture. Experiments by Nystrom et al. [1] found errors from 44% to 94% in turbulence intensity measurements. Gargett et al. [2,3] then showed that a 4-beam ADCP will give inaccurate data in the presence of anisotropies or when there are phase differences between the components of eddies. In this work, the ADCP is modelled as a low-pass filter to eddies, and significant loss of information is found to occur at lengthscales of up to ten times a typical tidal turbine blade chord**.** While this low-pass filtering may alter some statistics by truncating the observed spectrum, it is most damaging when data is extracted for a few particular frequencies, as a turbine designer might do when assessing fatigue life. An alternative probe is then suggested – a fast-response five-hole pressure probe, and results from prototype tests are shown. The reason for choosing a five-hole probe is that it represents a potentially low-cost alternative to deploying a large number of ADVs at a site. The use of fast-response five-hole probes in water turbines is being pioneered by Duquesne et al. [4], who have proven the concept on a small centrifugal pump.

Method

The work is in two parts: a theoretical study of the frequencies and lengthscales that a typical 4-beam, bottom-mounted ADCP can capture, and a study of a prototype fast-response pressure probe which could be used to supplement ADCP data and fill in the short lengthscale end of the turbulence spectrum in a tidal channel.

In the present work, the ability of a single beam to capture turbulent structures is assessed first (intra-beam filtering), before the effect of combining data from separate beams at different locations is discussed (inter-beam filtering). Three filters are developed to model the flow field that can be captured by an ideal ADCP beam. The first filter accounts for the damping caused by the failure of the back-scattering particles (suspended sand and organic matter) to follow the flow perfectly, while the second takes into account spatial averaging over the sampling volume of the beam and the third defines the effect of averaging over a number of samples.

In the second part of the work, alternative methods of capturing high-frequency, short-lengthscale disturbances are discussed. In particular, attention is drawn to a fast-response five-hole pressure probe, similar to those used in wind tunnel testing. A prototype device has been built and tested at IFREMER alongside an ADV and an LDV system and the results are compared. The configuration is shown in Figure 1. The probe (right-hand side) is positioned such that the head of the probe is aligned with the focus point of the ADV. The LDV system is 1.5 m upstream of the other devices.

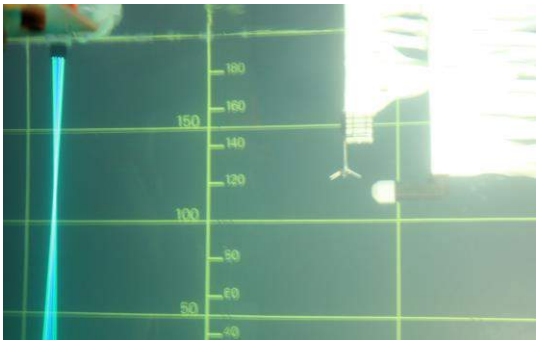

Figure 1 – Prototype probe in tank at IFREMER for comparative tests with ADV and LDV.

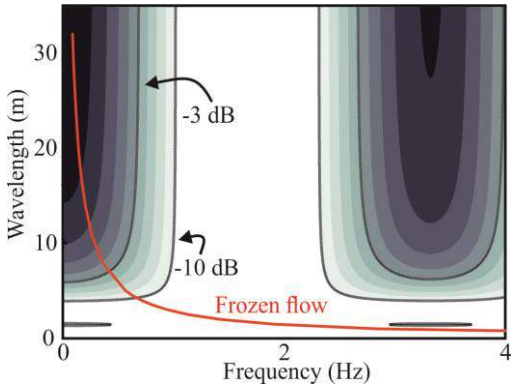

Figure 2 – Contours of ADCP attenuation compared to frozen flow advection.

Results

Figure 2 shows the streamwise filter at mid-depth in a typical 40m deep channel. The ADCP is found to act as a low-pass filter to turbulent structures. The key result is that information is lost for wavelengths below about 7-10 m. This lost information is in a dangerous range in that these lengthscales are too large to be predicted theoretically (as they will be affected by local bathymetry), while also being large enough to affect the tidal turbine. It was also found that the magnitude of the attenuation depends on whether the back-scattering particles are sand or organic – this is not usually known. The result of this relatively optimistic assessment is that a large proportion of the most damaging lengthscales will be severely attenuated by a typical ADCP. This suggests that ADCP data should be supplemented with data from a higher-resolution device over part of the channel.

The proposed higher-resolution device, a fast-response five-hole probe, has been tested in IFREMER, with initial results showing promise. These prototype tests show promise in terms of creating a low-cost, high-resolution device for supplementing ADCP data (i.e. a low-cost alternative to deploying multiple ADVs at a site).

Conclusions

The use of ADCPs for turbulence measurements requires serious thought, as there are fundamental limitations to the size and frequency of eddies that they can capture. In their conventional (4-beam, bottom-mounted) configuration, the divergence of the beams from their own axes and from each other creates a low-pass filter that increases quickly with distance from the sensor. This means that, at mid-depth in a typical channel, eddies shorter than 3-4 m are attenuated by more than 90%. Additionally, at high frequencies, there is the issue of whether the back-scattering particles follow the flow, or whether they will damp the oscillations. This limitation will apply to all Doppler-based measurement systems (ADVs etc).

To provide additional data at high frequencies, a novel device has been proposed: a fast-response five-hole pressure probe. Preliminary tests suggest that this device would produce clear data at higher frequencies, and it is believed that a fully-developed probe would be much lower cost than an ADV, allowing five-hole probes to be deployed at a tidal site prior to the turbine design process.

Acknowledgements:

The authors would like to thank EPSRC SUPERGEN and the Maudslay Society for the funding that made this work possible. They are also grateful to IFREMER for help with testing, and to Ivor Day for technical assistance.

References:

[1] Nystrom, E.A., Oberg, K.A., & Rehmann, C.R. (2002). Measurement of turbulence with acoustic Doppler current profilers – sources of error and laboratory results: *In Proc. Hydraulic Measurements and Experimental Methods Conference*, Estes Park, CO, USA. *U.S Geological Survey.*

[2] Gargett, A.E. Tejada-Martinez, A.E., & Grosch, C.E. (2008). Measuring turbulent large-eddy structures with an ADCP. Part 1: Vertical velocity variance. *J. Marine Research*, 66:155-189.

[3] Gargett, A.E. Tejada-Martinez, A.E., & Grosch, C.E. (2009). Measuring turbulent large-eddy structures with an ADCP. Part 2: Horizontal velocity variance. *J. Marine Research*, 67:569-595.

[4] Duquesne, P., Dan Ciocan, G., Aeschlimann, V., Bombenger, A., Deschenes, C. (2012). Pressure probe with five embedded flush-mounted sensors: unsteady pressure and velocity measurements in hydraulic turbine model. *J. of Expts in Fluids*, 54:1425, DOI 10.1007/s00348-012-1425-y.

Large Eddy Simulations to represent a full-scale tidal stream flow and turbine

Umair Ahmed, David Apsley, Tim Stallard, Imran Afgan, Peter Stansby
Modelling and Simulation centre, School of MACE, University of Manchester

Summary: CFD simulations are performed to represent the depth profile of velocity and turbulence measured at the deployment site of a full-scale tidal stream turbine to assess blade load predictions. Turbulent inflow conditions are defined using a Synthetic Eddy Method [1] based on precursor periodic channel simulations and with scaling applied to represent field measurements. The geometry of rotor and nacelle represent the 18 m diameter Alstom Ocean 1 MW tidal stream turbine. Simulations are conducted using Code_Saturne using a sliding mesh procedure [2]. LES simulations of a channel flow have also been conducted to determine the conditions incident to the rotor during operation. Turbulent kinetic energy spectra and instantaneous blade loads are compared for alternative inflow conditions and with field data.

Introduction

Computational Fluid Dynamics (CFD) simulations are performed with the open-source solver Code_Saturne for Alstom's 18-m diameter tidal-stream turbine currently being tested at the EMEC test site in the Orkneys. The CFD model couples a rotating mesh containing the turbine rotor with a stationary mesh containing the support tower via a sliding-mesh interface proposed by McNaughton et al [2]. To-date there has been a limited study of effect of both shear and turbulence with large-scale structure on turbine loading, particularly using CFD methods. CFD studies have been conducted with embedded blade element momentum models [3] and actuator line models [4] based on quasi-steady assumption of 2D lift and drag coefficients. For design optimisation purposes it is important to understand the accuracy with which blade-modelled CFD can be used for loading prediction. Blade modelled simulations have been conducted of lab-scale turbines with onset turbulence generated with synthetic turbulence methods. A recent study employs OpenFOAM for this purpose [5] although the onset flow was not intended to represent specific conditions. In this study an effort has been made to simulate a tidal-stream turbine subject to an approach flow with realistic levels of velocity shear, Reynolds stresses and length scales.

Methods

Large-eddy simulations (LES) with the dynamic (Germano/Lilly) model are performed using an inflow velocity profile representative of measurements obtained from a full-scale test site [6]. LES was used to investigate fluctuating loads (power coefficient; blade bending moments) and load spectra. Synthetic turbulence was prescribed at the inlet by using a Synthetic Eddy Method (SEM) proposed by Jarrin et al [1]. The vertical distribution of Reynolds stresses and length scales was defined from a channel-flow simulation with a stress free rigid lid and periodic boundary conditions. A first order forward Euler method is used to time advance the solution and a second order central differencing scheme is used for spatial discretisation. A computational mesh of approximately 18 million cells is used for the LES calculations. Flow and load is analysed for two inflow cases: Reynolds stresses and length scale profiles from the channel simulation scaled according to Reynolds number only and additionally scaled to match the on-site measured Reynolds stress profile and hub-height length scales. The details of the simulations are given in table below.

Case	Inlet mean velocity profile	Inlet turbulence	Tip speed ratio (TSR)
1	Precursor channel flow ($Re_\tau = 9300$)	SEM based on channel flow, Length scales × 0.5	5.2
2	Precursor channel flow ($Re_\tau = 9300$)	SEM based on channel flow, Length scales × 0.5, Reynolds Stress $\overline{u_i u_j}$ × 1.8	5.2

Results

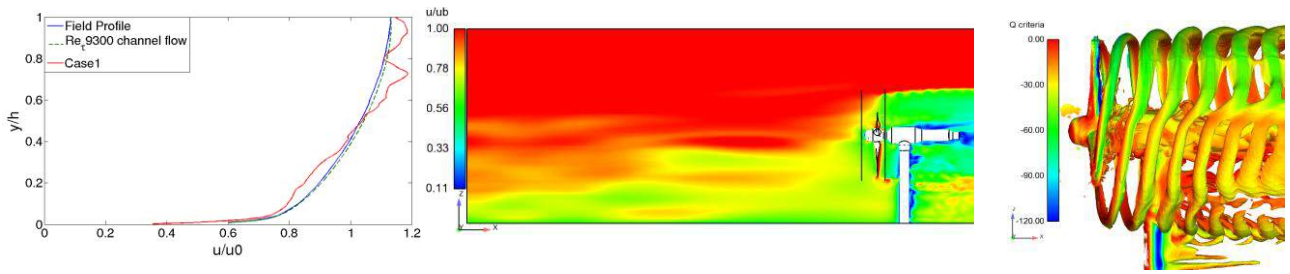

(a) Velocity profile at the rotor plane

(b) Upstream turbulence prescribed at the inlet

(c) Iso-surfaces of vorticity coloured by normalised Q-criterion

Figure 1: Turbulence and length scale stastics based on the precurser channel flow simulation

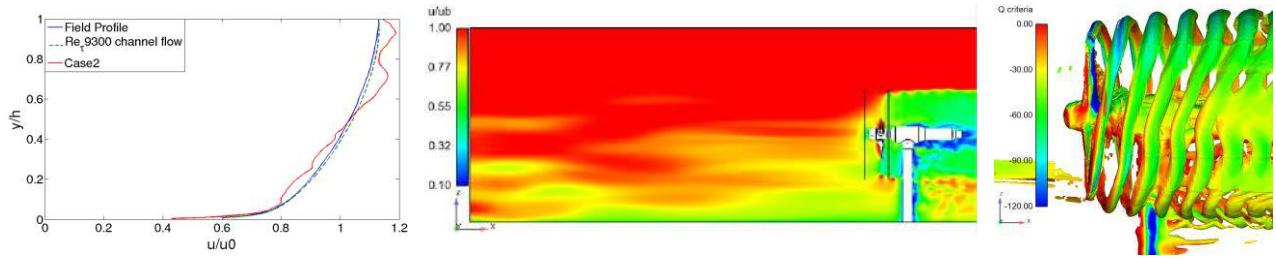

(a) Velocity profile at the rotor plane

(b) Upstream turbulence prescribed at the inlet

(c) Iso-surfaces of vorticity coloured by normalised Q-criterion

Figure 2: Turbulence and length scale stastics based on field measurements

Figures 1a and 2a show the averaged velocity at the rotor plane using different combinations of Reynolds stresses and length scales prescribed at the inlet. The influence of different inlet velocity, Reynolds stress and length scale profiles can be seen in Figures 1b and 2b. It can be seen in Figures 1c and 2c that the vorticity structures produced in the wake of the turbine differ with changes in the onset turbulence. Comparisons of turbulent kinetic energy spectra and instantaneous blade loads will be presented at the workshop.

Conclusions

Synthetic turbulence has been defined as inflow to large eddy simulations of a channel flow and tidal turbine to represent flow measurements obtained from a full-scale tidal stream site. The inflow characteristics are defined based on a periodic LES channel study and the flow at the rotor plane modelled by an open channel flow with synthetic turbulence inflow. A blade-modelled approach is employed to model the turbine. This approach is computationally costly and further analysis is ongoing for improved resolution of flow and load spectra. Simulations to-date indicate that use of LES results in blade generated turbulence, which is not captured by a RANS simulation. The introduction of onset turbulence increases loading over a range of frequencies and alters the tip-vortex structure immediately downstream of the rotor plane.

Acknowledgements:

This research was conducted as part of the Reliable Data Acquisition Platform for Tidal (ReDAPT) project commissioned and funded by the Energy Technologies Institute (ETI) and led by Alstom Ocean (previously TGL). The authors would also like to acknowledge EDF energy for additional funding, EDF energy and UKTC for access to HPC and the EPSRC funded project X-MED.

References:

[1] N. Jarrin, S. Benhamadouche, D. R. Laurence, R. Prosser, A synthetic-eddy-method for generating inflow conditions for large-eddy simulations, *International Journal of Heat and Fluid Flow* **27** (2006) 585–593. doi:10.1016/j.ijheatfluidflow.2006.02.006.

[2] J. Mcnaughton, I. Afgan, D. D. Apsley, S. Rolfo, T. Stallard, P. K. Stansby, A simple sliding-mesh interface procedure and its application to the CFD simulation of a tidal- stream turbine, *International Journal for Numerical Methods in Fluids* **74** (2014) 250–269.doi:10.1002/fld.3849.

[3] R. Malki, A. J. Williams, T. N. Croft, M. Togneri, I. Masters, A coupled blade element momentum-Computational fluid dynamics model for evaluating tidal stream turbine performance, Applied Mathematical Modelling **37** (5) (2013) 3006–3020. doi:10.1016/j.apm.2012.07.025.

[4] M. J. Churchfield, Y. Li, P. J. Moriarty, A large-eddy simulation study of wake propagation and power production in an array of tidal-current turbines., Philosophical transactions. Series A, Mathematical, physical, and engineering sciences **371** (1985) (2013) 20120421. doi:10.1098/rsta.2012.0421.

[5] T. P. Lloyd, S. R. Turnock, V. F. Humphrey, Assessing the influence of inflow turbulence on noise and performance of a tidal turbine using large eddy simulations, Renewable Energy **71** (2014) 742–754. doi:10.1016/j.renene.2014.06.011.

[6] D. Sutherland, B. Sellar, S. Harding, I. Bryden, Initial flow characterisation utilising turbine and seabed installed acoustic sensor arrays, in: EWTEC 2013, Aalborg, Denmark, 2013.

A Synthetic turbulence model for numerical simulation of marine current turbine

Clément Carlier[1,2], Grégory Pinon[1,*], Benoît Gaurier[2], Grégory Germain[2], Elie Rivoalen[3]
[1]*Laboratoire Ondes et Milieux Complexes (LOMC), UMR 6294, CNRS - Université du Havre, France*
[2]*IFREMER, Marine Structures Laboratory, Boulogne-Sur-Mer, France*
[3]*Laboratoire d'Optimisation et Fiabilité en Mécanique des Structures, INSA de Rouen, France*

Summary: The ambient turbulence intensity is a key factor in the study of marine current turbines. Indeed recent studies have shown that ambient turbulence intensity highly modifies the behavior of horizontal axis marine current turbines. Consequently numerical simulations have to represent the ambient turbulence or at least its effects on the performance and wake of the turbines. This paper presents the latest numerical developments carried out at LOMC in collaboration with IFREMER in order to take into account the effects of ambient turbulence.

Introduction

The recent experimental trials run at the IFREMER flume tank of Boulogne-Sur-Mer, France, have shown that ambient turbulence intensity I_∞ (eq. (1)) highly modifies the behavior of horizontal axis marine current turbines [1,2].

$$I_\infty = 100\sqrt{\frac{\frac{1}{3}\left[\sigma^2(u_\infty)+\sigma^2(v_\infty)+\sigma^2(w_\infty)\right]}{\overline{u}_\infty^2+\overline{v}_\infty^2+\overline{w}_\infty^2}} \quad (1)$$

One of the most noticeable influence can be observed in the wake, downstream of the turbine. Indeed as shown in Fig. 1, the higher the turbulence intensity is, the faster the wake effects decrease. Moreover the interactions between turbines are also highly modified by the effect of the ambient turbulence as shown by Mycek et *al.* [2] for interactions between two turbines.

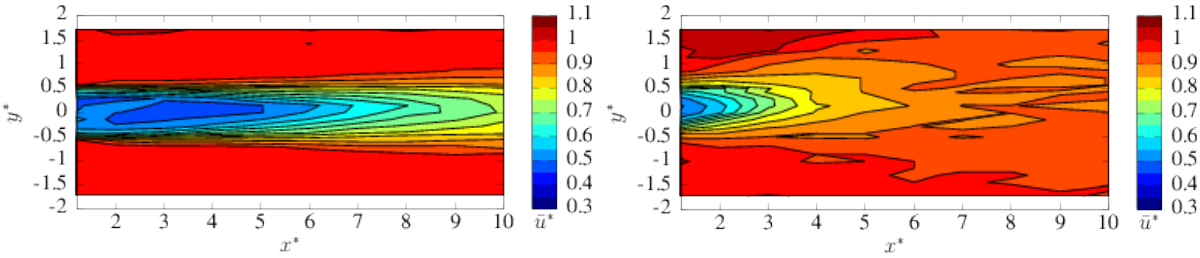

(a) I_∞ = 3% (b) I_∞ = 15%

Fig. 1. Wake behind a turbine with TSR=3.67, U_∞=0.8 m.s^{-1} for different ambient turbulences.

In order to take into account the effect of the ambient turbulence in our numerical simulations, a new module was integrated in the three-dimensional software developed at LOMC [3].

Methods

The software developed at LOMC is based on an unsteady Lagrangian method: the Vortex method [4], a velocity-vorticity numerical implementation of the Navier-Stokes equations. In this method, the turbines are represented using a panel method and the flow is discretised with vorticity-carrying particles emitted at the trailing edge of the turbines blades.

* Corresponding author. *Email address*: gregory.pinon@univ-lehavre.fr

In order to represent the ambient turbulence effects in our three-dimensional software the Synthetic-Eddy-Method [5] was chosen. Togneri *et al.* [6] already adapted this model to their BEMT code for tidal turbines. The Synthetic-Eddy-Method generates a flow with a given turbulence intensity I_∞ and a given anisotropic ratio $(\sigma_u : \sigma_v : \sigma_w)$ by adding a perturbation term to the upstream velocity of the flow U_∞. This perturbation term is calculated as the influence of N generated "turbulent structures" randomly dispatched in the studied space. In our software the "turbulent structures" are advected using the upstream velocity U_∞ and, for each structure leaving the studied space, a new one is generated on the inlet.

Results

Figure 2 displays preliminary results obtained with the Synthetic-Eddy-Method. It shows example of perturbed flow-field generated with the model for the same anisotropic ratio ($\sigma_u : \sigma_v : \sigma_w$) and different turbulence intensities I_∞.

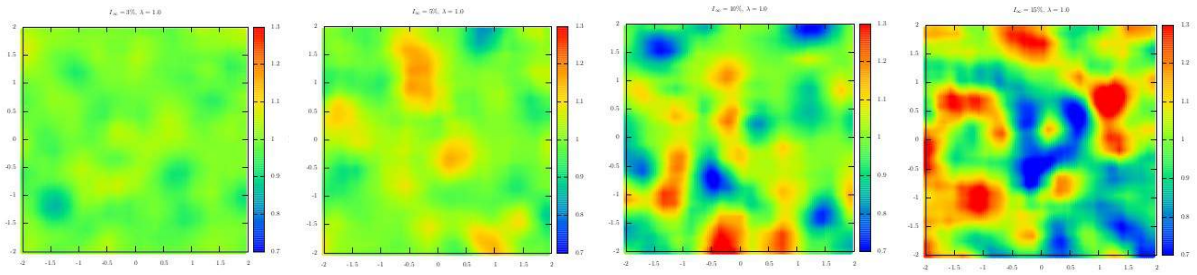

(a) I_∞ = 3% (a) I_∞ = 5% (a) I_∞ = 10% (a) I_∞ = 15%

Fig. 2. Example of velocity field provided by the ambient turbulence model for different value of I_∞.

Conclusions and Further Works

A new module was added to our three-dimensional software to represent the ambient turbulence and its effects on the behavior of marine current turbines. The next step in this work is to use this ambient turbulence model with one marine current turbine and confront the numerical results obtained with experimental data [1] for I_∞ = 3 and 15%. The final goal of this study is to simulated an entire farm of marine current turbines for any turbulent intensity.

Acknowledgements:

The authors would like to thank Haute-Normandie Regional Council and Institut Carnot IFREMER Edrome for their financial supports for C. Carlier Ph.D. Grant and "GRR Energie" programs. The authors also would like to thank the CRIHAN (Centre des Ressources Informatiques de Haute-Normandie) for their available numerical computation resources. Finally the authors would like to thank M. Togneri and I. Masters for the fruitful discussions at the 3rd Oxford Tidal Energy Workshop on the Synthetic-Eddy-Method.

References:

[1] Mycek, P., Gaurier, B., Germain, G., Pinon, P. and Rivoalen E. (2014). Experimental study of the turbulence intensity effects on marine current turbines behavior. part I: One single turbine. *Renewable Energy*. **66**, 729-746.

[2] Mycek, P., Gaurier, B., Germain, G., Pinon, P. and Rivoalen E. (2014). Experimental study of the turbulence intensity effects on marine current turbines behavior. part II: Two interacting turbines. *Renewable Energy*. **68**, 876-892.

[3] Pinon, G., Mycek, P., Germain, G. and Rivoalen, R. (2012). Numerical simulation of the wake of marine current turbines with a particle method. *Renewable Energy.* **46**, 111-126.

[4] Leonard, A. (1980). Vortex methods for flow simulation. *Journal of Computational Physics*. **37**, 289-335.

[5] Jarrin, N., Benhamadouche, S., Laurence, D. and Prosser, R. (2006). A synthetic-eddy-method for generating inflow conditions for large-eddy simulations. *International Journal of Heat and Fluid Flow*. **27**, 585-593.

[6] Togneri, M. and Masters, I. (2014). Synthetic Turbulence Generation for Turbine Modelling with BEMT. In: *Proc. 3rd Oxford Tidal Energy Workshop*, Oxford, UK.

Modelling Hydrodynamic and Morphodynamic Effects at Ramsey Sound

David Haverson*
Industrial Doctoral Centre for Offshore Renewable Energy, Edinburgh, UK
John Bacon
Centre for Environment, Fisheries and Aquaculture Science, Lowestoft, UK
Helen Smith
Department of Engineering, University of Exeter, Penryn, UK

Summary: A Telemac2D hydrodynamic model has been used to determine the impact of a 10MW tidal array at Ramsey Sound. Predicted sediment maps have been created using bed shear stress. Results show the tidal array causes alterations to eddy propagation in the order of 30km, but their impact should be minimal. However, the tidal array reduces the local bed shear stress causing an accumulation of sediment within the array and in its wake.

Introduction

Understanding the environmental impacts of renewable energy projects is of growing importance. The dominant hydrodynamic impact of a tidal stream device is the reduction of flow in the device's wake. The resultant impact of this will be seen predominantly on the benthic environment through changes in bed characteristics and sediment dynamics. A number of sites around the UK are being considered for development, one of which is Ramsey Sound, where flows are accelerated, up to 3.5 m/s, in a channel between Ramsey Island and the mainland. In 2011, Tidal Energy ltd (TEL) was given consent to test a prototype of their Delta Stream device in Ramsey Sound. Following successful testing, TEL is intending to develop a 10MW demonstration array just north of the Sound at St David's Head. The aim of this research is to investigate the impact of this 10MW array.

Methods

A 2D depth-averaged hydrodynamic model of the area has been simulated using Telemac2D. The unstructured triangular mesh has 300,948 elements, with a 3.6km resolution along the open boundary, focusing down to 10m to resolve key bathymetric features. The open boundary is forced using the OSU TPXO European Shelf 1/30° regional model. The effect of the tidal array is introduced into the model as an extra sink in the momentum equations. The tidal turbines impose a drag on the flow in two parts: a thrust force produced by the rotor due to energy extraction and a drag force caused by the supporting structure. The 10MW array is modelled as nine devices. Each Delta Stream device consists of three 15m rotors in a triangular arrangement. Thus, each device is modelled as the combined total force of all three rotors and support structure. This force is spread over 8 elements, covering an area of 40m x 40m. A detailed description of the model and methodology is presented in [1].

The methodology used to determine the impact on sediment dynamics was originally presented by Martin-Short [2]. As explained, due to lack of data for forcing boundary conditions, it is difficult to model suspended and bed load transport. However, as bed shear stress is the primary driver in sediment movement, it can be used as a predictor to understand the regime in the region. Bed shear stress is calculated as

$$\tau = \rho C_d ||\mathbf{u}|| \mathbf{u}. \quad (1)$$

where ρ is the density of seawater, C_d is the bottom drag coefficient and $||\mathbf{u}||$ is the magnitude of the velocity vector. This method *"can be used to determine the finest grain size that can be deposited in a region."* As the main driver in sediment prediction is velocity, the impact of the tidal array will be through the local reduction/increase in flow conditions and not through altering drag characteristics of the sediment.

Results

Ramsey Sound is a naturally very turbulent area, due to bathymetric effects, with the formation of large eddies. The resulting effect of the tidal array causes alterations to the dispersion of these eddies in the order of 30km away. However, the dispersion of these eddies are naturally variable due to other drivers (such as winds)

* Corresponding author.
Email address: D.Haverson@ed.ac.uk

not present in the model. Therefore, the benthic habitat is realistically already adapted to these large scale variations. However, the resulting change to the mean bed shear stress, over 30 days, is much more localised, as shown in Figure 1. It can be seen that the tidal array reduces the flow directly in its wake, reducing the mean bed shear stress. This will result in sediment accumulation. However, there is also a small area of increased bed shear stress, which will lead to an increased erosion. This is due to flows being accelerated between the array and the headland in order to maintain the momentum in the flow. Figure 2 shows the estimated sediment maps during a snap shot of peak flood. Over the full tidal cycle, the predicted sediments show good agreement with EUNIS habitat maps. It can be seen that the presence of the array leads to a localised accumulation of sediment within the array and in its wake.

Conclusions

As expected, the presence of the tidal array locally reduces the bed shear stress leading to an accumulation of sediment. However, there are limitations to this methodology. Whilst insights can be gathered into the likely changes, this method only determined variations in bed shear stress due to skin friction. It does not take into account changes in bed formation nor can it determine sediment transport rates. Further modelling will be required to quantify these parameters.

Acknowledgements:

The Industrial Doctorate Centre for Offshore Renewable Energy is funded by the Energy Technologies Institute and the RCUK Energy Programme, grant number (EP/J500847/1).

References:

[1] Haverson, D., Bacon, J., Smith, H. (2014) Modelling the far field impacts of a tidal energy development at Ramsey Sound. In: *Proc. 21st Telemac User Conference*, Grenoble, France, 119-124.

[2] Martin-Short, R., Hill, J., Kramer, S.C., Avdis, A., Allison, P.A., Piggott, M.D. (2015) Tidal resource extraction in the Pentland Firth, UK: Potential impacts on flow regime and sediment transport in the Inner Sound of Stroma. *Renewable Energy*, 76, 596-607.

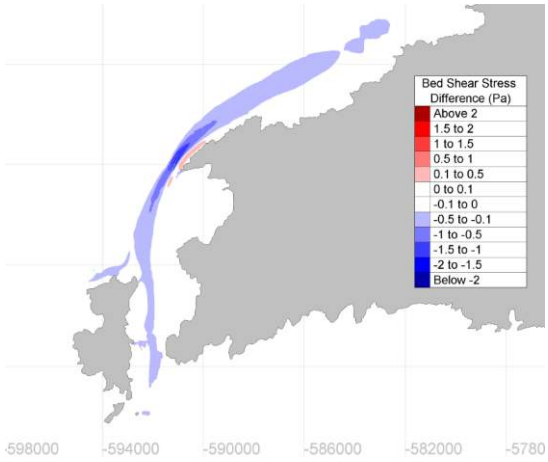

Fig. 1. Mean difference in bed shear stress

Fig. 2. Estimated sediment maps for no (left) and 9 (right) devices during peak flood (south-north flow).

The distribution of the Irish Sea tidal-stream resource

Matt Lewis*, Simon Neill, Peter Robins
School of Ocean Sciences, Bangor University, UK

M. Reza Hashemi
Department of Ocean Engineering, University of Rhode Island (USA)

Summary: The tidal-stream resource of the Irish Sea was investigated with a 3D hydrodynamic model. Devices currently require water depths (*h*) between 25–50m and peak spring tidal current speeds (SV) of 2.5m/s. An operational power curve was applied to model-simulated currents (assuming a typical device density). The resource was found to be extremely limited by current deployment criteria (*h* of 25-50m & SV>2.5m/s), however, the resource could increase five fold if turbines are developed to harvest lower velocities sites (SV>2m/s) and be deployed in deeper water. Oceanographic conditions of potential future sites are discussed, such as the assumption of rectilinear flow.

Introduction

Tidal-stream resource estimates are often based on hydrodynamic tidal models with spatial resolution in the order of kilometres, which could be considered unsuitable [1] as differences of up to 2 m/s have been noted between resource maps [2]. Presently, tidal-stream energy technology requires peak spring flows (SV) in excess of 2.5 m/s, and water depths between 25-50 m [3]. Regions suitable for such "1st generation" technology are sparse, and typically the result of topographic/bathymetric flow enhancement. As competition for sea-space intensifies or the phasing potential of the tidal resource is realized [4], tidal-stream energy sites beyond the typical 1st generation locations will need to be developed; especially as any potential concentrated exploitation of the resource could lead to significant feedbacks between the resource and the environment [5]. Therefore, the potential sea space of these 1st generation sites needs to be better quantified, and future directions for the most effective and beneficial development of tidal-stream energy technology needs to be better understood.

Methods

The Irish Sea tidal-stream energy resource was quantified using the 3D Regional Ocean Modelling System (ROMS), which simulates tidal hydrodynamics using finite-difference approximations of the Reynolds-Averaged Navier-Stokes equations with hydrostatic and Boussinesq assumptions, and has been successfully applied for a number of resource studies (e.g. [4]). To better understand hydrodynamic model uncertainties two tidal forcing products, each with ten constituents, were compared (TPXO and FES2012 [6]). The computational grid extended 51°N to 56°N and 7°W to 2.7°W, and three model spatial resolutions were compared: 1/60°, 1/120° and 1/240°.

The spatial distribution of the undisturbed spring-neap cycle mean kinetic energy (KE_{s-n}) for the Irish Sea was calculated from the simulated depth-averaged velocity time-series ($\overline{U}_t$) using Equation 1. Further, to estimate the practical power available, the measured power curve of the twin-rotor 16m diameter (~40m device width) Seagen device (www.marineturbines.com), was applied to simulated tidal currents at suitable sites – assuming a device spacing of 3 device widths laterally and 7 device widths downstream (two devices, or four rotors, per fine resolution model cell). Feedbacks between energy extraction and the resource, such as inter-device and inter-array interactions (see [7]), and practical considerations (such as distance to grid connection) were not included.

$$KE_{s-n} = \frac{1}{14.77days}\sum\left[\iiint \frac{1}{2}\left(\overline{U}_t\right)\delta m\right]\delta t \cong \frac{1}{n}\sum_0^{14.77days}\left\{\sum_A\left[\frac{1}{2}\rho\left(\overline{U}_t\right)^2 h_t \delta x \delta y\right]\right\}\delta t \quad (1)$$

where *n* is the number of observations, *m* is mass, ρ is density, and the volume per computational cell is calculated as the multiple of cell width (δx), cell length (δy), and time-varying water depth (h_t).

Results

All three spatial resolution tidal models validated well (to within 10% for both elevations and currents using 147 observations), however a 9% improvement in simulated elevations was found when using the FES2012 product for boundary conditions. The distribution of the tidal-stream energy resource assuming current ("1st generation") and future (beyond "1st generation") device deployment criteria is shown in Fig. 1. The tidal-stream resource was found to be extremely limited assuming 1st generation device deployment criteria; annual available practical power resource of 24GWh was calculated within an areal extent of 90km^2 – assuming an M2 and S2 tidal

* Corresponding author.
Email address: m.j.lewis@bangor.ac.uk

cycle only. Analysis revealed that including "2nd generation" technologies (SV> 2m/s and including deeper water locations) would increase the available resource to 111GWh with a near ten-fold increase in the available sea space (800km^2). All three spatial resolution models were found to be in general agreement with our 1st generation resource estimate; however our 1/60° model appeared to over-predict the resource by 31GWh when including 2nd generation sites. Moreover, we found potential sites were more likely to be rectilinear in the plane of flow between peak ebb and flood tide, with a 20° average error in this assumption for 1st generation sites reducing to an average of 3° for 2nd generation sites; which could have a significant impact on practical resource estimates if a turbine cannot yaw to face the direction of flow [6].

Conclusions

Extending the operational range of a turbine appears to be an important step to ensuring the growth of the industry and that tidal-stream energy can make a meaningful contribution to low carbon electricity generation. Increasing turbine deployment to lower tidal velocities sites and deeper water locations will reduce sea space pressures, increase phasing potential (constant electricity production), and reduce potential tidal current misalignment issues. Moreover, larger basin-scale tidal resource maps should consider finer spatial resolution than currently practiced if "2nd generation" technologies are developed, and future work needs to reduce some of the assumptions made within this study; for example, energy extraction terms within the hydrodynamic model and economic costing of distance to grid connections.

Acknowledgements:

The tidal model simulations were made possible thanks to High Performance Computing (HPC) Wales. The authors would like to acknowledge the financial support of EPSRC Supergen project EP/J010200/1 and the SEACAMS project (www.seacams.ac.uk).

References:

[1] O'Rourke F, Boyle F, Reynolds A. Tidal current energy resource assessment in Ireland: current status and future update. Renewable and Sustainable Energy Reviews 2010; 14: 3206-3212.
[2] Black and Veatch. Phase II. UK tidal-stream energy resource assessment. London: The Carbon Trust; 2005.
[3] Iyer A, Couch S, Harrison G, Wallace A. Variability and phasing of tidal current energy around the United Kingdom. Renewable Energy 2013; 51: 343 – 357.
[4] Neill SP, Hashemi MR, Lewis MJ. Optimal phasing of the European tidal-stream resource using the greedy algorithm with penalty function. Energy 2014; 73: 997-1006.
[5] Neill SP, Jordan JR, Couch SJ. Impact of tidal energy converter (TEC) arrays on the dynamics of headland sand banks. Renewable Energy 2012; 37(1): 387-397.
[6] Lewis M, Neill SP, Robins PE, Hashemi MR. Resource assessment for future generations of tidal-stream energy, Energy 2015: http://dx.doi.org/10.1016/j.energy.2015.02.038
[7] Draper S, Borthwick AGL, Houlsby GT. Energy Potential of a tidal fence deployed near a coastal headland, Philosophical Transactions of the Royal Society 2013, Part A, 371:20120176

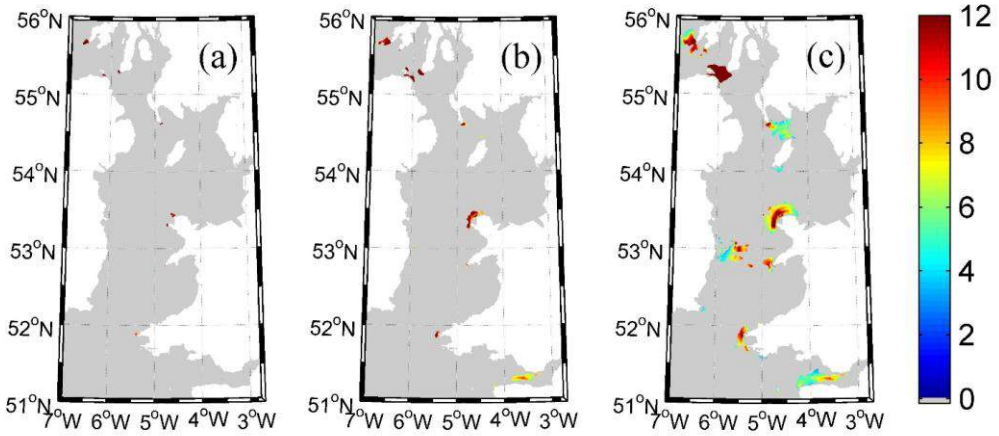

Fig. 1. Estimated undisturbed mean kinetic energy flux (GJ) of the Irish Sea assuming; (a) 1st generation (SV>2.5m/s and 25<h<50 m), (b) 2nd generation (SV>2m/s and h>25m), and (c) 3rd generation (SV>1.5m/s and h>25m) technologies. Unsuitable regions are shaded grey.

The sensitivity of tidal resonance in the Bristol Channel

Chanshu Gao*, Thomas A. A. Adcock and Sena Serhadlıoğlu
Department of Engineering Science, University of Oxford, UK

Summary: The energy resource in the Bristol Channel is of national strategic significance to meet the future demand for low carbon energy, and it is the single largest resource area for tidal energy in the UK. However, the complex tidal dynamics of the Bristol Channel are not yet fully understood, in particular the sensitivity of the tidal dynamics to changes such as those caused by energy extraction. This is the motivation for the development of a simplified two-dimensional model to simulate the tidal flows in Bristol Channel. The tidal resonance in Bristol Channel has been investigated by exciting the model with a single tidal component and a series of sensitivity tests have been carried out on tuneable model parameters.

Introduction

The semi-diurnal tides observed in the Bristol Channel are one of the largest in the world with a mean tidal range of 12.2 m at spring tides, which is driven by two main mechanisms: one is the funnelling effect at the upper reaches of the Bristol Channel due to its wedge-shaped geometry and shallow bathymetry; and the other is the quarter-wave length resonance of the Channel with the Atlantic tidal wave [1]. Resonant systems are typically very sensitive to small changes, but will be highly site dependent and further work is needed to fully understand them [2]. Therefore, a simplified two-dimensional model has been developed to investigate the resonances in Bristol Channel using the discontinuous Galerkin (DG) version of ADCIRC, which is a well-developed hydrodynamic finite element model. The DG-ADCIRC solver is capable of using highly flexible unstructured grids that are used to solve the governing equations for coastal and ocean circulations problems [3].

Methods

Fig. 1 shows the overall computational mesh with 16 selected observation stations (From ST1 to ST16) used to model the Bristol Channel. This unstructured grid allows a large variation in the scales of regions of interest, which in this study varies from 500m to 5000m. The open boundaries are forced with a single sinusoidal constituent with an amplitude distribution across the boundary given by that of the M_2 constituent interpolated from a larger model [1]. The DG-ADCIRC modelling parameters were set as constant throughout the study: most of the parameters were attained as the default values recommended by the ADCIRC model developers and used in Serhadlıoğlu *et al.* [4]; while the rest, such as time step, bottom friction, wetting and drying were determined using equations and a parameter sensitivity analysis for the area of focus. Four stations (ST3/5/7/9) were chosen to represent the inner section of the Channel while three stations (ST11/13/15) represent the outer Channel. Water level, nodal factor and bed friction parameters were chosen for the sensitivity tests.

Results

The response curves of the Bristol Channel have been investigated by exciting the model using artificially altered M_2 forcing frequencies (ω), and applying a ratio (ω/ω_{M2}) varying between 0.5175 and 5.175 (Fig. 2). All the stations show a peak in response at around a ratio of 1.2-1.4 which indicates the quarter-wave length resonance of the system with a period of approximately 8.6-10 hours. The inner section of the Bristol Channel (ST3/5/7/9) shows an amplified response over the frequency range ω/ω_{M2}ratio of 1.2-1.4 while the outer part of the Channel (ST11/13/15) exhibits an apparent resonance around the ratio of 3.1-3.6.

The results of the sensitivity test on water level, nodal factor and bed friction in both inner (ST5) and outer (ST11) parts of the Channel are shown in Fig. 3. The response tides are driven by natural frequency (ω/ω_{M2}=1). With water level varying from 4 m lower to 4 m higher than the real situation, the tidal heights do not present visible change. Over a period of 9.3 years, the M_2 nodal factor changes from its minimum (maximum) value, to its maximum (minimum); however, during this time period the M_2 tidal heights almost remain the same. The bed friction is seen to be a dominant effect on the tidal response, since the M_2 amplitude at ST11 decreases by around 0.2m with the quadratic friction coefficient increasing from 0.0025 to 0.005. The bed friction has even greater influence on the shallower areas: at ST5 the amplitude change reaches more than 0.3m.

* Chanshu Gao.
Email address: chanshu.gao@eng.ox.ac.uk

Conclusions

Preliminary studies show that the quarter-wavelength resonant period of the Bristol Channel is close to but shorter than the semi-diurnal tidal band, suggesting that the basin length of the Bristol Channel is shorter than the resonant quarter-wavelength. The response curve obtained in the study suggests that there is another resonance occurring in the Bristol Channel, which might be the resonant response of the Bristol Channel itself. The bed friction chosen has a significant effect on the response of the inner channel location when forced by an M_2 tide, which may have implications for tidal energy extraction. Neither the amplitude on the boundary, nor the mean water level, has a significant impact on the resonant response, suggesting that the nodal factor of the tide, or any possible sea-level rise, will not have a dramatic effect on tidal response in the Channel. Further investigation of the idealised 2-D model and consideration of the real situation of tidal dynamics in the Bristol Channel are necessary to take this analysis further.

References:

[1] Serhadlıoğlu, S. (2014). Tidal stream resource assessment of the Anglesey Skerries and the Bristol Channel. DPhil. University of Oxford.

[2] Adcock,T.A.A., Draper, S. and Nishino, T. (2015). Tidal power generation — a review of hydrodynamic modelling. In press, *Proc. IMechE, Part A: Journal of Power and Energy*.

[3] Kubatko, EJ., Westerink, J.J. and Dawson, C. (2006) hp Discontinuous Galerkin methods for advection dominated problems in shallow water flow, *Computer Methods in Applied Mechanics and Engineering*, 196(1–3) 437-451

[4] Serhadlıoğlu, S., Adcock, T.A.A., Houlsby, G.T. Draper, S. and Borthwick, A.G.L. (2013) Tidal Stream Energy Resource Assessment of the Anglesey Skerries, *International Journal of Marine Energy* 3-4 e98-e111.

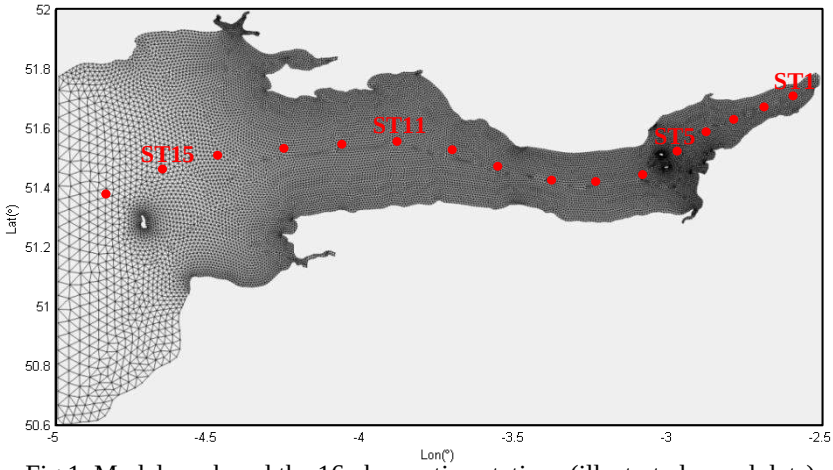

Fig.1. Model mesh and the 16 observation stations (illustrated as red dots).

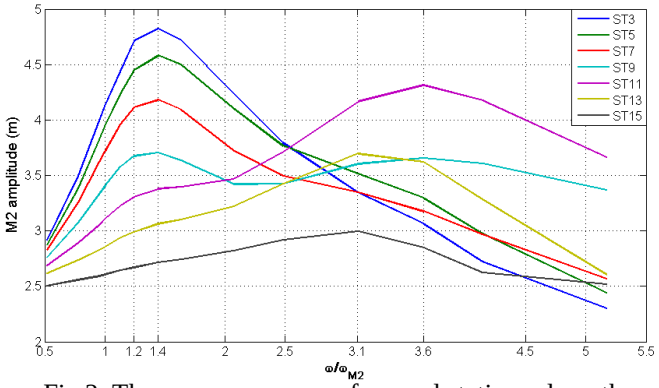

Fig.2. The response curves of several stations along the Bristol Channel: ST3, ST5, ST7 and ST9 represent the inner Channel response; ST11, ST11 and ST15 represent the outer Channel response.

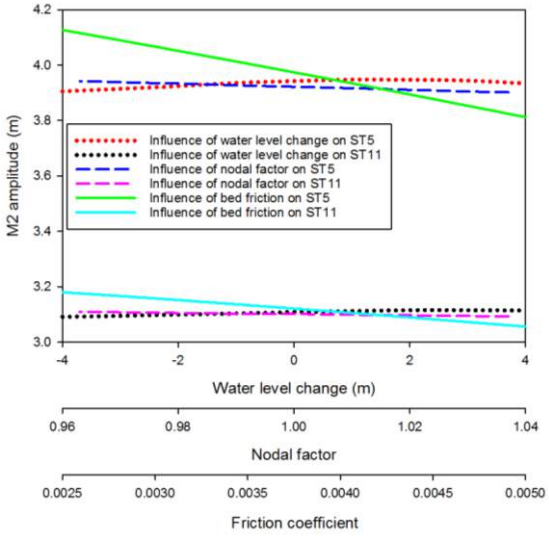

Fig.3. Sensitivity test results on water level (dotted lines), nodal factor (dash lines) and bed friction (solid lines) at ST5 and ST11.

Impacts of In-Stream Tidal Current Turbines on Sediment Dynamics in the Minas Basin, Bay of Fundy, Canada

Ryan P. Mulligan*, Logan Ashall
Department of Civil Engineering, Queen's University, Canada

Brent Law
Bedford Institute of Oceanography, Fisheries and Oceans Canada, Canada

Danika van Proosdij
Department of Geography, Saint Mary's University, Canada

Summary: The Bay of Fundy has strong tidal currents making it an ideal place for tidal power extraction using in-stream tidal current turbines. The implications of constructing a large-scale turbine farm in Minas Channel and the impacts on suspended sediment in the Minas Basin are investigated using a 3D hydrodynamic and sediment model validated using observations from ship-based and bottom-moored instruments. A turbine farm is simulated by adding semi-permeable structures that induce local energy losses over part of the water column. The results suggest that a large-scale tidal energy farm could reduce suspended sediment concentrations which would impact environmental processes, particularly on fine-grained intertidal areas around the macrotidal basin.

Introduction

The Bay of Fundy is a near-resonant macrotidal embayment connected to the Gulf of Maine in Eastern Canada (Fig. 1a). The semi-diurnal tidal range is the highest in the world (up to 16 m), with the strongest currents up to 5 ms^{-1} in Minas Channel. It is ideal location for tidal power extraction by harnessing potential energy using tidal barrages [1] or kinetic energy using in-stream turbines [2]. Numerical modelling efforts [3] have determined that 7 GW of mean power can be extracted by a turbine farm and interest in deployment of in-stream tidal energy extraction devices heightens the importance of understanding the basin-wide hydrodynamics and sediment dynamics. Minas Basin has high suspended sediment concentrations (SSC) [1,4] and a turbine farm could have far-field impacts on the physical and biological environment. The goal of this study is to simulate the processes in Minas Basin using a 3D numerical model validated with field observations, to investigate the implications of tidal power extraction from a turbine array on suspended sediment transport.

Methods

The Delft3D [5] hydrodynamic and sediment model coupled to a surface wave model is used in this study, with a domain consisting of two connected grids with coarse (800 m) and fine (200 m) horizontal resolution, and four topographically-following vertical layers representing 5, 15, 30 and 50% of the water depth. The model is forced by tidal observations near the entrance to the Bay of Fundy and wind observations over a simulation period of 30 days. The model is initialized with a sediment distribution map to define the location of fine muddy (cohesive) material on the intertidal flats, coarse sands (non-cohesive) in intermediate depths and exposed bedrock (no sediment) in deep areas scoured by tidal currents [6]. Sediment and morphological input parameters are selected based on previous numerical results [4]. Turbines are parameterized as semi-porous hydraulic structures that induce local losses of energy over the lower 20% of the water column (6-20 m near the bed in 30-100 m water depths) in Minas Channel. The turbine regions (groups of turbines at close spacing of less than the model resolution) were implemented in individual grid cells over the lower two vertical layers for two different scenarios representing low (16 turbine regions) and high (41 turbine regions, Fig. 1c) tidal power extraction cases. Observations from May-June 2013 that include water levels, currents profiles, surface waves and SSC profiles, obtained from bottom-moored Acoustic Doppler Current Profilers and sensors deployed from an oceanographic research vessel, are used to validate the numerical model.

* Corresponding author.
Email address: mulligar@queensu.ca

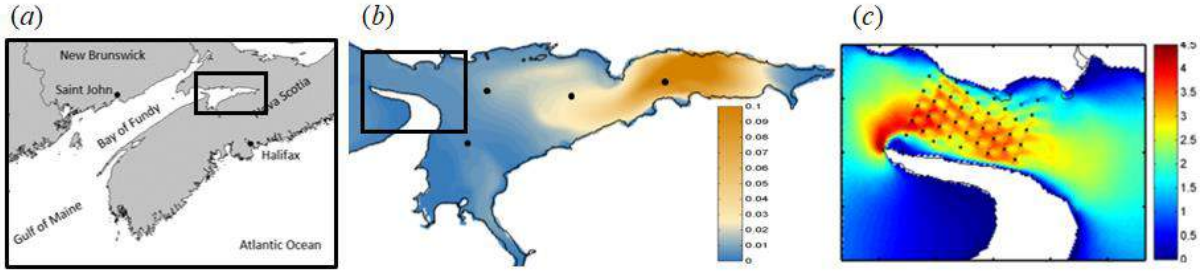

Fig. 1. The Bay of Fundy, Nova Scotia, Canada: a) geographical location; b) predicted depth-averaged SSC (mgL^{-1}) in Minas Basin at high tide (June 12, 2013) with black dots indicating observing stations; and c) predicted surface tidal current magnitude (ms^{-1}) in Minas Channel during a flood tide (June 7, 2013) with a farm of 41 turbine regions in a high tidal power extraction simulation.

Results

The low and high power extraction scenarios result in 1% and 15% decreases in tidal amplitude in Minas Basin, corresponding to 0.8 and 5.6 GW of mean tidal power respectively [3]. Simulated tidal currents during a flood tide with turbines are shown on Fig. 1c, for high tidal power extraction case. The current speed is significantly altered by a turbine farm in Minas Channel with localized differences (from a simulation without turbines) in surface velocity up to 1.5 ms^{-1}. The reduced flows influence the Minas Basin where currents are reduced by up to 0.6 ms^{-1} at the observation sites in the centre of the basin. Lower velocities reduce the simulated rates of sediment erosion and deposition, and the highest impacts occur further from the turbines in the eastern end of the basin with lower tidal current speeds where the fractional change in velocity is highest. The averaged SSC were calculated at 5 stations from the observations and the model simulations (e.g. Fig. 1b), and the results suggest that SSC is reduced by 6% and 37% in the eastern end of the basin for the low and high tidal power extraction scenarios respectively.

Conclusions

Hydrodynamics and sediment transport in the Bay of Fundy are investigated using a coupled hydrodynamic, wave and sediment model. Idealized model scenarios were used to numerically simulate different sizes of in-stream turbine farms. In the high tidal power extraction scenario, far-field intertidal areas are the most affected, with a decrease of 70 mgL^{-1} in mean SSC, while very small changes occur at other stations. Overall, the change in SSC averaged over time and throughout the water column at 5 stations indicates that the implementation of low and high tidal power extraction turbine arrays could cause a reduction in SSC in the Minas Basin which would affect small-scale physical and biological processes particularly on the fine-grained intertidal areas around the macrotidal basin. This research provides a foundation for investigating the potential change in currents and suspended sediment concentrations due to tidal power farms and could lead to a more efficient turbine arrays with lower impacts on the marine environment.

Acknowledgements: We thank the crew of the CCGS Hudson at the Bedford Institute of Oceanography. This research was funded by the Offshore Energy Research Association (OERA) of Nova Scotia.

References:

[1] Greenberg, D.A. and Amos, C.L. (1983) Suspended sediment transport and deposition modeling in the Bay of Fundy, Nova Scotia - a region of potential tidal power development. *Can. J. Fish. Aqua. Sci.*, **40**:s20-34.

[2] Mulligan, R.P., Smith, P.C., Hill, P.S., Tao, J., van Proosdij, D. (2013). Effects of tidal power generation on hydrodynamics and sediment processes in the Bay of Fundy, *Proc. Can. Soc. Civ. Eng.*, Montreal, 10p.

[3] Karsten, R.H., McMillan, J.M., Lickley, M.J., Haynes, R.D. (2008). Assessment of tidal current energy in the Minas Passage, Bay of Fundy. *Proc. Inst. Mech. Eng., Part A: J. Power and Energy*, **222**(5), 493–507.

[4] Tao, J., Hill, P.S., Mulligan, R.P., Smith, P.C., 2014. Seasonal variability of total suspended matter in Minas Basin, Bay of Fundy. *Estuar. Coast. Shelf Sci.*, **151**, 169-180, doi: 10.1016/j.ecss.2014.10.005.

[5] Lesser, G. R., Roelvink, J. A., van Kester, J., Stelling, G. S. (2004). Development and validation of a three-dimensional morphological model. *Coast. Eng.*, **51**(8-9), 883-915.

[6] Amos, C.L., Long, B.F.N. (1980). The sedimentary character of the Minas Basin, Bay of Fundy. *Littoral Processes and Shore Morphology, Geological Survey of Canada*, 80-10, 123–152.

Characterising the variability of the tidal-stream energy resource over the northwest European shelf seas

Peter Robins, Matt Lewis, Simon Neill, Sophie Ward
School of Ocean Sciences, Bangor University, UK

Summary: The spatial distribution of the tidal currents over the northwest European shelf seas were examined using a 3D model (ROMS) at ~1 km spatial resolution. Tidal analysis of the depth-averaged velocities were applied to the power curve of a prototype tidal-stream device, post-simulation. We show that the ratio of the amplitudes of the M_2 and S_2 tidal currents generates significant variability in annual practical power – variability that is not accounted for when considering only the mean peak spring currents. Diurnal inequalities (governed by K_1 and O_1) and tidal asymmetries (governed by the relationship between M_2 and M_4) can further affect power generation. We find that mean peak spring tidal velocities can under-estimate the resource by up to 25%, and that annual practical power generation can vary by ~15% for regions experiencing similar mean peak spring tidal velocities, due to the influence of other tidal constituents.

Introduction

The tidal-stream renewables industry is at a crucial stage, where devices are grid-connected at high-energy sites (e.g., marineturbines.com; openhydro.com). The next stage – the construction of arrays – has been granted consent at several sites (e.g., fundayforce.ca; emec.org.uk), where site selection has been informed by relatively superficial resource assessment models (e.g., BERR Atlas of UK Marine Renewables; renewables-atlas.info), based on the peak spring tidal currents. Yet, little research has been conducted on the temporal variability, and how this varies spatially, which is essential when considering the ultimate goal of firm power generation. For example, a site which has lower peak tidal currents than another may actually have a greater net resource, because the time series velocities are more consistent or more symmetrical [1]. We investigate the spatial and temporal variability of the tidal currents and potential power production across the northwest European shelf seas, with the aim of improving our understanding of the net tidal-stream energy resource and optimising energy yield.

Methods

Three-dimensional tidal currents were simulated over the northwest European shelf using ROMS [2]. Our domain (14°W to 11°E, and 42°N to 62°N) had a resolution of ~1/60° (latitude) and 1/100° (longitude). Tidal elevation and tidal velocity forcing was obtained from TPX07 global tide data, and simulated 30 days, after a model spin-up, which is sufficient for tidal analysis of the following constituents: M_2, S_2, K_1, O_1, and M_4. Our model was validated against data (ntslf.org), producing scatter indices (SI), i.e. root mean squared error normalised by the mean of the observations, ≤ 8% SI for elevations and ≤ 12% SI for tidal currents.

Variability in the tidal currents over the lunar cycle was quantified according to the following ratio (R):

$$R = 1 - (\overline{U}_{S2}/\overline{U}_{M2}) \quad (1)$$

where $\overline{U}_{M2}$ and $\overline{U}_{S2}$ denote the amplitudes of the depth-averaged tidal velocity. We also investigate the daily modulation of consecutive tides, due to the declination of the Moon and described by K_1 and O_1. Diurnal inequalities may cause power generation to become sub-optimal for one of these tides per day. Next, we look at M_4-generated tidal asymmetries and variability in power generation over semi-diurnal timescales. The above processes are not routinely incorporated into tidal-stream resource maps or resource optimisation studies. Our approach investigates the variability of the principal tidal constituents discretely, in order to improve the overall resource characterisation. We consider the extractable resource for an observed power curve from a grid-connected turbine – the Seagen-S twin 600 kW (net 1.2 MW), 16 m diameter, turbine deployed in Strangford Narrows, UK (marineturbines.com). The cut-in and rated power speeds are 1.0 and 2.7 m s^{-1}, respectively.

Results

The spring-neap ratio R (Eq. 1) was calculated for the northwest European shelf seas (Fig. 1). The black contours in Fig. 1 denote potential tidal-stream sites – within which R varies from 0.59 (a relatively large variability between springs and neaps) to 0.82 (a relatively low variability between springs and neaps). Larger R ratios will generate a more continuous energy yield over the lunar cycle and, therefore, could be an important factor in resource exploitation and optimisation. When we examine all potential tidal-stream sites, we show that more practical power can be extracted when R is greater (Fig. 2).

Diurnal inequalities are generated in regions where the combined $\overline{U}_{K1}$ and $\overline{U}_{O1}$ current amplitudes are significant. Simulated variability in diurnal inequalities, for the northwest European shelf seas, were small. However, for any given velocity, a greater diurnal inequality generally produced significantly less practical power, than semi-diurnal tides. Finally, we calculate the contribution of the M_4 tide to practical power, which

generally reduces power production. There is a weak relationship based on tidal asymmetry; less net power production tends to occur when the tidal currents exhibit stronger asymmetry.

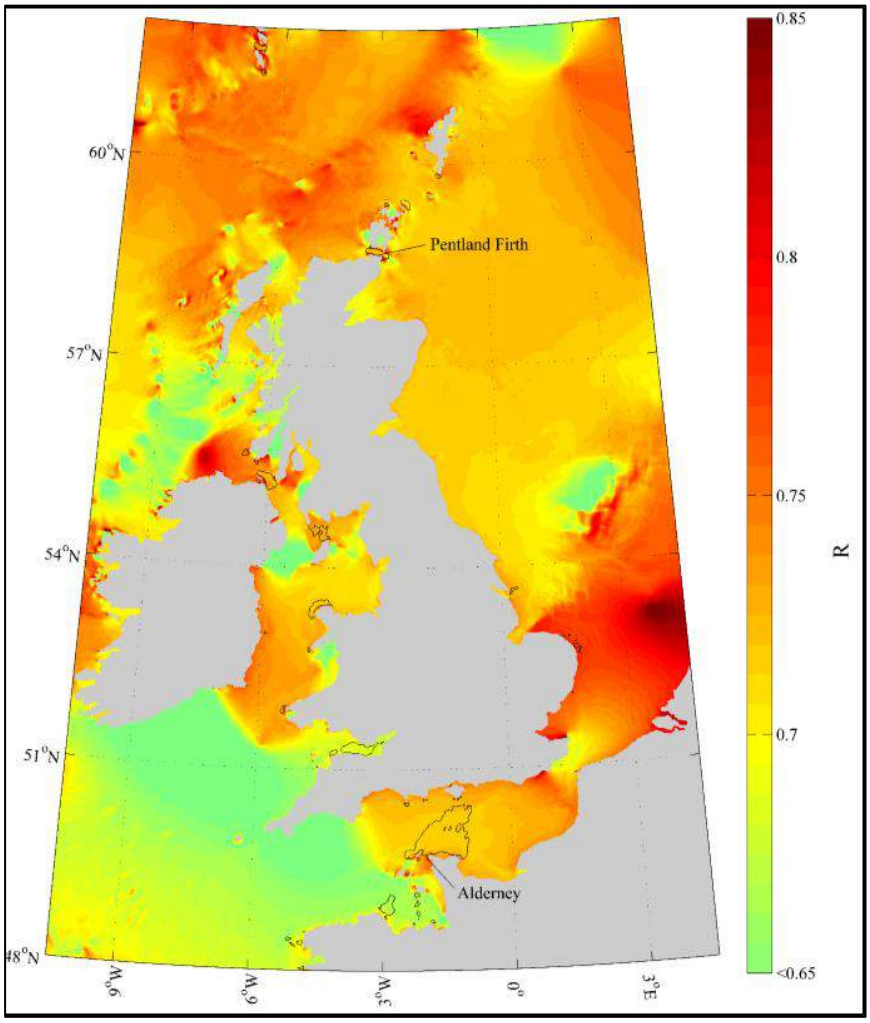

Fig. 1. Spatial variability in the spring-neap ratio *R* (Eq. 1). The black contours denote potential TEC sites – where water depths exceed 25 m and peak velocities exceed 2 m s^{-1}.

Conclusions

We calculate the European tidal-stream energy resource – a region with high tidal dissipation and surrounded by nations that are motivated to invest in marine renewables. Harmonic variabilities can cause variabilities in the available annual practical power. However, there tends to be less variability (~10%) between 'second-generation sites' (mean peak spring velocities ~2 m s^{-1}), than between 'first-generation sites' (velocities >2.5 m s^{-1}). Counter-intuitively, site selection based on lower rated turbines, where a larger sea space is available, may generate more electricity than higher rated turbines over a relatively limited sea space. Traditionally calculating the resource based on the mean spring-neap tide inaccurately represents the resource by up to 25%. Therefore, it will be important to resolve other tidal constituents and relate energy production to daily and seasonal energy demand.

Acknowledgements:
The authors acknowledge the support of the Welsh Government, HEFCW, WEFO, ERDF, and High Performance Computing Wales. (Grants: LCRI-M 80284, SEACAMS 80366, EPSRC EP/J010200/1).

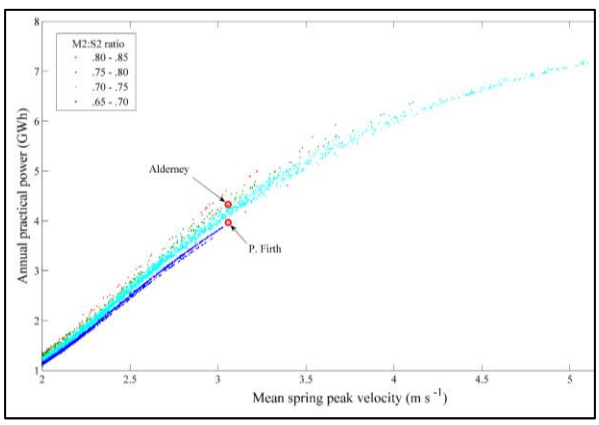

References:
[1] Neill SP, Hashemi MR, Lewis MJ. 2014. The role of tidal asymmetry in characterizing the tidal energy resource of Orkney. Ren. Energy 68: 337-350.
[2] Shchepetkin AF, McWilliams JC. 2005. Regional Ocean Model System: a split-explicit ocean model with a free-surface and topography-following vertical coordinate. Ocean Modelling 9: 347-404.

Fig. 2. Mean spring peak velocity plotted against annual practical power, for potential tidal-stream sites (i.e., 9,500 km^2), coloured corresponding to their spring-neap ratio *R*. Example sites signify Alderney (*R* = 0.75) and Pentland Firth (*R* = 0.69).

Wave-current interaction in the Bristol Channel and the implications of a Severn Barrage on wave climate

Iain Fairley[1], Ian Masters
College of Engineering, Swansea University, UK

Reza Ahmadian
School of Engineering, Cardiff University, UK

Summary: Wave current interaction leads to wave a significant tidal modulation of wave heights in the Bristol Channel. Proposals exist for a Severn Barrage to generate electricity and these will impact on the tidal regime in the area. The aim of this work is to determine the impact of these changes to wave climate in the region. Measured data is used to illustrate the tidal modulation of wave height and a spectral wave model used to test the impact of the barrage. Barrage implementation reduces the tidal modulation of wave heights. In general changes to wave height forced by the barrage are small, differences over a tidal cycle being ±5% of the natural case.

Introduction

Tidal energy extraction has the potential to alter tidal currents and elevations. Academic research has initially focussed on these hydrodynamic impacts but more recently second order effects of hydrodynamic change such as impacts on sediment transport [1, 2] and ecosystems have been considered. One area of impact is on wave climate via wave-current interaction. Wave-current interaction is a well-researched process [3]: waves propagating through a current will both affect and be affected by the current. This contribution focusses on the latter. The motivation is primarily to understand impacts of the Severn Barrage but this contribution can also be considered illustrative of potential impacts of large tidal stream arrays.

The Severn Estuary has one of the largest tidal ranges in the world (14m) and hence a range of schemes have been proposed to generate electricity either via lagoons, barrages or tidal fences. Recent reports have suggested that a barrage from Cardiff to Weston could generate 5% of the UK's electricity supply [4], however such a large structure would have a range of environmental impacts e.g. [5, 6].

The Severn Barrage, will impact wave condition in two ways: to the east of the barrage, waves incident from the Atlantic will be blocked by the structure; to the west, waves will be affected by altered water levels and currents. In this paper only the second is considered based on numerical modelling. A SWAN wave model is run for characteristic wave conditions. This model is forced with water level and current outputs from a DIVAST hydrodynamic simulation [7] for scenarios with and without a barrage in place. It is recognised that wave current interaction can be problematic in spectral wave models [8, 9]: in this contribution a version of SWAN modified by van der Westhuysen [9, 10] to better cater for wave current interaction is used. In this version an additional source term for current induced white-capping is included [9, 10]. The work that will be presented is based on work described in [11]

Results

Figure 1 shows a plot of the spectral density of the wave height record at the Scarweather Sands wave buoy in the centre of the Bristol Channel. A peak in the spectral density at 1.9 cycles a day can be seen; this corresponds to the semi-diurnal tidal frequency and demonstrates the tidal modulation of wave height. Similar results are observable in other wave buoys in the region.

Figure 2 shows a plot of water levels and wave heights over a tidal cycle at the Scarweather Sands wave buoy. It can be seen that wave heights are greatest at mid tide on the incoming tide and lowest at mind-tide on the outgoing tide. This corresponds to times of maximum current. Implementation of the Severn Barrage reduces the magnitude of the ebb current and hence reduces the

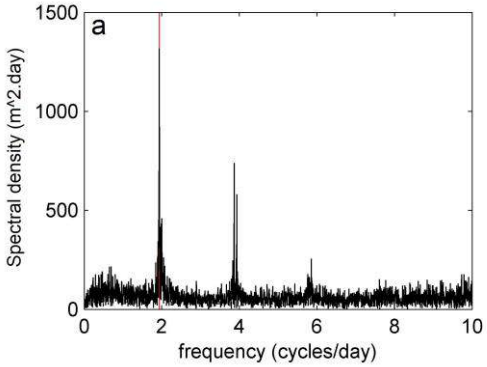

Figure 1: The spectral density of significant wave height from the Scarweater Sands wavebuoy

[1] Corresponding author.
Email address: i.a.fairley@swansea.ac.uk

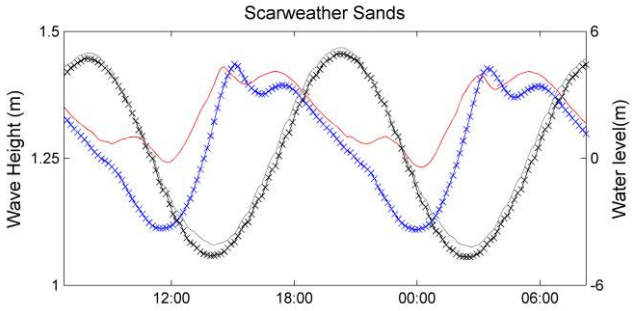

Figure 2. A plot showing the tidal modulation of wave height at Scarweather sands. The black crossed line shows without barrage water level and the grey line with barrage water level. Wave heights are shown by the blue crossed line (without barrage) and the red line (with barrage).

modulation of wave heights. This means that wave heights are greater on the out-going tide for the barrage case.

Conclusions

Implementation of a Severn Barrage will affect tidal range and currents in the Bristol Channel. This contribution shows that this will lead to a reduction of tidal modulation of wave heights: peak wave heights will remain at a similar level but reduction in wave heights on the out-going tide will be less. When wave heights are averaged over a tidal cycle

Acknowledgements:

This research has been carried out as part of both the LCRI and MAREN projects, which are part funded by the Welsh Government, the Higher Education Funding Council for Wales, the Welsh European Funding Office, and the European Regional Development Fund (ERDF) Convergence and Atlantic Area Transnational (INTERREG IV) Programmes. The authors wish to acknowledge their financial support. The authors acknowledge the use of Battri and Triangle in mesh generation. Andreas van der Westhuysen is thanked for providing his modified SWAN source code which allowed us to use his improvements that better cater for wave-current interaction.

References:

[1] I. Fairley, I. Masters, and H. Karunarathna, "The cumulative impact of tidal stream turbine arrays on sediment transport in the Pentland Firth " *Renewable Energy*, vol. (under review), 2015.

[2] S. P. Neill, E. J. Litt, S. J. Couch, and A. G. Davies, "The impact of tidal stream turbines on large-scale sediment dynamics," *Renewable Energy*, vol. 34, pp. 2803-2812, Dec 2009.

[3] J. Wolf and D. Prandle, "Some observations of wave-current interaction," *Coastal Engineering*, vol. 37, pp. 471-485, Aug 1999.

[4] DECC, "Severn Power Tidal Power Feasibility Study Conclusions and Summary Report," 2010.

[5] M. W. Aprahamian, C. D. Aprahamian, and A. M. Knights, "Climate change and the green energy paradox: the consequences for twaite shad Alosa fallax from the River Severn, U.K," *Journal of Fish Biology*, vol. 77, pp. 1912-1930, Nov 2010.

[6] M. Kadiri, R. Ahmadian, B. Bockelmann-Evans, W. Rauen, and R. Falconer, "A review of the potential water quality impacts of tidal renewable energy systems," *Renewable & Sustainable Energy Reviews*, vol. 16, pp. 329-341, Jan.

[7] J. Q. Xia, R. A. Falconer, and B. L. Lin, "Hydrodynamic impact of a tidal barrage in the Severn Estuary, UK," *Renewable Energy*, vol. 35, pp. 1455-1468, Jul.

[8] R. C. Ris and L. H. Holthuijsen, "Spectral modelling of current-induced wave blocking," presented at the 25th International Conference on Coastal Engineering, Orlando, Florida, 1996.

[9] A. J. van der Westhuysen, "Improved modelling of wave-current interaction in SWAN," presented at the Coastal Engineering 2010, Hamburg, 2010.

[10] A. J. van der Westhuysen, "Spectral modeling of wave dissipation on negative current gradients," *Coastal Engineering*, vol. 68, pp. 17-30, Oct 2012.

[11] I. Fairley, R. Ahmadian, R. A. Falconer, M. R. Willis, and I. Masters, "The effects of a Severn Barrage on wave conditions in the Bristol Channel," *Renewable Energy*, vol. 68, pp. 428-442, Aug 2014.

Investigation on the hydrodynamics of the catamaran hull of a floating tidal power generation device

Yuanchuan Liu and Qing Xiao*
Department of Naval Architecture, Ocean and Marine Engineering, University of Strathclyde, UK

Summary: Tidal energy as an alternative clean and renewable energy source has recently aroused much interest among both academia and industry. Floating tidal power generation devices are also under development worldwide. In this paper, hydrodynamics of the catamaran hull of a floating tidal power generation device is investigated using a CFD solver. As an initial step, the tidal turbine is not considered. Motion and force responses of the floating platform subject to regular waves are presented and analysed.

Introduction

Over the last several decades, energy crisis, together with the public concern about environmental pollution caused by traditional fossil energy sources such as coal and oil, has motivated more and more researchers and enterprises to develop clean and renewable energy sources as alternatives. Among them, tidal energy has gradually aroused interest in many countries mostly thanks to its higher predictability than other renewable energy sources like wind and solar energy [1]. Previously, most of tidal energy devices were designed to be installed on fixed structures sitting on the seabed. Nowadays some floating structures are under development as they are comparatively cheap to construct and install as well as easy to maintain [2, 3]. In that case, the floating structure might affect the position of the tidal turbine thus play a significant role in the performance of power generation. As a result, study on the interaction between the floating structure and the tidal turbine has recently become a hot topic.

In this paper, hydrodynamics of the catamaran hull of a floating tidal power generation device is investigated using a CFD solver based on open source CFD toolbox OpenFOAM [4]. As an initial step, only the supporting hull is considered and the tidal turbine is temporarily not attached. Numerical results such as motion and force responses are presented and analysed for the floating catamaran hull subject to the regular waves.

Methods

The present solver [5] used in this paper is developed in OpenFOAM, where the two-phase incompressible RANS equations are solved by Finite Volume Method (FVM), the surface interface is captured by a VOF method with bounded compression technique, and the pressure-velocity coupling is handled by the PIMPLE algorithm which combines the well-known PISO and SIMPLE algorithms.

The solver is integrated with a numerical wave tank module for wave generation and damping, as well as a body motion system including a 6DoF motion solver and a mooring system analysis module to deal with the complex motion responses. All of these newly added modules make the existing solver ideal for simulating hydrodynamic problems for ships and floating structures in the naval architecture and ocean engineering industry.

Computational Model

The tidal turbine is supported by a catamaran hull for the floating tidal power generation device [6]. The whole structure is comprised of two identical demihulls separated by a given distance as shown below in Fig. 1. The fore and aft parts of the hull are symmetric. The structure is moored by four lines for position keeping as shown in Fig. 2. The elastic coefficient for all lines is selected as a constant as 28.23 g/mm while pretension is set to be 15 N.

Simulation has been performed in a model scale of 13.333 under regular incident wave conditions. The wave height is 0.06 m and wave length is the same as the hull length [6]. The Stokes first order deep water wave theory is adopted for wave generation. Surge, heave and pitch are free and the mooring system also works to prevent the structure from drifting away. Since the two demihulls are identical, only half of the structure is considered.

Results

The motion responses of the platform, namely surge, heave and pitch, are illustrated in Fig. 3. Surge response is constrained by the mooring lines. Otherwise, the structure will drift away with the wave. Heave response oscillates about -0.002 m rather than 0 m due to initial imbalance between the displacement and total mass. Pitch response, on the other hand, moves between 2 and -2 degrees.

* Corresponding author.
Email address: qing.xiao@strath.ac.uk

Tension force for the mooring lines is shown in Fig. 4. It is shown that the average tension for the upstream line #2 between 9 s and 15 s is 15.34 N, which is larger than 14.45 N for the downstream line #1. This is due to the fact that the structure tends to move towards the downstream region under the influence of incident waves.

Conclusions

In this paper, the hydrodynamics of a catamaran hull for a tidal turbine is investigated in waves, using a CFD solver developed in OpenFOAM. Motion and force responses are obtained and analysed, showing the ability of this solver in simulating hydrodynamic problems for floating structures. Following steps involve taking into consideration the effects of the tidal turbine, carrying out a comprehensive study under different working conditions and comparing numerical results with experimental data available.

References:

[1] Wikipedia. Tidal power. 9 Feb 2015. http://en.wikipedia.org/wiki/Tidal_power.
[2] Bluewater. BlueTEC: Bluewater's Tidal Energy Conversion platform. 9 Feb 2015. http://www.bluewater.com/products-technology/tidal-energy-conversion-tec/.
[3] Ltd S. T. P. Scotrenewables Tidal Turbine SR250. 9 Feb 2015. http://www.scotrenewables.com/technology-development/250kw-prototype/sr250-construction.
[4] OpenFOAM. The OpenFOAM website. 25 November 2014. http://www.openfoam.com/.
[5] Shen Z., Cao H., Ye H. *et al.* (2013). Development of CFD Solver for Ship and Ocean Engineering Flows. In: *8th International OpenFOAM Workshop*, Jeju, Korea.
[6] Ma Y., You S., Zhang L. *et al.* (2013). Tests for oscillation and wave response of a floating tidal power generation device. *Journal of Vibration and Shock.* **32** (2), 14-17.

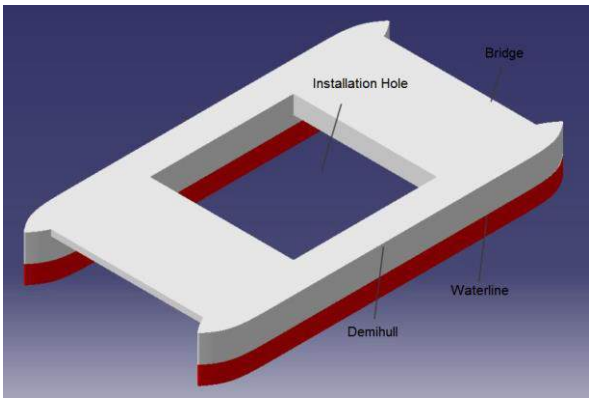

Fig. 1. Geometry of the catamaran hull

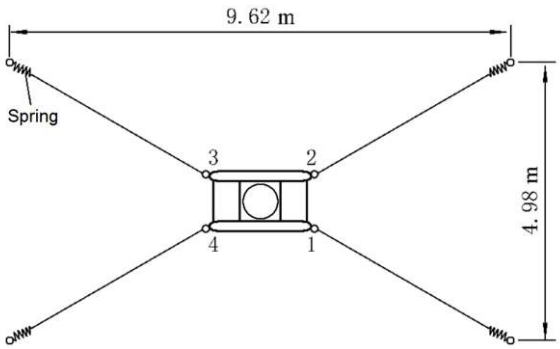

Fig. 2. Mooring system configuration

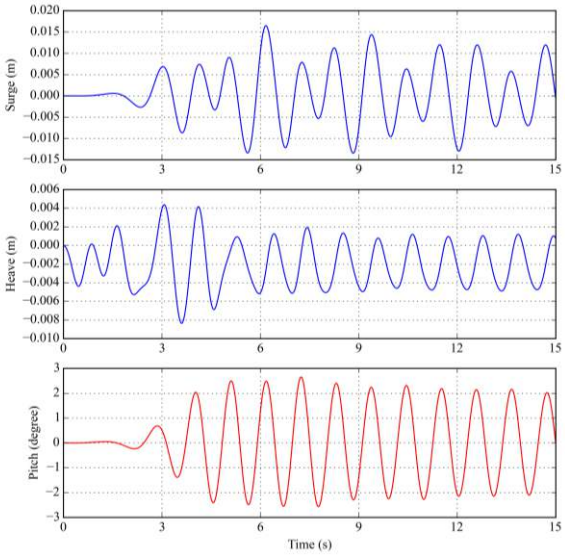

Fig. 3. Motion responses of the structure in waves

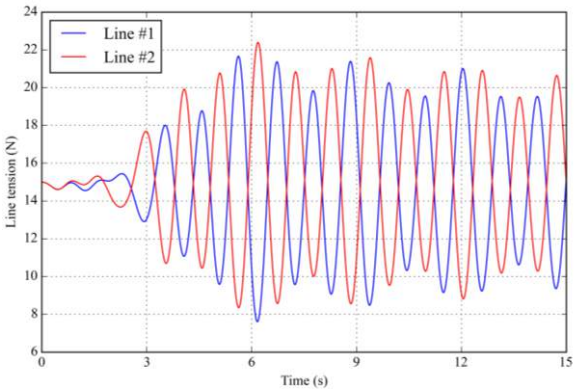

Fig. 4. Tension force for two lines

3D extraction of tidal energy from a ROMS model

Alice J. Goward Brown*, Simon P. Neill
School of Ocean Science, Bangor University, UK

Summary: Using a method developed by T.Roc et al., tidal energy extraction is implemented within a 3D ROMS (Regional Ocean Modelling System) model. This method applies actuator disk theory whereby each turbine is treated as a mid-water perturbation and accounts for both momentum and turbulent hydrodynamic effects. Here we examine the method of 3D tidal energy extraction within an idealised tidal channel to examine the potential hydrodynamic effects of energy extraction.

Introduction

Tidal stream energy devices generate power from fast flowing tidal streams. The designs of the devices are highly variable and thus will all influence the flow in different ways. The method for tidal energy extraction presented here is fundamentally based upon the actuator disk concept, where the loading of the turbine blades is uniformly distributed over a disk - acting as a discontinuity in pressure within the tidal flow (Figure 1(a)). Subsequently this method is most relevant for devices which follow the horizontal axis turbine design (Figure 1(b)) [1],[2]. The methodology behind the tidal energy extraction is described in great detail in [3] and has been shown to validate well against flume experiments which, until flow field data from around *in situ* tidal energy devices is available to validate models, gives us confidence in the method described. Here we use the aforementioned method to examine 3D energy extraction within an idealised channel with the future aim of investigating the hydrodynamical impact of tidal energy extraction within an area of high tidal flow [4], [5].

A. Overview of Energy Extraction Method

The tidal energy extraction technique used is a modification of an existing ocean circulation model, ROMS. ROMS is a 3-D, free-surface, terrain-following, hydrostatic primitive equation oceanic model [6]. The turbulence parameter used in the tidal extraction technique is the generic length scale (GLS) closure model. The vertical grid in ROMS is a terrain following sigma grid which adds a level of complexity within the turbine resolution.
Sensitivity experiments by [3] have come up with a rule of thumb for the spatial turbine resolution (Figure 1(c)). Readers are directed to consult [3] for a more detailed overview of the theoretical background behind the turbine implementation in the model but in brief, the method used accounts for both the momentum balance through the thrust force ~ Ft (Equation 1) and turbulence balance perturbations represented by turbulence correction terms, P_p; P_b; $P\varphi$. A term is added to each of the two k-φ generic length-scale turbulence closure model's equations to simulate reduced turbulence length scales ($P\varphi$) and additional production of wave turbulence due to the presence of the turbine (P_k) (Equations 2 and 3). It is worth noting that in this method the thrust coefficient (C_t) is calculated for an unconstrained flow and subsequently boundary/blockage effects are accounted for through the set of momentum and turbulence source terms [1], [7].

$$\overrightarrow{Ft} = \frac{1}{2}\rho A_d C_t(|u_\infty|u_\infty)\vec{n} \tag{1}$$

Where ρ is the water density, A_d is the actuator disk surface $Ct = 4a(1-a)$ the thrust coefficient, u_∞ the unperturbed flow velocity and $\vec{n}$ the unitary vector normal to the actuator disk.

$$P_k = C_1\frac{u^3}{\Delta x} - C_2\frac{u.k}{\Delta x} = P_p - P_d \tag{2}$$

$$P\varphi = C_3\frac{P^2}{\varepsilon} \tag{3}$$

Where k is the turbulent kinetic energy (TKE) per unit mass. P represents the production of TKE by shear, ε is TKE dissipation and C_1, C_2 and C_3 are given by [8], [9].

The ability to define individual turbines in x,y,z space will enable device scale applications and thus provide the means for array design to be examined on a regional scale.

* Corresponding author.
Email address: a.j.gowardbrown@hotmail.co.uk

Methods

For the purposes of this study we have created a channel comparable to that described in [4] with a width of 1km, a length 4km and an input water depth of 60m which decreases linearly to an exit depth of 59.6m. The channel has two no-slip closed (North and South) and two open (East and West) boundaries. A semi-diurnal M2 tide is applied at the open boundaries with Chapman and Flather boundary conditions. The turbulence closure scheme chosen was the k- ε scheme since it gave the lowest error values in a comparison study performed by [7] and the bottom roughness is representative of a turbulent channel flow regime with a value of 3×10^{-3} [6], [10].

In this initial test case the turbine itself was positioned in the centre of the channel mid-way in the water column and had a 20m diameter. The purpose for this study is to investigate the impact of turbines on channel hydrodynamics and to test a new method of tidal energy extraction modelling.

Acknowledgements:

I would like to thank my supervisor for his help and direction and Thomas Roc for his generous distribution of the turbine code. Thanks also goes to Fujitsu who in partnership with HPC wales are funding this PhD work without which none of the research would be achievable.

References:

[1] J. Whelan, M. Thomson, J. Graham, and J. Peiro, "Modelling of free surface proximity and wave induced velocities around a horizontal axis tidal stream turbine," in Proceedings of the 7th European Wave and Tidal Energy Conference, 2007.

[2] T. Burton, D. Sharpe, N. Jenkins, and E. Bossanyi, Wind energy handbook. John Wiley & Sons, 2001.

[3] T. Roc, D. C. Conley, and D. Greaves, "Methodology for tidal turbine representation in ocean circulation model," Renewable Energy, vol. 51, pp. 448–464, Mar. 2013. [Online]. Available: http://linkinghub.elsevier.com/retrieve/pii/S0960148112006106

[4] I. G. Bryden and S. J. Couch, "ME1marine energy extraction: tidal resource analysis," Renewable Energy, vol. 31, no. 2, pp. 133–139, Feb. 2006. [Online]. Available: http://linkinghub.elsevier.com/retrieve/pii/S096014810500220X

[5] S. P. Neill, J. R. Jordan, and S. J. Couch, "Impact of tidal energy converter (TEC) arrays on the dynamics of headland sandbanks," Renewable Energy, vol. 37, no. 1, pp. 387–397, Jan.2012. [Online]. Available: http://linkinghub.elsevier.com/retrieve/pii/S0960148111003855

[6] A. F. Shchepetkin and J. C. McWilliams, "The regional oceanic modelling system (roms): a split-explicit, free-surface, topography-following coordinate oceanic model," Ocean Modelling, vol. 9, no. 4, pp. 347–404,2005.

[7] T. Roc, D. Greaves, K. M. Thyng, and D. C. Conley, "Tidal turbine representation in an ocean circulation model: Towards realistic applications," Ocean Engineering, vol. 78, pp. 95–111, 2014.

[8] K. Rados, J. Prospathopoulos, N. Stefanatos, E. Politis, P. Chaviaropoulos, and Z. A, "Modelling of free surface proximity and wave induced velocities around a horizontal axis tidal stream turbine," in European Wind Energy Conference, 2009.

[9] P.-E. M. Rethore, N. N. Sørensen, A. Bechmann, and F. Zahle, "Study of the atmospheric wake turbulence of a cfd actuator disc model," in 2009 European Wind Energy Conference and Exhibition, 2009.

[10] S. P. Neill, M. R. Hashemi, and M. J. Lewis, "The role of tidal asymmetry in characterizing the tidal energy resource of orkney," Renewable Energy, vol. 68, p. 337350, 2014. [Online]. Available: http://www.sciencedirect.com/science/article/pii/S0960148114000099

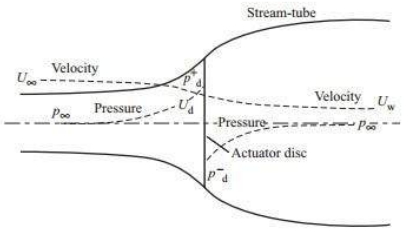

Figure 1(a) Actuator disk theory [2]

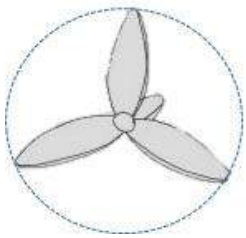

Figure 1(b) Example of a horizontal axis turbine, blue dashed circle indicates the swept area

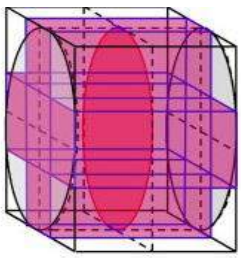

Figure 1(c) Numerical control-volume approximation with the exact smeared control volume (blue cylinder). The red disc represents the actuator disk [3]

Flexible Blades for Tidal Turbines

Ignazio Maria Viola*, Susan Tully, Jean-Baptiste Richon,
Abel Arredondo Galeana, Rowan Eveline Muir
Institute for Energy Systems, School of Engineering, University of Edinburgh, UK

Summary: The combination of highly turbulent flow and wave-induced currents within a tidal stream leads to continuous load variations on the blades of tidal turbines and limits their survivability and fatigue endurance. We propose the use of flexible turbine blades to decrease the amplitude of the load fluctuations and thus increase their durability. We developed a numerical model of a turbine blade; we show the extreme flow variations that it experiences and we show that a blade with a flexible trailing edge can result in reduced amplitude load fluctuations. Preliminary results of ongoing complementary experiments have confirmed the predicted trends.

Introduction

Recent reviews [1,2] show that flexible foils have been effectively exploited for energy harvesters, particularly for wind turbine blades [2]. Foils with flexible trailing edges can decrease the maximum load fluctuations and, if properly tuned, can also increase mean performance. For instance, oscillations of the trailing edge can allow negative drag on a plunging foil [3]. This is due to the positive interaction between the leading and trailing edge vortices [4]; an interaction that can be more easily controlled and exploited when the flow fluctuations are periodic and predictable. Therefore flexible blades have the potential to negate the negative impact of periodic wave-induced currents on the fatigue life of turbine blades and instead, turn them into an opportunity to improve endurance and performance.

Method

We developed a simple model of both a fixed and a rotating blade. The fixed blade model consists of a 2D blade section at a fixed depth below the mean water line experiencing turbulent current and wave-induced flow. Whilst the rotating blade model considers a 2D foil-section taken as the blade section at 3/4th of the blade span and accounts for the variable vertical position and angular velocity of the blade as it rotates. The loads on the blade and its deformation can be computed for a range of tidal flow speeds, amplitudes and wave frequencies. Waves are regular, propagate in line with the current and conform to the kinematics of small-amplitude deep water waves. The combination of tidal-stream current and wave-induced current leads to a variable incident flow speed and angle of attack. Loads are computed for a NACA 4415 foil, where the distribution of the pressure difference ΔC_p between the pressure and suction side of the foil is almost triangular, with a maximum at the leading edge and zero at the trailing edge of the foil. The maximum Δp is proportional to the angle of attack (AoA) and Δp is modelled as constant for $AoA < -10°$ and $AoA > 10°$. The foil is modelled as a cantilever beam subjected to a triangular load. Since the displacement of the trailing edge leads to a different AoA and in turn, to a different load, an iterative fluid-structure coupling is implemented.

Experiments on a 1:15th scale blade section are currently ongoing in the University of Edinburgh's flume in order to gather a detailed description of the flow field around the blade. The flume is 0.4 m wide and has a water depth of 0.4 m. Three extruded NACA 4415 blade sections, all with a rigid nose but different degrees of flexibility in the trailing edge, were 3D printed. The blades have a chord of 0.15 m and a span of 0.3 m (0.1 m lower than the flume width) and each blade is tested at a depth of 0.15 m below the static free surface. End plates parallel to the flume's side walls are used in order to hold the blade tips outside of the side-wall boundary layers. The end plates are connected to two single axis load cells which measure the lift and the drag respectively. PIV flow measurements are performed on the blade's symmetry plane while turbulence data are simultaneously recorded via LDV six chord lengths upstream of the blade. In this abstract we present preliminary results that were achieved with the most flexible tested blade whose specially-designed structure is equivalent to a blade with a rigid nose and, from 2/3rd of the chord, a flexible trailing edge with a Young's Modulus of $E = 5.6$ kPa. The blade was held at a static AoA of 5° in a current of $U_0 = 0.2$ m/s, in waves with an amplitude of 0.04 m and frequency of 1 Hz.

Rotating flexible blades will be tested on a 1:20th scale tidal turbine at Ocean University of China in April 2015. For these tests a 3D twisted and flexible blade was 3D printed with a rigid nose and, from 11/20th of the chord, a flexible trailing edge with $E = 0.2$ MPa. Hereby we present a numerical simulation of the tests with a current of $U_0 = 0.2$ m/s, a tip speed ratio of five and waves, travelling perpendicular to the rotor plane, with amplitude of 0.3 m and frequency of 0.5 Hz.

* Corresponding author. *Email address*: i.m.viola@viola.ac.uk

Results

Figs. 2-4 refer to the fixed blade simulations. Fig. 2 shows the resulting streamwise $(U+u)$ and vertical (v) velocity components and the combined flow speed (Tot) over a wave period. Fig. 3 shows the large variation of instantaneous AoA, which is almost certainly leading to a dynamic stall process. Since the load increases linearly with the AoA and with the square of the flow speed, only the combination of extreme AoA and high flow speed leads to a blade deflection. This is clearly show by Fig. 4 which shows the mean Δp divided by the reference dynamic pressure $(q_0 = 1/2\rho U_0^2)$, for both the flexible and a rigid blade. The flexible blade carries the same Δp as the rigid blade near the mean conditions, but admits lower load peaks. Preliminary experiments verified the computed trend. Fig. 5 shows the measured normal force coefficient over a wave period for both the flexible and rigid blade. Figs. 4-5 show similar trends despite the rough approximation in the definition of Δp. The smoother experimental trends compared to the numerical ones are possibly due to the large turbulence intensity in the flume $(T_u = 7\%)$ and insufficient endplate length stopping 2D flow conditions from being achieved. Current experiments are focused on flow measurements and results will be discussed in the oral presentation.

A rotating blade experiences a more complicated relative flow velocity. Fig. 6 shows the mean $\Delta p/q_0$ over two consecutive wave periods for a flexible and a rigid blade. It can be clearly seen that, even when blade rotation is accounted for, the blade flexibility is able to generate thrust and limit load peaks.

Conclusions

Preliminary results suggest that flexible blades can achieve similar mean forces to rigid blades but limit load peaks and therefore could be effectively exploited to enhance the durability of tidal turbines. Further research is necessary to understand the underlying vortex flow dynamics and thus enable the optimum design of blades.

Acknowledgements:

This work was supported by the EPSRC, grant number EP/M02038X/1

References:

[1] Xiao, Q., Zhu, Q. (2014). A review on flow energy harvesters based on flapping foils. *J. Fluid Struct.*, **46**, 174-191.
[3] Cleaver, D. J., Gursul, I., Calderon, D. E., Wang, Z. (2014). Thrust enhancement due to flexible trailing-edge of plunging foils. *J. Fluid Struct.*, **51**, 401-412.
[2] Lachenal, X., Daynes, S., Weaver, P. M. (2013). Review of morphing concepts and materials for wind turbine blade applications. *Wind Energy*, **16**, 283-307.
[4] Rival, D., Trangemeier, T., Tropea, C. (2009). The influence of airfoil kinematics on the formation of leading-edge vortices in bio-inspired flight. *Exp. Fluids*, **46**, 823-833.

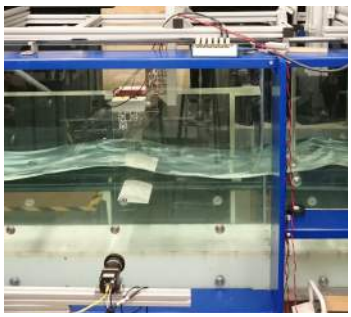

Fig. 1. Fixed blade exp. setup

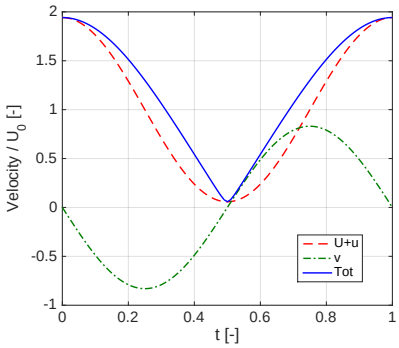

Fig. 2. Flow speed

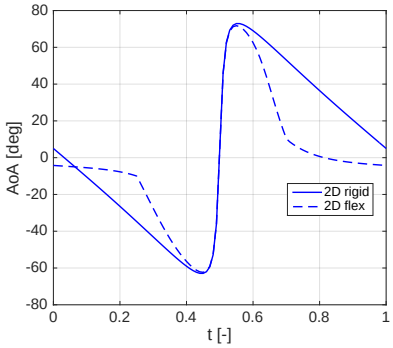

Fig. 3. Angle of attack

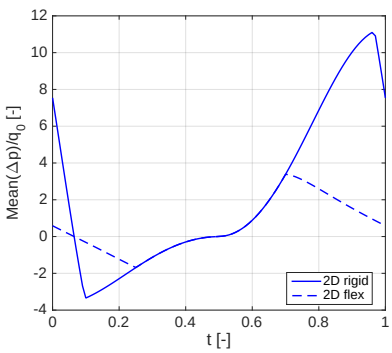

Fig. 4. Computed Δp

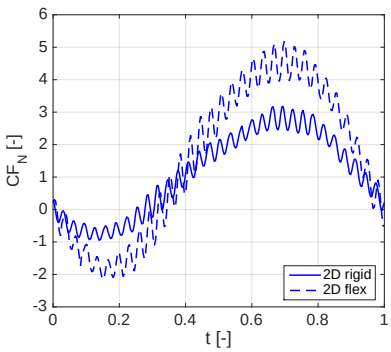

Fig. 5. Measured CF_N

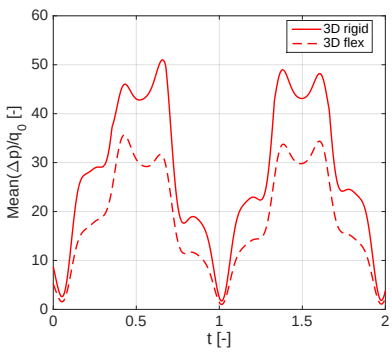

Fig. 6 Computed Δp rotating blade

A Blade Design Method of the Horizontal Axis Tidal Current Turbine

Xiaohang Wang*, Qihu Sheng, Ke Sun
College of Shipbuilding Engineering, Harbin Engineering University, Harbin, China

Summary: A contour map method is developed to design the blade of a horizontal axis tidal current turbine based on BEM (Blade Element Method). When a blade element profile and the local tip speed ratio (TSR) of a tidal turbine's blade are defined, the power of the element provided to the turbine shaft is determined by the chord length and attack angle. Our design method shows the power coefficient contour of each element variable with chord length and attack angle based on the BEM. Targeting the best efficiency and other constraints, the design parameters of the blade element can be searched in the contour map directly. This method can make the blade design process more efficient and the assessment of the rotor's hydrodynamic performance more accurate.

Introduction

For tidal current turbines, we usually pay more attention to achieving the maximum efficiency of energy capture. In traditional blade design methods, the energy utilization efficiency of the rotor is the primary optimized objective. However, blade design should consider many different factors due to the turbine operating in complex ocean conditions. The contour map method developed based on BEM could satisfy multi-criteria optimisation such as the hydrodynamic load distribution, the ability to self-start and the choice of processing technique etc.

Methods

The contour map method has different initial values, sequence of iteration solution, hypotheses and convergence criteria compared to the traditional BEM method [1-3]. For the initial values, the range of blade chord length and attack angle can be obtained with empirical formulas. Once the blade element's chord length and attack angle are confirmed, the flow angle and induced factors can be obtained with two relation equations from BEM theory and the velocity triangle by iterative calculation. The relationship between power coefficient (C_p) and geometric parameters (such as the chord length and the attack angle) is thus established as a contour map (see Figure 1). Compared with the traditional BEM method [4], the blade elements' drag can be considered through different initial parameters and iterative sequence. Although solving the problem difficult, the numerical solution can be obtained quickly.

If a 2% reduction of C_p can be accepted as a constraint, then the chord length and twist angle can be chosen within a range, as shown in Figure 2 and Figure 3. Model-1 is the rotor with blades designed using the contour map method with single optimal objective of maximum C_p. Model-2 is carried out using the C_p contour map of Model-1with multi-criteria constraints. The design parameters are shown in Table 1.

Tab.1The basic design parameters of blade model

Model	Blade Numbers	Element profile	*TSR*	Diameter[m]	Optimization conditions	Maximum C_p
Model-1	3	FFAW3211	5.5	1.0	Single optimization Maximum C_p	45%
Model-2	3	FFAW3211	5.5	1.0	Multi-factorial optimization including C_p	43%

In order to make the *TSR* range for power output wider, attack angles of each blade element are set as variables, but this reduces the maximum C_p and significantly affects the chord and twist angle distribution along the blade radius. Generally, the larger lift value is assigned to the blade root, which can make the root's chord length reduce. The distribution of the attack angle α_r can be given as a function of power in order to obtain an approximate linear distribution of chord length as shown in Equations 1-3.

$$\alpha_r = \alpha_2 r_c^{\,B} \tag{1}$$

$$B = \ln(\alpha_1 / \alpha_2) / \ln(r_{root}) \tag{2}$$

Where, r_c is the relative position to rotor radius; r_{root} is the relative position of the cross-section nearest to the root. α_1 is the attack angle corresponding 95% of the maximum lift value; and α_2 is defined as follows:

$$\alpha_2 = 2\alpha_{Cl/Cd\max} - \alpha_1 \tag{3}$$

*Corresponding author.
Email address: kikiwxh@163.com

Results

From CFD results in Figure 4, the peak C_p of Model-1is very high at the design point *TSR*=5.5 using the single objective optimal design. However, the total curve has a smaller operating *TSR* range for high efficiency, which is not conducive to the stability of power output. At the same time, in the lower *TSR* range, the C_p decreases so fast that the rotor will have difficult self-starting. For Model-2, the maximum C_p is slightly lower than that of Model-1 after the multi-criteria optimization, but the C_p in the low *TSR* range is improved greatly, which will more easily achieve self-starting. The total curve becomes smooth and greatly widened near the peak value, indicating that the contour map method is feasible and reasonable.

Conclusions

The contour map method combines blade element hydrodynamic performance more accurately than traditional BEM theories. This method has more degrees of freedom of optimal objectives, for example adding other constraints besides the maximum C_p. The best advantage of contour map method is to establish the relationship between the performance and the control parameters of the blade intuitively, so the rotor's C_p at various *TSR* can be precisely controlled. This method can make the blade design and optimization process more efficient because it no longer relies on the blind parameter test.

References:

[1] G. Ingram. *Wind turbine blade analysis using the blade element momentum method*. Durham University, 2011

[2] P. Giguère and M.S. Selig. *Design of a tapered and twisted blade for the NREL combined experiment rotor*. NREL/SR-500-2617, April 1999

[3] J.N. Goundar and M.R. Ahmed. *Design of a horizontal axis tidal current turbine*. Applied Energy, 111(2013), 161-174

[4] B.G. Wu, X.M. Zhang and J.M. Chen. *Design of high-efficient and universally applicable blades of tidal stream turbine*, Energy, 60(2013), 187-194

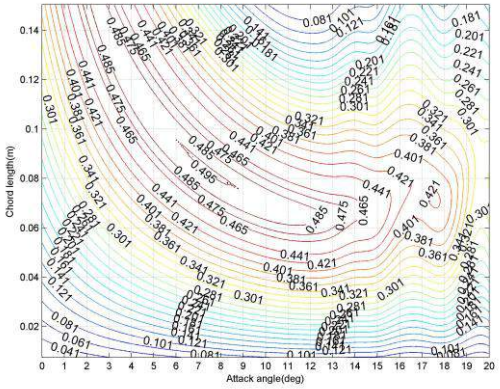

Fig.1 C_p contour of the first blade element

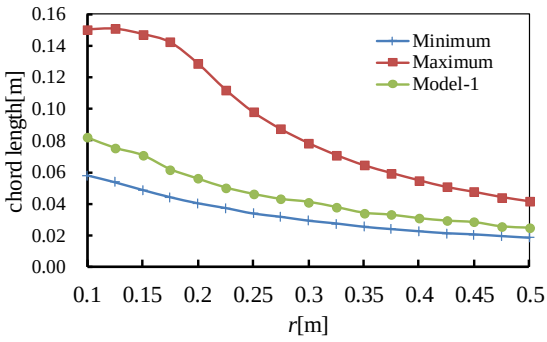

Fig.2 Chord length range of the blade element

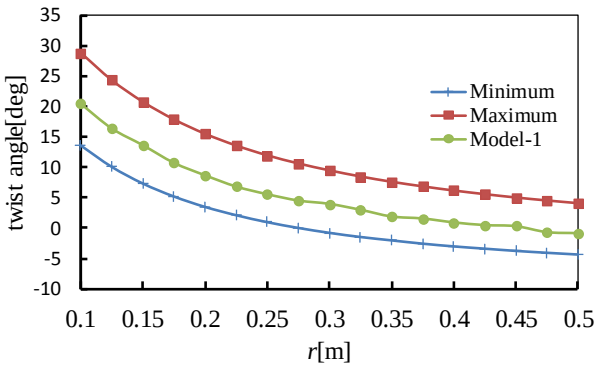

Fig.3 Twist angle range of the blade element

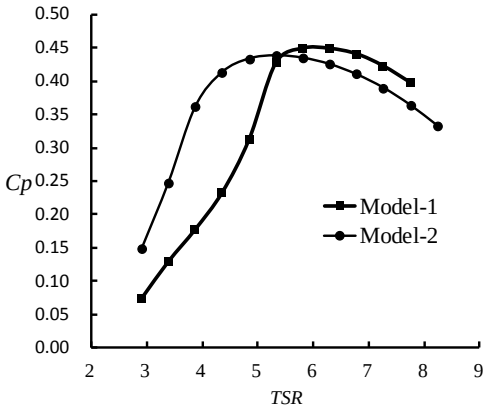

Fig.4 Power coefficient comparison with single and multi-criteria optimization

Power and Thrust Behaviour in a Porous Disc Fence Array Experiment

Susannah Cooke*, Richard H. J. Willden, Byron W. Byrne
Department of Engineering Science, University of Oxford, UK

Summary: A set of experiments were carried out using porous discs to simulate a fence array of tidal turbines. Measuring disc thrust and flow behaviour behind the discs, the behaviour of 'inferred power' was considered across a range of disc porosities and inter-disc spacings. The inferred power coefficient behaviour of the fence array showed similar behaviour to that predicted by 'partial fence' theory.

Introduction

An analytical model for the behaviour of a partial fence array of tidal turbines has been previously developed by Nishino and Willden [1], showing that greater power is available if a fence of turbines within a tidal channel is carefully arranged to exploit the effects of local blockage. This behaviour has been further investigated in computational analysis [2], but no experimental work had previously been undertaken to fully investigate the assumptions and results of this model. A previous small scoping experiment using 5 porous discs had previously considered thrust behaviour only [3], and a broader experiment involving eight porous discs was therefore designed to allow thrust and flow behaviour to be measured around such a fence array.

Experimental Arrangement

A partial fence array of eight porous discs was investigated. Sets of eight discs were manufactured at different porosities from $\Theta = 0.3$ to $\Theta = 0.6$, where Θ is the open area ratio. A first approximation of the relationship between Θ and the pressure resistance coefficient, κ, can be used as defined in [4] to show that these open area ratios are equivalent to disc resistance coefficients of $\kappa = 1.8$ to $\kappa = 10$. Each fence array tested was made up of eight discs of the same porosity, representing an array of identical turbines.

Inter-disc spacing, s, was varied from $0.1d$ up to $0.4d$, where d is the disc diameter of 270mm. This resulted in array widths varying from 2.38m up to 3.02m, maintaining a sufficient array bypass flow width of approximately 1m on each side. Multiple disc porosities were tested at each spacing to fully investigate the parameter space.

Testing was carried out in the 5m wide flume at the University of Manchester, with discs placed at mid-depth within a still water depth of 0.45m, as shown in Figure 1, resulting in a global blockage ratio of 0.2. Disc thrust was measured individually through strain gauges affixed to the towers, and flow speeds behind the array were measured using a Nortek Vectrino+ Acoustic Doppler Velocimeter (ADV). Flow values were sampled at 200Hz for at least 60 seconds to ensure robust measurements, based on previous work done in the same facility [3].

Disc arrays were mounted 6.1m downstream of the flume inlet porous weir. Flow measurements, downstream of the disc plane, were taken only at the centreline of the array and taken as representative mean flow speeds. The average centreline freestream flow speed through the working area was found to be 0.466m/s, which has been taken as the undisturbed channel flow speed for all power and thrust coefficient calculations.

An 'inferred power' was calculated following the assumption for an actuator disc that power extracted from the flow (comprising both useful device power and also power lost to wake mixing) is equal to the disc thrust multiplied by the average flow speed through the disc. With real porous discs rather than actuator discs, however, it is not possible to directly measure the flow speed through the disc. The closest point downstream of the discs at which flow speeds could be accurately measured, without introducing reflections and noise into the

Figure 1 – Experimental Set-Up

* Corresponding author.
Email address: susannah.cooke@eng.ox.ac.uk

ADV signal, was 0.3*d* (81mm). This speed will always be lower than the true flow speed through the disc plane, since flow continues to decelerate behind a device; however, it will vary in line with this true disc flow speed. It was therefore decided to calculate an inferred power from:

$$P_{inferred} = T_{disc} U_{disc,0.3d} \quad (1)$$

for each disc. The average flow speed at 0.3*d* behind each disc, used for this calculation, was found using a weighted sum of the flow measurements taken by the ADV probe 0.3*d* downstream of each disc.

Results

In total, fifteen configurations of inter-disc spacing and disc porosity were tested. Twelve of these focused on the area of highest thrust, with disc porosities between 0.3 and 0.4, while an additional three tests were carried out on higher porosities (i.e. lower disc thrust) at an intermediate spacing of $s/d = 0.2$.

An inferred global power coefficient C_{PG} was found as shown in Figure 2a for the 12 high thrust (low disc porosity) cases. It should be noted that the contours here are extrapolations between the individual 12 cases included to show the shape of the trends more clearly.

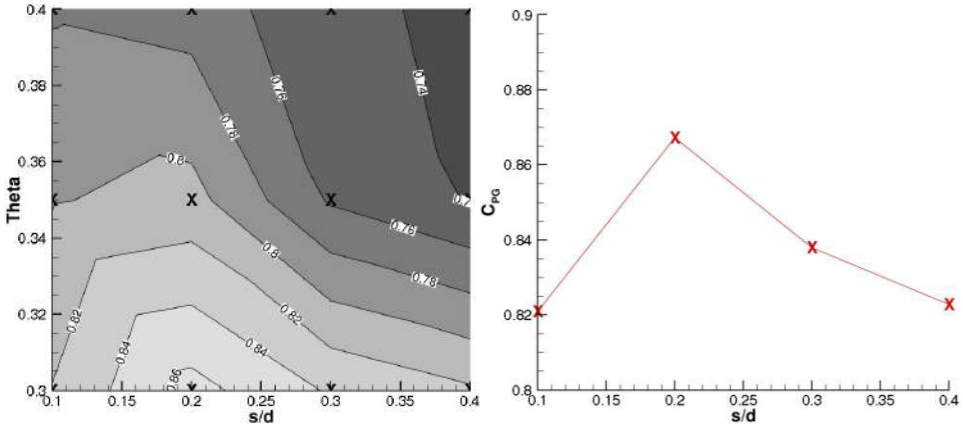

Figure 2: Plots of inferred C_{PG} variation with spacing and disc porosity: a) extrapolated contours from the 12 configurations measured (each marked with **X**), b) values of C_{PG} for the highest thrust discs, $\Theta = 0.3$.

It can be seen that, when thrust and power behaviour are compared to the analytical model of Nishino and Willden [1], similar behaviour is seen to that expected from theory, namely an available power peak at high thrust and close spacing. Thrust is seen to increase as disc porosity reduces, i.e. as individual disc resistance increases. Power is also seen to increase with reducing disc porosity, but also drops off when too much thrust is applied in too closely spaced an array. This is shown most clearly in the $\Theta = 0.3$ plot in Figure 2b, where C_{PG} is lower at $s/d = 0.1$ than it is at any higher spacing, and a clear power peak is seen at $s/d = 0.2$.

Conclusions

These experiments using porous discs have shown fundamental trends of available power behaviour in tidal turbine arrays to be similar to those expected from partial fence theory. A peak in 'inferred power' is seen for a high thrust, closely spaced array, however a steep drop-off in power is observed if spacing is further reduced.

Acknowledgements:

The authors would like to acknowledge the support of the SuperGen UK Centre for Marine Energy Research (UKCMER) and the Oxford Martin School, which have funded this work. Some equipment employed at UoM was partly developed during the PerAWAT project, commissioned by the ETI. The authors would also like to thank their colleagues at Manchester for assistance with this work, in particular Tim Stallard and Alex Olczak.

References:

[1] Nishino, T., Willden, R. H. J. (2012). The efficiency of an array of tidal turbines partially blocking a wide channel. *J. Fluid Mech.* **708**, 596–606.

[2] Nishino, T., Willden, R. H. J. (2013). Two-scale dynamics of flow past a partial cross-stream array of tidal turbines. *J. Fluid Mech.* **730** , 220–244.

[3] Cooke, S. C., Willden, R. H. J., Byrne, B. W., Stallard, T., Feng, T. (2014). An experimental investigation of blockage in a short fence array of tidal turbines. In: *Proc. 1st RENEW conf, 2014.* Lisbon, Portugal

[4] Taylor, G. I. (1944). Air resistance of a flat plate of very porous material. *ARC Reports and Memoranda*

Hydrodynamic and Ecological Impacts of Turbine Structures: Insights from the FLOWBEC Platform

Shaun Fraser*, Vladimir Nikora
School of Engineering, University of Aberdeen, AB24 3UE, UK

Benjamin J. Williamson, James Waggitt, Beth E. Scott
Institute of Biological and Environmental Sciences (IBES), University of Aberdeen, AB24 2TZ, UK

Summary: This paper describes insights from a novel experimental approach to collecting field data in tidal test sites. Deployments of the FLOWBEC platform around tidal turbine structures gives insights into the impacts of marine energy extraction. Analysis of velocity and backscatter data reveal key hydrodynamic effects and indicate important ecological implications of turbine structure presence.

Introduction

The hydrodynamic and ecological effects of tidal energy extraction are still poorly understood, and there is still a significant lack of field data in tidal sites and around test devices. Despite much work published on simulations and scale experiments for hydrodynamic characterisation of tidal sites and analysis of turbine wakes, published accounts of field work in tidal channels and around full-scale devices are limited. Similarly, quantitative assessment of bird, fish, and marine mammal behaviour in tidal sites is rare. With very little field data around real tidal turbine structures, the ecological impacts of energy extraction remain highly uncertain.

The NERC/Defra collaboration FLOWBEC-4D (Flow, Water column & Benthic Ecology 4D) is addressing this lack of knowledge with the development and deployment of an innovative self-contained multi-instrument platform [1]. Five 2-week deployments were completed in 2012 and 2013 at wave and tidal energy sites (Figure 1), both in the presence and absence of renewable energy structures at the European Marine Energy Centre (EMEC), Orkney, UK [2].

Methods

The FLOWBEC sonar platform combines a number of instruments to record information over a range of physical and multi-trophic levels at a resolution of several measurements per second (Figure 2). High resolution acoustic backscatter data comes from an upward-facing multifrequency Simrad EK60 echosounder (38, 120 and 200 kHz) synchronised with an upward-facing Imagenex Delta T multibeam sonar (260 kHz) aligned with the tidal flow. A Sontek ADV is used for high frequency 3D local current and turbulence measurements (sampling volume approx. 0.85m above seabed). Novel hydrodynamic analysis methods and algorithms for noise removal and detection of biological targets have been developed, revealing key physical characteristics of the study sites and the behaviour and interactions of biological targets in the area. Data recorded 20m from a turbine gravity base structure (approx. 10m high including central piling) and subsequent control deployment (adjacent but out of the structure wake) at the Fall of Warness tidal test site allows preliminary analysis of device impacts.

Figure 1. Deployment of the self-contained FLOWBEC platform at EMEC.

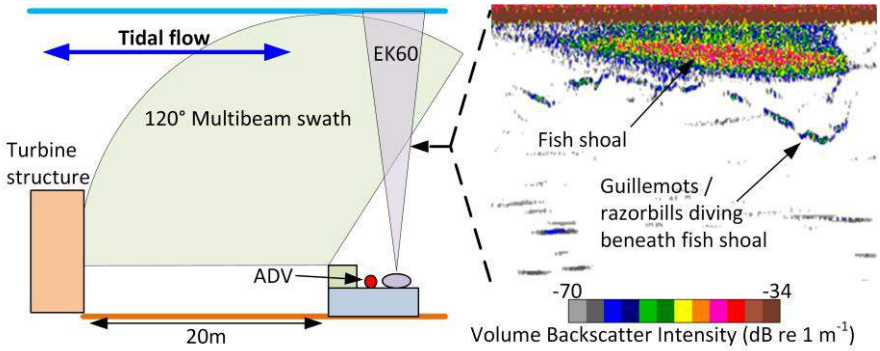

Figure 2. Platform setup and instrument arrangement on the seabed in the presence of a turbine structure. On the right shows a 5-minute excerpt of echosounder data demonstrating diving seabirds feeding on a fish shoal.

* Corresponding author.
Email address: s.fraser@abdn.ac.uk

Results

Comparison of data collected in the presence of tidal turbine structures with control data is demonstrated with some key parameters plotted below in Figure 3 using data selected over similar meteorological and tidal conditions. Although some natural variation may be present between deployments, preliminary results indicate important consequences of turbine structure presence. A clear reduction in peak mean velocity and much higher turbulence energy is apparent downstream of the turbine structure when compared with the control. The absence of any significant ADV velocity cross-correlation only during the period where the structure is upstream is consistent with the disruption of large scale coherent motions in the wake of the structure. Early results indicate these hydrodynamic impacts affect fish shoal distributions and behaviour; fish shoals are closer to the seabed, with less variance in height when in the wake of the turbine structure, compared to the control site.

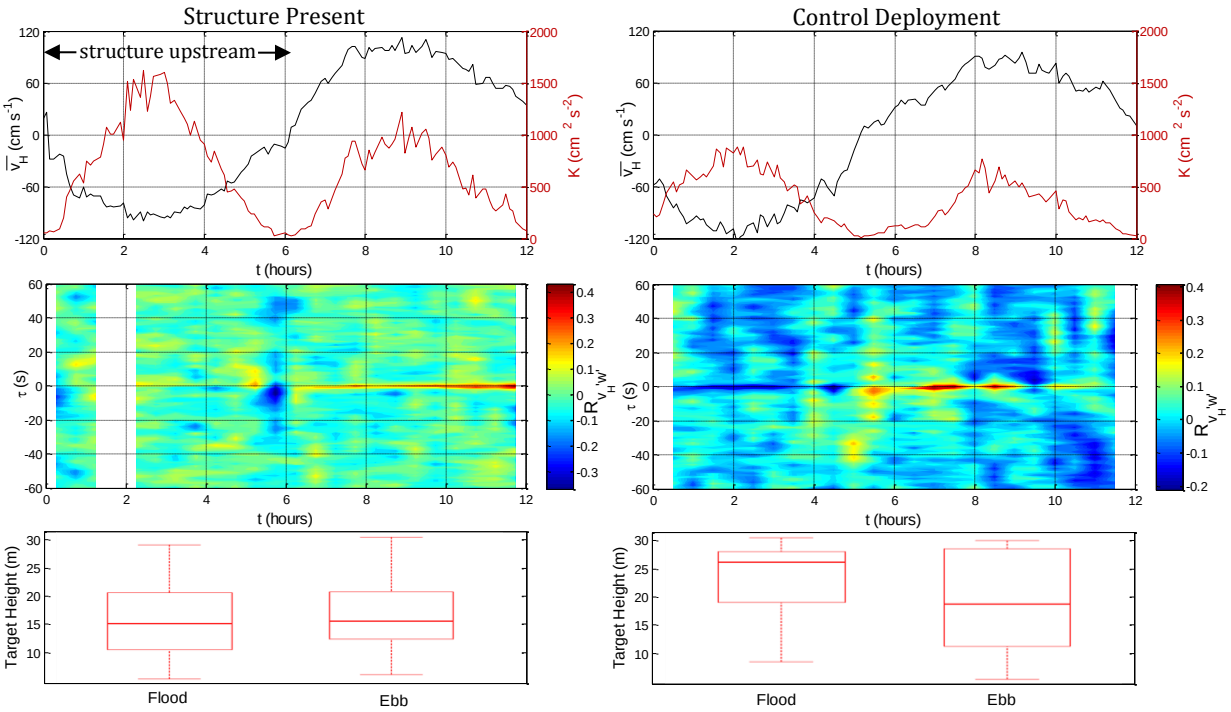

Figure 3. All figures on the left are in the presence of the turbine structure, with the instrument platform downstream for approximately first 6 hours. Figures on the right are from the control deployment. Top: mean horizontal velocity $\overline{v_h}$ and turbulence energy K computed over 5 minute sections from ADV data; negative $\overline{v_h}$ corresponds to flood measurements and positive $\overline{v_h}$ corresponds to ebb. Middle: cross-correlation function through time for the fluctuating horizontal velocity $v_H{}'$ and vertical velocity w' where τ is the time lag. Bottom: descriptive statistics of fish shoal distributions, target height is distance to detected shoal from the platform.

Conclusions

The FLOWEC project and platform contributes to an understanding of the hydrodynamic and ecological significance of the impacts of marine renewable devices in tidal sites. Novel processing and analysis procedures for velocity and backscatter data have been developed, and preliminary results of field data indicate important hydrodynamic effects of structure presence and behavioural changes of marine species. On-going analysis aims to inform quantitative appraisal of the environmental impacts of marine energy extraction on a wider scale.

References:

[1] Williamson, B.J., Blondel, Ph., Armstrong, E., Bell, P.S., Hall, C., Waggitt, J.J., Scott, B.E., 2015. A Self-Contained Subsea Platform for Acoustic Monitoring of the Environment around Marine Renewable Energy Devices – Field Deployments at Wave and Tidal Energy Sites in Orkney, Scotland. Oceanic Engineering, IEEE Journal of (in press).

[2] Williamson, B. J., Scott, B. E., Waggitt, J. J., Hall, C., Armstrong, E., Blondel, P., & Bell, P. S. (2014, September). Field deployments of a self-contained subsea platform for acoustic monitoring of the environment around marine renewable energy structures. IEEE Oceans

Field characterisation of currents and near surface eddies in the Pentland Firth

Jonathan Hardwick*, Ian Ashton, Lars Johanning
Renewable Energy, University of Exeter, UK

Summary: This study reports on ADCP field measurements in the Inner Sound of the Pentland Firth. The ADCP deployment was undertaken with the aim of identifying the currents likely to be experienced by a vessel installing or operating on tidal stream turbines. Both mean flow and turbulence metrics are investigated. Of particular interest is the difference in turbulence characteristics between ebb and flood tidal periods. The turbulence intensity is calculated and was found to be greater during the ebb tides. Auto-correlation of the data is analysed to enable the calculation of the length scale of the turbulence. This study was done as part of a TSB funded consortium facilitating the design of a new high flow installation vessel.

Introduction

A major obstacle in the development of large scale tidal energy arrays is the cost of installation and subsequent routine maintenance checks. Currently, this is done using vessels from the offshore wind and oil and gas sectors which are expensive and not tailored for tidal energy installations. The design of new deployment vessels that are able to operate continuously in an energetic tidal race will be a key factor in driving the installation down to commercially viable levels. It will be essential for such vessels to hold station and heading at small offset, which requires equipping these vessels with sophisticated dynamic positioning systems. A major operational challenge however is negotiating the near surface eddies, which can be strong enough to destabilise a vessel. The findings of this study will go towards providing an assessment towards design optimisation of cost effective installation vessels.

Methods

This study thus focuses on understanding the characteristics of near surface eddies using field measurements. To achieve this, an ADCP was deployed in the energetic tidal site of Pentland Firth, Scotland. A 600 kHz 4-beam ADCP has been configured to sample continuously at 2Hz to measure current particulate velocities at a vertical bin resolution of 1m, the ADCPs were also measuring wave elevation and direction.

Current data from the bottom-mounted, upward looking ADCP is analysed to investigate the characteristics of the mean and turbulent current flow, focusing in particular on the near surface eddies. The turbulence intensity is calculated and periods of high turbulence are examined in detail. The autocorrelation of turbulent fluctuations was analysed to determine the spatial variation in time scales of turbulent eddies near the surface and their affect to station keeping of installation vessels.

Results

Mean flow

Current speeds of up to 5 ms^{-1} were experienced throughout the deployment with greater velocities measured during the flood. The current does not flow in and out at opposite compass points (figure 1), the flow follows a path related to the local geography and bathymetry at the site.

Turbulence

One of the main problems with using ADCP measurements to calculate turbulence measurements is that at the top of the water column the ADCP beam spread is sufficiently large (12m at the surface) that smaller eddies and surges cannot be resolved. This study however is interested in turbulence that may cause an installation vessel to alter position, small eddies will not have a significant effect on the vessels position and the ADCP measurements can be used to investigate the turbulence metrics of the lager structures.

The turbulence intensity was calculated throughout the deployment [1] and was found that the value was larger on the ebb that the flood at 17% and 13% respectively (figure 2), slightly larger than other tidal sites[2], the intensity of turbulence was considerably higher at slower tidal speeds. Close investigations of periods of high turbulence showed that at certain periods when when wave and tide were in the same direction, the fluctuations

* Corresponding author.
Email address: j.p.hardwick@exeter.ac.uk

were dominated by orbital motions whereas when the waves and tides were opposed the turbulence was much more random.
The length scales of the turbulence were calculated by analysing the auto-correlation of the turbulent fluctuations[3], it was found that these length scales varied considerably throughout the deployment however there was a correlation with the current speed with larger length scales corresponding to faster tides. Eddies of scale within the range to effect the installation vessel (50-60m) were measured at current speeds above 2.5ms^{-1} and could be of sufficient force to destabise a vessel attempting to maintain DP.

Conclusions

The flow conditions were found exhibit large differences between ebb and flood flow patterns. The current direction was found to be non-symmetrical, the location of the deployments close to the island of Stroma would likely explain the current direction as the tides move through the Inner Sound past the island. Turbulence data was calculated from the ADCP, the spatial dimensions of turbulent eddies could not be directly calculated however statistical calculations were done to acquire values for the turbulence intensity, Reynolds stresses and the length scales of the eddies. For a future study it would be interesting to investigate the structure of eddies by deploying multiple measurement devices over a significant area. The data was used in the modelling and tank testing of the DP system for the installer. This study was undertaken as part of the high flow (HF4) TSB project led by Mojo Maritime.

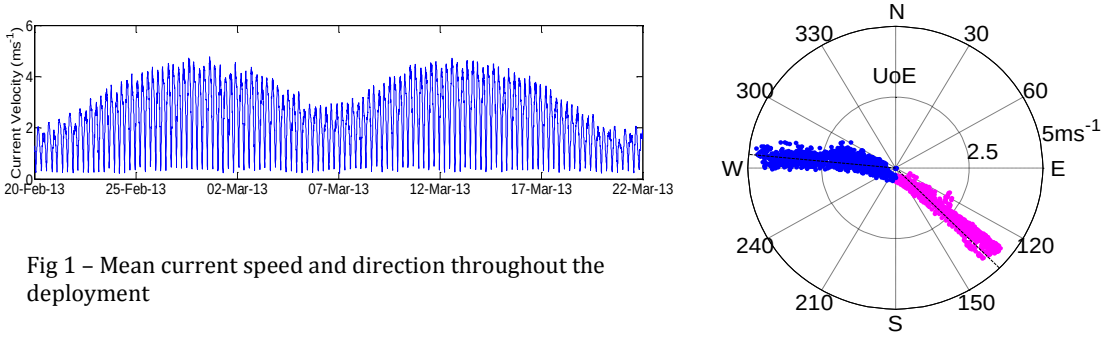

Fig 1 – Mean current speed and direction throughout the deployment

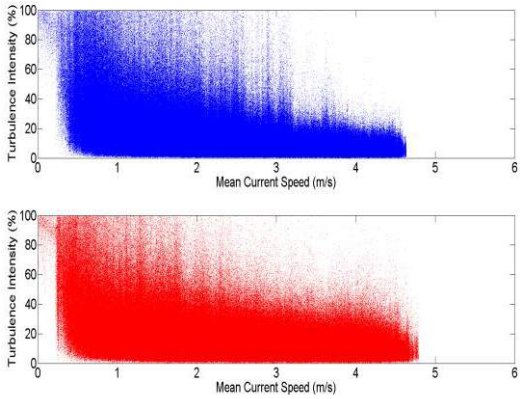

Figure 2 – Turbulence intensity during flood (top) and ebb (bottom) tides

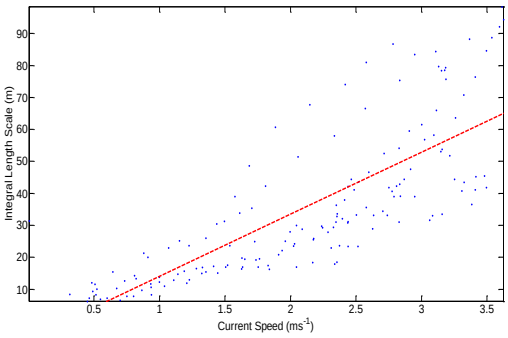

Figure 3 –Relationship between length scale and current speed

References:

[1] J. Thompson, B. Polagye, M. Richmond, V. Durgash, "Quantifying Turbulence for Tidal Power Applications" OCEANS 2010, 1-8
[2] I. A. Milne, R. Sharma, R. G. J. Flay, and S. Bickerton, "Characteristics of the turbulence in the flow at a tidal stream power site", *Phil. Trans. R. Soc. A*., vol. 371, pp.1-14, January 2013.
[3] M. T. Stacey, S. G. Monismith, and J. R. Burau, "Measurements of Reynolds stress profiles in unstratified tidal flow", *Journal of Geophysical Research*., vol. 104, pp. 10,933-10,949, May 1999.

Traditional turbulence methods and novel visualisation techniques for coastal flow model in order to deploy tidal stream turbines

I. Masters*, E. Zangiabadi, M. Edmunds, A. J. Williams and T. N. Croft
Marine Energy Research Group, Swansea University
Singleton Park, Swansea, UK
http://www.swansea.ac.uk/engineering/marine-energy/

Summary: Knowing the characteristics of the current is necessary in order to estimate the energy a TST can extract from a site. These characteristics are strongly influenced by the topography of the seabed. For a potential TST deployment site the bathymetry is surveyed using an echosounder and the resulting data is used in the development of the geometric model. The steady state k-ε and transient Large Eddy Simulation (LES) turbulence methods are employed. The results of all cases are compared with the flow data transect gathered by Acoustic Doppler Current Profiler (ADCP). Despite some simplifications in the model, the results show a relatively good agreement with the real site data.

Introduction

Marine and estuarine environments are characterised by roughness and irregularity in topography and three-dimensional (3D) turbulent flows, which can hugely affect the performance of Tidal Stream Turbine (TST) and should be investigated carefully [1]. Commercial codes like DELFT3D, MIKE3, etc. only provide information about the general properties of the flow and steady state turbulence. In this research both steady state and transient turbulence models are employed to model the turbulence in the coastal regions. Using time dependent solutions resolves the instantaneous properties of the flow but have the disadvantage of having a greater computational cost. The turbulence models are used to simulate flow over a rigid surface with consideration of the seabed geometry and without considering any vegetation and sediment transport.

Methods

One of the most commonly used RANS turbulence models is the standard k-ε turbulence model. Due to its nature, the k-ε method is not able to provide sufficient details on the formation of eddies and vortices.
To resolve the transient small scale turbulences of the flow Large Eddy Simulation (LES) is used. Using LES allows one to solve explicitly the large eddies by using a filtered approach of Navier-Stokes equation in which the filter is the grid size and implicitly account for the small eddies by using a subgrid-scale model (SGS model). The stream surface visualisation method employed has important inherent characteristics that can enhance the visual perception of complex flow structures [2]. Lighting and shading reinforce the perception of shape and depth, images or textures can be mapped to the surface primitives providing additional visual information, colour and transparency can be used to convey additional data attributes. Surfaces in general are able to not only capture the features within the flow, but can reduce the visual clutter when compared to using glyphs or streamlines [3]. A stream surface is the integration of a one dimensional curve through 3D steady flow. The resulting surface is everywhere tangent to the local flow [2]. The use of these surfaces revealed a complex eddy close to the outlet of the domain (Figure 1a).

Results

The selected bathymetry covers an area of about 1800 m length and 800 m width. It contains two pinnacles; the largest of these, Horse Rock, is surface piercing at low tide and is observed to shed vortices. Two different coarse (3.7 M) and a fine (36.2M) element grids are created and the same geometry is used to run the simulation for both the k-ε and LES turbulence models using a standard finite volume. ANSYS FLUENT® is used to perform all the simulations. The inlet velocity for the *k-ε* case is set to be 1.5 m/s and the turbulent intensity of 20 % along with the turbulent viscosity ratio of 100 were chosen. For the transient flow problem, the Large Eddy Simulation with Smagorinsky-Lilly subgrid-scale turbulence method is selected. Again the same inlet velocity as for the k-ε model has been chosen for the flow and the Vortex Method is used to create random fluctuation at the

* Corresponding author:
Email address: i.masters@swansea.ac.uk

inlet. For the bed boundary condition a no slip wall with roughness height (k_s) of 5.4 meters with roughness constant of 0.9 is selected.
Velocity values are extracted at 775m from the inlet (a location for which boat data is available) across the channel at the depth of -10 (15 meters below the surface) and the results then compared with the boat data (Fig 1b). The boat data is unsmoothed instantaneous ADCP data from a single transect. Having an averaged velocity would reduce the noise seen in the boat data but there was lack of survey data. Formation of at least one eddy behind the Horse rock was also observed. The two bodies of water coming from each side of the Rock are circling around the generated eddy before joining each other again further downstream. In Figure 1c it can be seen that the eddy is very flat. It starts its movement upward but then it seems that because of the fast water flowing overhead, it is crushed. The shear profile for the two models is given in Fig 1d, however there is a lot of spatial variability given the rapidly changing topography.

Conclusions

It has been understood that the k-ε method can predict the flow pattern with relatively good accuracy near the main features of the domain which are Horse Rock and the deep valley towards the end of the domain. The LES model has the ability to simulate some important flow patterns because of the bathymetry (i.e. formation of eddies). The results also show that it is necessary to customise the bed roughness parameters in a way that can compensate for the effects of simplifying the bathymetry and sub grid scale features. It is also observed that high frequency turbulence is smoothed out in the results shown in Figure 1a and 1c. Reynolds number calculations show that the element length should be reduced and the total mesh increased to approx. 140M elements to be able to observe this complexity.

Acknowledgements:

This work was undertaken as part of the Low Carbon Research Institute Marine Consortium (www.lcri.org.uk). The authors are grateful for the guidance, support and resources of the Marine Energy Task Group for Wales and High Performance Computing Wales (HPCW).

References:

[1] S. Kang, I. Borazjani, et al., *Numerical simulation of 3D flow past a real-life marine hydrokinetic turbine.* Advances in Water Resources, 2012. **39**(0): p. 33-43.
[2] M. Edmunds, R.S. Laramee, et al., *Surface-based flow visualization.* Computers & Graphics, 2012a. **36**(8): p. 974-990.
[3] M. Edmunds, R.S. Laramee, et al., *Automatic Stream Surface Seeding: A Feature Centered Approach.* Comp. Graph. Forum, 2012c. **31**(3.2): p. 1095-1104.

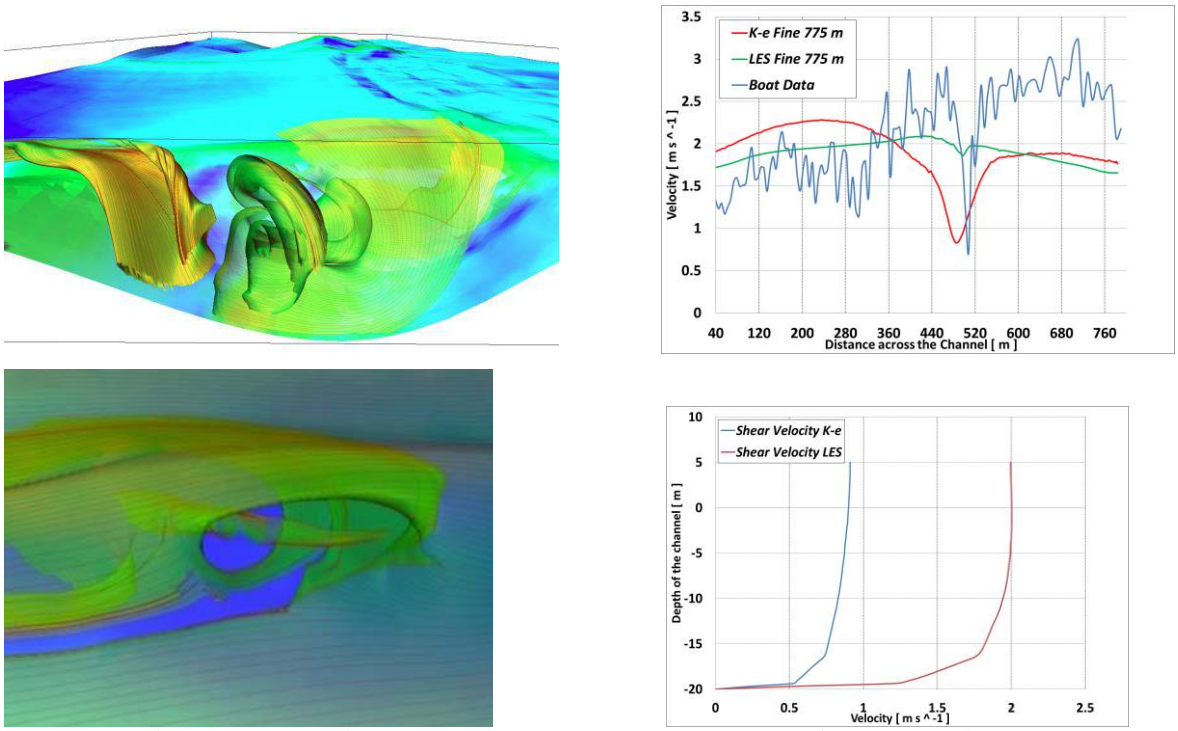

Figure 1 (a top left) The very turbulent flow with eddies and swirls, (b top right) Comparison of the velocity profile across the channel at 775m from the inlet, (c bottom left) the eddy behind Horse Rock and (d bottom right) the shear profile behind Horse Rock

Simplified Wake Models for Small Tidal Farms: Reduced Scale Evaluation and Array Loading Study

David Sudall[1], Alex Olczak, Tim Stallard, Peter Stansby
School of Mechanical, Aerospace and Civil Engineering, University of Manchester M13 9PL, UK

Summary: Various models have been employed to estimate velocity deficit downstream of horizontal axis tidal turbines. In this study, prediction of loads on downstream turbines using self-similar superposition, developed in [1], is compared to experiments and RANS-BEM models for multiple rows of scaled rotors. It is found to compare well for centre array turbines but less so on outer array edge turbines. The superposition model is employed to evaluate the impact of yaw strategy on energy yield and load variation from a small tidal farm at the MeyGen site. Continuous yaw offers 24% greater energy yield over a fixed system. Peak mean loads on the most heavily loaded turbine in the array are 17% greater than the least loaded turbine.

Introduction

To accurately predict energy yield and loading of individual turbines within an array, methods for modelling the wake profiles of upstream turbines are being developed. Actuator disc models embedded into shallow water solvers have been used to represent energy extraction from multiple turbines [2], whereas RANS-BEM has been used to model arrays of tidal turbines at the individual device scale (e.g. [3]). These modelling approaches have a relatively high computational demand. As such simplified approaches are of value, particularly for initial assessments of long-term yield and load variation for evaluation of alternative farm layouts or control strategies.

Wake Model Evaluation

The wake of a horizontal axis tidal stream turbine comprises an initially axisymmetric shear layer that expands to reach the wake centreline and, further downstream, develops to a self-similar transverse profile of streamwise velocity [1]. Experimental measurements indicate the width of the shear layer is linear with downstream distance, with a lower expansion rate in the vertical direction, and these shear layers merge between 2-3 diameters (D) downstream. From around 6D downstream the transverse profile of velocity follows a self-similar Gaussian form, with a centreline velocity deficit, ΔU_{max}, proportional to $x^{-1/2}$ and half wake width $y_{1/2}$, proportional to $x^{1/2}$. For small numbers of turbines, superposition of multiple self-similar wakes provides an approximation for the transverse velocity profile downstream of a row (fence) of multiple turbines (Fig. 1) neglecting wakes.

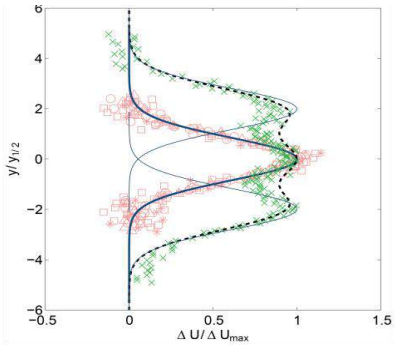

Fig. 1: Transverse profile of normalized velocity for experimental study of a single rotor wake, at X = 4D(△), 6D(○), 8D(□) and 10D(*) with self-similar Gaussian profile (▬) and 6D downstream of a fence of 3 rotors (×), with single wakes (—) and superposition (- -).

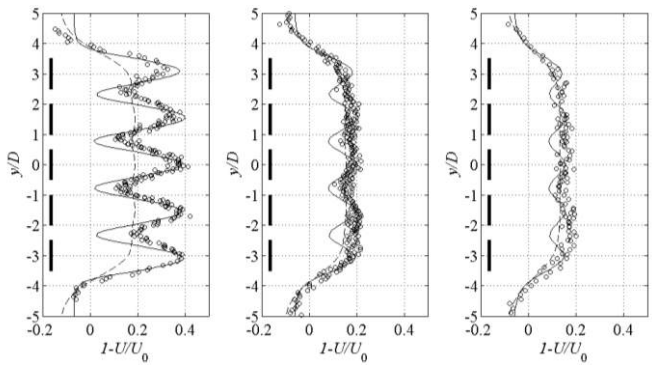

Fig. 2: Transverse profiles of velocity deficit for a single row of 5 rotors at 1.5D lateral spacing by superposition (--), RANS-BEM (-) and experiment (°) for X = 4D (left), 8D (centre) and 10D (right) downstream. Rotor plane (▬).

[1] *Email address*: david.sudall@postgrad.manchester.ac.uk

For larger numbers of turbines per row, this approach combined with a correction based on mass flux conservation and channel wall reflections, provides the wake and bypass flow velocity (Fig. 2). This is comparable to a RANS-BEM prediction for downstream distance greater than 6D. The RANS-BEM model is implemented in STAR-CCM+ with the k-ω SST model with values of k and ω representing experimental measurements. Accuracy of this superposition approach is evaluated for small groups of rotors of two to three rows and with rotors aligned and staggered relative to the preceding row. The average of the square of velocity, determining thrust, over the extent of five rotors located 8D downstream of a row of five rotors is obtained to within 2% of measurements for the central rotors compared to 11% with RANS-BEM. For rotors at the edge of the row, transverse shear differs between both predictions and experiment with the superposition model under-predicting velocity squared by over 30% whereas RANS-BEM over-predicts by 4%.

Energy Yield and Mean Load Modelling

The superposition wake model has been used to evaluate the influence of turbine arrangement and yaw control strategy on net energy yield and individual turbine loading. A rectilinear array of 20 turbines with 6D transverse spacing and 20D spacing between 4 rows is considered with flow speed and direction data for the MeyGen site from FOAM [4]. Each turbine is rated at 1MW with power coefficient 0.44 below rated speed. A continuous yaw strategy generates over 24% higher energy yield than a fixed yaw mechanism. A control strategy which yaws once per tide, slack tide yaw, generates only 3% less than the continuous strategy. Low capacity factors are observed since the current velocity is below the cut-in speed of the turbine for 45% of a year. Thrust force on the turbine and a tripod support structure are obtained by a C_T(TSR) curve and a drag coefficient based on BS EN 1993-3-1:2006 [5] for lattice structures. Drag applies to the stationary blades and structure during shutdown. Net force at rated speed is 1 MN with a base over-turning moment of 17.5 MNm. Variation of loading between turbines is considered to assess standardisation. The 98th percentile load differs by 17% and mean load by 12% (Fig. 3).

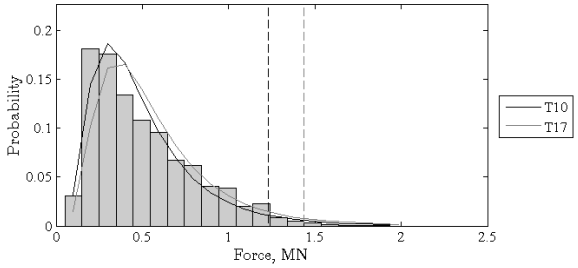

Fig. 3: Histogram of net horizontal force probability distribution on the least loaded turbine (T10) and with log-normal fit for both T10 and T17, the greatest loaded turbine, and their respective 98th percentiles (dashed).

Conclusions

A simplified wake model is evaluated for prediction of downstream velocity and thrust by comparison to experiment and RANS-BEM. Velocity prediction is of comparable accuracy to the CFD model for central turbines, but is under-predicted for turbines exposed to the shear between wake and bypass flow. Different yaw strategies are compared. Continuous yaw provides greatest yield although, for this location, yaw during slack-tide only reduces yield by 3%. Peak loading on turbines differs by 17% between individual support structures. This informs a study of the placement, loading and yield of co-located farms of offshore wind and tidal stream turbines.

References:

[1] T. Stallard, T. Feng and P.K. Stansby (2014). Experimental Study of the Mean Wake of a Tidal Stream Rotor in a Shallow Turbulent Flow, *J. Fluids and Structures*. DOI: 10.1016/j.jfluidstructs.2014.10.017

[2] S. Draper, A.G.L. Borthwick, G.T. Houlsby (2013) Energy potential of a tidal fence deployed near a coastal headland, *Phil. Trans. R. Soc. A.* DOI: 10.1098/rsta.2012.0176

[3] M. Edmunds, R. Malki, A.J. Williams, I. Masters, T.N. Croft (2014) Aspects of tidal stream turbine modelling in the natural environment using a coupled BEM-CFD model, *Int. J. Marine Energy* **7**(1), 20-42.

[4] Met Office (2014) Forecasting Ocean Assimilation Model 7km Atlantic Margin model (FOAM AMM7). Accessed via. myocean.eu

[5] European Committee for Standardization (2006) BS EN 1993-3-1:2006 Eurocode 3 - Design of steel structures – Part 3-1: Towers, masts and chimneys – Towers and masts.

Micrositing and Turbulence

Michael Togneri and Ian Masters
College of Engineering, Swansea University, UK

Summary: We present turbulence results from two acoustic Doppler current profiler measurement campaigns carried out in Ramsey Sound at two locations within 50m of one another. The campaigns were not simultaneous, but both covered at least one complete spring-neap cycle. We briefly describe the methods by which we calculate the parameters used to characterise the turbulence (turbulent kinetic energy, turbulence intensity and integral lengthscales). We find that both measurement campaigns exhibit strong flood-ebb asymmetry, but that otherwise many features differ significantly. We investigate the correlation between lengthscales and turbulent kinetic energy and find it is site-specific; in other words, it is not safe to assume *a priori* that more energetic turbulence has concomitantly larger eddies or vice versa.

Introduction

Turbulence in tidal currents will induce fluctuating loads on tidal stream turbines. These fluctuations are a vital engineering consideration in that they influence not only the fatigue life of mechanical components but also that they will induce strong transient peak loads. Understanding turbulence at deployment sites is therefore significant for device developers, as well as interesting scientifically. Although there are many studies from individual sites (e.g. [1,2]), no general model exists and so it is necessary to investigate turbulence on a site-by-site basis. Here, we examine two sets of results from a single site at slightly different positions ("micrositing"). No similar study of the dependence of turbulence on location at this small scale is attested in the literature.

The site in question is Ramsey Sound, between Ramsey Island and the Pembrokeshire coast; the mean flow characteristics as measured by boat transects are reported in [3]. The bathymetry of the sound, as seen in Fig. 1, is complex; notable features include a central channel up to 70m deep, a surface-piercing stack in the eastern half of the channel and a large ridge extending from Ramsey Island into the middle of the channel.

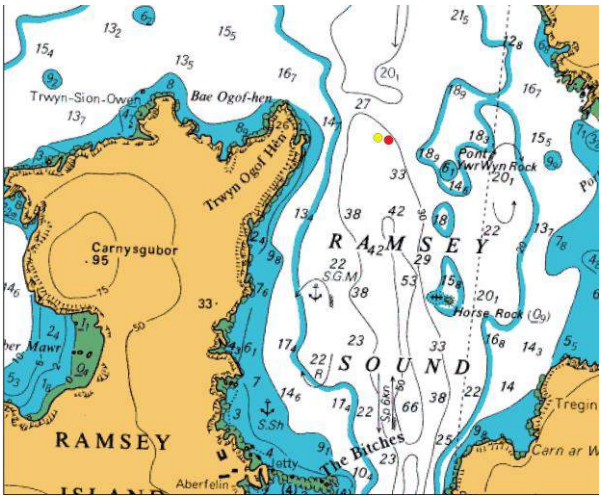

Fig. 1: Admiralty chart showing northern end of Ramsey Sound, with measurement locations marked by circles (yellow for campaign A, red for campaign B).

The first set of measurements ("campaign A") was carried out in 2009, the second ("campaign B") in 2011. The same model of 4-beam ADCP was used on both campaigns: an RDI Workhorse Sentinel, operated with a ping frequency of 600kHz and sampling at 2Hz.

Methods

The most important characteristics of marine turbulence are the strength and size of eddies present. The most direct metric of the strength of turbulence is the turbulent kinetic energy (TKE), usually reported as the TKE density and denoted $\frac{1}{2}q^2$. Turbulence strength is also reported with the turbulence intensity (TI), which is the magnitude of the turbulent velocity fluctuations expressed as a fraction of the magnitude of the mean velocity. TKE is calculated with the variance method, which is well-attested in the literature [4]. In short, the variance method relates the statistical properties of the along-beam velocity measurements to the bulk fluid properties in the ADCP's measuring volume, by assuming statistical homogeneity and stationarity over a reasonable averaging period.

A measure of the eddy size is obtained by calculating the lengthscale. Note that although these have units of length, they should not be interpreted as the size of any particular structure; instead, they increase and decrease in proportion to the average eddy size. We elect to measure the lengthscale with an integral technique, which

calculates the time-lagged autocorrelation coefficient for the along-beam velocity and integrates between a lag of zero and a lag large enough that the beam velocity is uncorrelated with itself. Note that this integration yields a timescale rather than a lengthscale; to get the desired dimension, we multiply by the mean velocity. Also note that since we use data from only a single beam, we can obtain four independent measures of lengthscale.

Results

Fig. 2 shows TKE profiles from both measurement campaigns, split into floods and ebbs. We can see there are two important asymmetries, firstly between ebb and flood, which is present in both measurement campaigns, and secondly between campaign A and campaign B, which is more noticeable on the ebb than the flood.

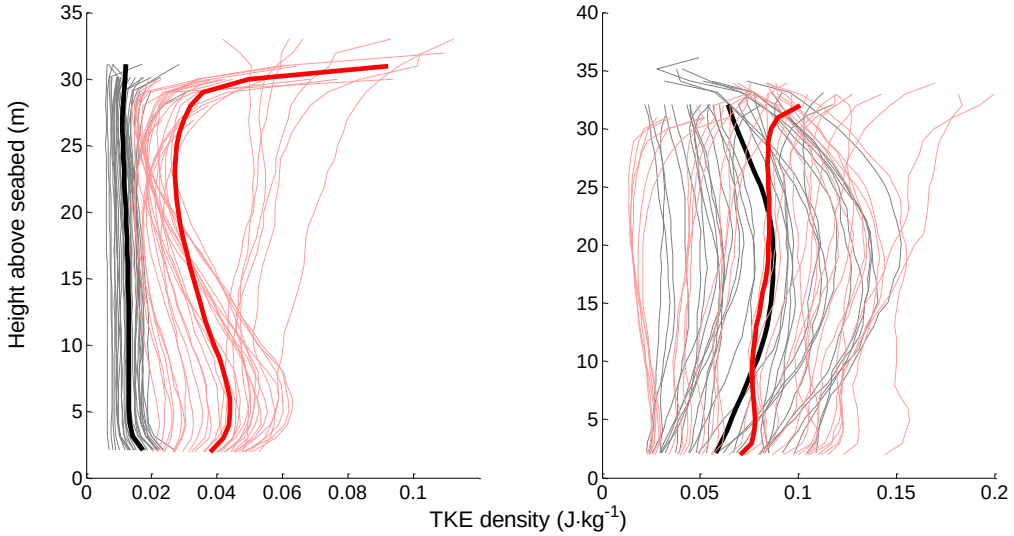

Fig. 2: Comparison of mean TKE profiles from ebbs (left) and floods (right). Campaign A results are in black, campaign B results in red. Pale lines show profiles of individual phases, while bold lines show overall ebb or flood profiles for a given campaign.

In both campaigns, the flood phases are more energetic than the ebbs. However, although floods are fairly similar, with the mean differing by less than 5%, this is not the case with ebbs. Here, campaign B ebbs are roughly 3 times as energetic as in campaign A, and the profile shapes differ significantly.

Acknowledgements:

This work was undertaken as part of the LCRI Marine Consortium, and as part of the SuperGen UKCMER Phase 3. The authors wish to acknowledge the financial support of the Welsh Assembly Government, the Higher Education Funding Council for Wales, the Welsh European Funding Office and the European Regional Development Fund Convergence Programme. The authors would also like to acknowledge the assistance of Paul Evans and Rob Poole.

References:

[1] Osalusi, E., Side, J., Harris, R. (2009). Structure of turbulent flow in EMEC's tidal energy test site, *Int. Commun. Heat Mass* **36**, 422-431

[2] Thomson, J., Polagye, B., Durgesh, V. (2012). Measurements of Turbulence at Two Tidal Energy Sites in Puget Sound, WA, *IEEE J. Oceanic Eng.* **37**(3), 363-374

[3] Fairley, I., Evans, P., Wooldridge, C, Willis, M., Masters, I. (2013). Evaluation of tidal stream resource in a potential array area via direct measurements, *Renew. Energ.* **57**, 70-78

[4] Lu, Y. Y., Lueck, R. G. (1999). Using a broadband ADCP in a tidal channel. Part II: Turbulence, *J. Atmos. Oceanic Technol.* **16**(11), 1568-1579

Predictability and temporal variation of tidal stream power

Thomas A. A. Adcock*
Department of Engineering Science, University of Oxford, UK

Summary: This abstract uses numerical models of several candidate sites around Great Britain to consider the predictability and temporal variations in tidal stream power.

Introduction

One of the key advantages given for tidal power is that it is predictable. This is true in principle but can be difficult to predict in practice. Set against this, a key disadvantage of tidal power is that it is intermittent. This paper uses examples to highlight the problems with predictability and intermittency of tidal power.

Methods

The results presented in this paper are mainly derived from a number of numerical models of several candidate sites for tidal stream energy extraction around Great Britain. These are models of the Pentland Firth [1], Portland Bill and the tidal race to the south of the Isle of Wight [2]. The models use the discontinuous Galerkin version of ADCIRC to solve the shallow water equations. The presence of tidal turbines is simulated using actuator disc theory to represent the thrust from the turbines and to differentiate between the power available for generation, from the power extracted from the flow.

Results — Predictability

The most straightforward way to predict tidal power at some point in the future is to model the physics of the tidal flow. Accurate and robust modelling remains difficult without tidal turbines and almost impossible when tidal turbines are present. Developing these models is vital to the future of the industry, but they will always be computationally expensive and we will need to use computationally inexpensive methods to extrapolate to arbitrary times in past or future. The standard approach taken to do this is harmonic analysis. This technique works well for predicting water levels, and slow tidal currents, but is well known to produce poor results in fast tidal races.

As an example of the inaccuracy of harmonic analysis, we have investigated the numerical model of tidal hydrodynamics used in [1]. A location was selected in the Inner Sound (Pentland Firth), which is one of the first areas where a large array of tidal turbines is planned. A point at 58.6624N 3.1244E was analysed. Harmonic analysis was carried out on this timeseries using the industry standard T_Tide software, using all available tidal constituents. Fig. 1 shows the power (kinetic flux) predicted directly by the numerical model, and the kinetic flux predicted by harmonic analysis of the model data. There is clearly a substantial mis-match, with the harmonic analysis failing to pick up many of the oscillations in the data.

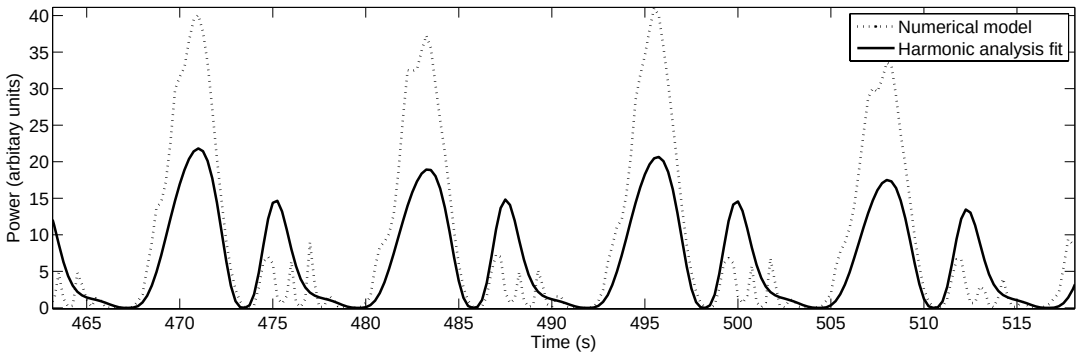

Fig. 1. Comparison of kinetic flux predicted from numerical model of Inner Sound with kinetic flux predicted by harmonic analysis of the model

* Corresponding author.
Email address: thomas.adcock@eng.ox.ac.uk

Results — Temporal variation

It is useful to consider a variety of timescales, ranging from daily variations, to variations in power output over many years, when analysing the temporal variations in tidal power output [3].

First consider the variation in power over a day. No power can be generated at slack water or when the flow is below the cut-in speed of the turbine. The amount of daily variation is strongly dependent on the cut-in speed and power capping strategy used by the turbines. At a national scale, the phase difference between spatially distant sites will help to smooth out the variations in power and, in principle, the timing of power production could even be varied at large sites [4].

The next longest important time scale is the spring/neap tidal cycle. When analysing this scale it is useful to consider the average power produced over a single M_2 tidal cycle and to consider the ratio of the power produced at a neap cycle with that on a spring cycle [5]. This ratio varies significantly between different sites. The ratio between power at neaps to power at springs for the Pentland Firth is around 1:8 to 1:10, whereas this drops to 1:4 for Portland Bill and 1:6 for the Isle of Wight tidal race. Again, these figures are dependent on the power capping strategy adopted. Unlike the daily variation the spring/neap cycle is in phase all over the world, and hence there will be a significant variation in the total output of tidal power plants over a period of a fortnight.

It is also important to consider the variation in power output over a timescale of years [6]. The dominant physics that leads to a change in the power availability at this scale is the variation in "nodal factor" — the correction to the amplitude of the M_2 tide to account for variation in the plane of the Moon's orbit relative to the equator. This varies over a period of 18.6 years. This leads to a small but significant variation in the power a tidal stream farm can be expected to produce from year to year. For the Pentland Firth the model predicts the variation shown in Fig. 2 for two different turbine configurations.

References:

[1] Adcock, T.A.A., Draper, S., Houlsby, G.T., Borthwick, A.G.L., Serhadlıoğlu, S. (2013). The available power from tidal stream turbines in the Pentland Firth. *Proc. R. Soc. A*, **469,** 20130072.

[2] Adcock, T.A.A., Draper, S. (2014). On the tidal stream resource of two sites in the English Channel: Portland Bill and Isle of Wight, In: *33rd OMAE*, San Francisco, USA.

[3] Adcock, T.A.A., Draper, S., Nishino, T. (2015). Tidal power generation — a review of hydrodynamic modelling, in press, *J. Power and Energy*

[4] Vennell, R., Adcock, T.A.A. (2014) Energy Storage Inherent in Large Tidal Turbine Farms, *Proc. R. Soc. A* 20130580.

[5] Adcock, T.A.A., Draper, S. (2014). Power extraction from tidal channels — multiple tidal constituents, compound tides and overtides, *Renewable Energy* **63** 797-806.

[6] Stock-Williams C., Parkinson S., Gunn K. (2013). An investigation of uncertainty in yield prediction for tidal current farms. In: *10th European wave and tidal energy conference (EWTEC)*, Aalborg, Denmark.

[7] Adcock, T.A.A., Draper, S., Houlsby, G.T., Borthwick, A.G.L., Serhadlıoğlu, S. (2014). Tidal stream power in the Pentland Firth — long-term variability, multiple constituents and capacity factor, *J. Power and Energy* **228**(8) 854–861.

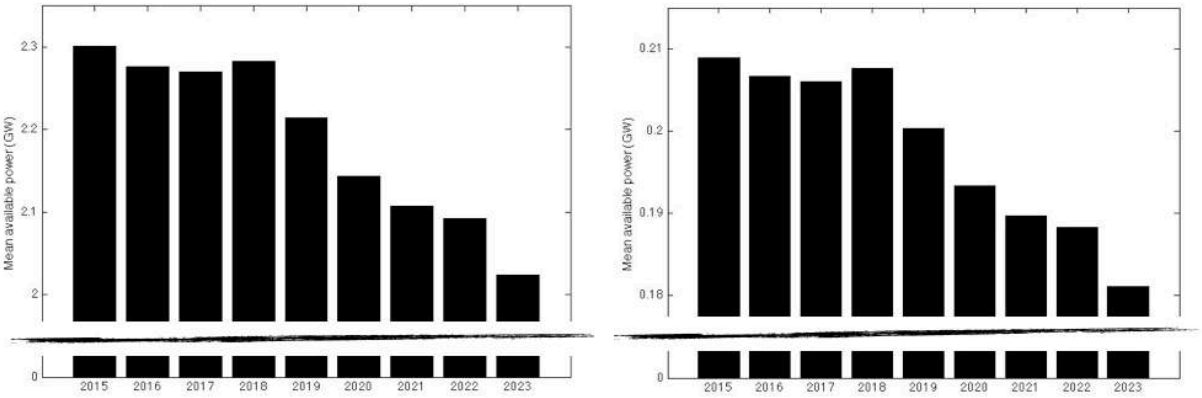

Fig. 2. Mean annual power predicted for two configurations of tidal turbines in the Pentland Firth. Left: 3 rows of high blockage turbines; right: 1 row of low blockage turbines

The importance of tidal phasing on leasing for tidal energy schemes

Simon P. Neill*, Matt J. Lewis
School of Ocean Sciences, Bangor University, Menai Bridge, UK

M. Reza Hashemi
Department of Ocean Engineering, University of Rhode Island, USA

Summary: The high tidal stream regions of the NW European shelf seas are approximately in phase with one-another. It is therefore possible, under a leasing system that is governed by demand for high tidal stream sites, that the power generated by the first generation of tidal stream arrays will similarly be in phase. We apply a 3D model of the NW European shelf seas to demonstrate that lower energy sites offer considerably more phase diversity, and hence more scope for generating baseload to the electricity grid. We therefore suggest that a state-led leasing strategy, favouring the development of sites which are complementary in phase, and not simply sites which experience the highest current speeds, would encourage a sustainable tidal energy industry.

Introduction

Although tidal currents are predictable, this form of renewable energy resource, in common with other forms of renewable energy like wind, wave, and solar, is intermittent [1], from semi-diurnal through to spring-neap (and longer timescale) variability. However, there is scope for exploiting our knowledge of the phase relationship between tidal energy sites by aggregating the electricity generated by a number of geographically distributed sites, leading to firmer power generation to the electricity grid [2]. Consideration of the phase relationship between sites is not reflected in the current leasing process for tidal energy schemes. For example, in the UK, The Crown Estate (as manager of the UK seabed) grants rights for tidal energy developers to operate on the seabed. At present, with the exception of Holyhead Deep (Minesto UK Ltd), developers are exclusively interested in high tidal energy sites, as evidenced by the 31 tidal stream sites that are currently leased from The Crown Estate. However, there is minimal phase diversity among these high tidal energy sites [3], and if all such sites were to be developed, the aggregated electricity generated would be characterised by strong semi-diurnal intermittency [4].

In this presentation, I discuss the implications of such a leasing strategy, and suggest ways in which phase diversity could be increased, such as developing lower tidal stream sites in parallel with high tidal stream development. I also discuss how a state-controlled leasing system, working in conjunction with privatised or centralised electricity networks, could lead to increased phase diversity, and hence the ultimate success of a sustainable tidal energy industry.

Phase diversity

Instantaneous velocity u for the M2 (principal lunar semi-diurnal) tidal constituent is

$$u = H_u \sin(\omega_{M2} t - g_u) \tag{1}$$

where H_u and g_u are the M2 current amplitude and phase, respectively, ω_{M2} is the angular frequency of the M2 tidal constituent, and t is time. Since tidal energy devices will extract energy on both flood and ebb phases of the tidal cycle, we are interested in the absolute value of u, and for $t = 0$

$$|u| = H_u |\sin(g_u)| \tag{2}$$

and so we can characterise the phase effect as $|\sin(g_u)|$ (Fig. 1b); hence two ideal complementary sites will have a difference in $|\sin(g_u)|$ of 1 (which represents a time lag of around 3.1 h, i.e. a quarter of a tidal cycle). Examining this plot in some detail, and in conjunction with the plot of current amplitude (Fig. 1a), it is clear that the electricity generated by many of the high tidal energy sites throughout the NW European shelf seas would be in phase. For example, the Pentland Firth is in phase with the high tidal stream sites along the east coast of Scotland and England, and these sites are also in phase with the key sites in the English Channel. Further, in the Irish Sea, Pembrokeshire is approximately in phase with NW Anglesey. It is clear from Fig. 1 that significantly more phase diversity can be

* Corresponding author.
Email address: s.p.neill@bangor.ac.uk

introduced into a large-scale tidal energy strategy by considering lower tidal stream sites in addition to developing regions of strong tidal flow.

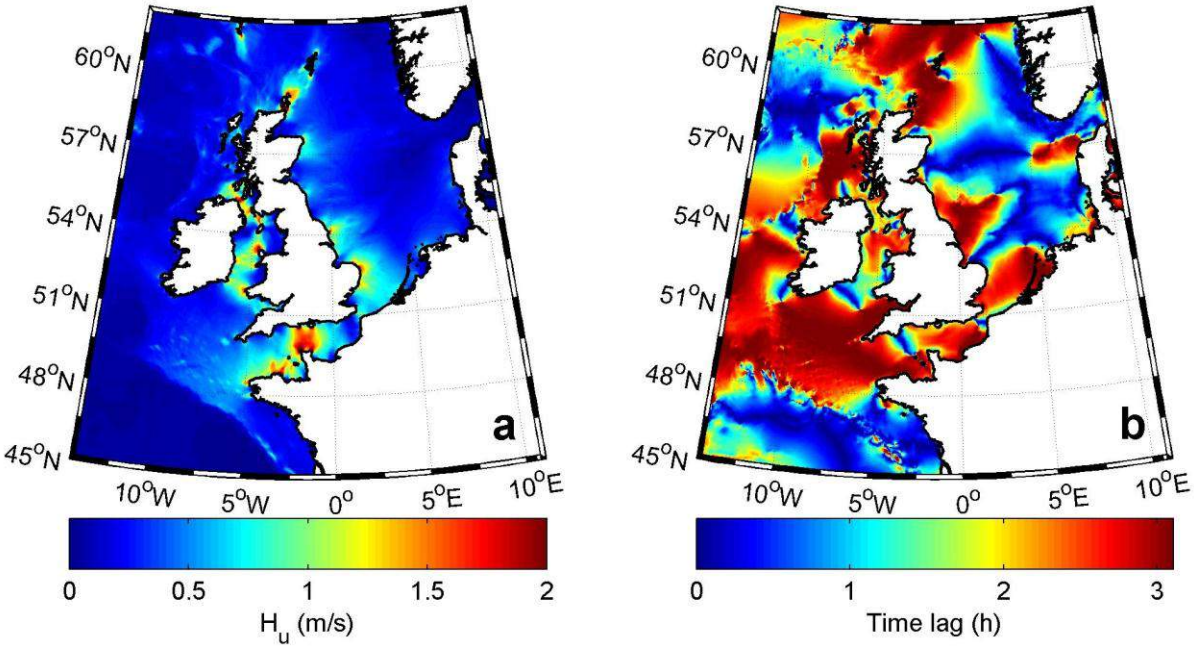

Fig. 1. Tidal current (a) amplitude and (b) phase over the NW European shelf seas. (a) is a plot of the semi-major axis of the M2 tidal current ellipse, and (b) is a plot of $T_{M2}|\sin(g_u)|/4$, where T_{M2} is the period of the M2 tidal constituent (approximately 12.42 h), and g_u is tidal current phase.

Discussion and conclusions

Our analysis of tidal current phasing throughout the NW European shelf seas reveals that there is considerably more phase diversity in the lower tidal flow regions, compared to the phase diversity offered by high tidal flow regions. In particular, and in agreement with previous studies of the region [3-4], the high tidal flow regions are in phase with one-another (Fig. 1). Therefore, should all these high tidal flow regions be developed, the aggregated electricity generated would be characterised by very strong semi-diurnal intermittency. Clearly, development of lower tidal stream sites would diversify this phasing, and generate firmer power with less intermittency. However, it is important to note that these lower tidal stream sites also experience intermittency over semi-diurnal timescales and, as shown in the presentation, the peak in aggregated power generation would be shifted by at best 1.25 h for lower tidal stream sites, in comparison to high tidal stream sites.

Acknowledgements:

S.P. Neill acknowledges the support of the Welsh Government Sêr Cymru programme through the National Research Network for Low Carbon Energy and the Environment.

References:

[1] Vlachogiannis, J. G. (2014). Marine-current power generation model for smart grids. *J. Power Sources* **249**, 172-174.

[2] Clarke, J. A., Connor, G., Grant, A. D., Johnstone, C. M. (2006). Regulating the output characteristics of tidal current power stations to facilitate better base load matching over the lunar cycle. *Renew. Energ.* **31**, 173-180.

[3] Iyer, A. S., Couch, S. J., Harrison, G. P., Wallace, A. R. (2013). Variability and phasing of tidal current energy around the United Kingdom. *Renew. Energ.* **51**, 343-357.

[4] Neill, S. P., Hashemi, M. R., Lewis, M. J. (2014). Optimal phasing of the European tidal stream resource using the greedy algorithm with penalty function. *Energy* **73**, 997-1006.

The effects of tidal farms in estuaries under extreme coastal and fluvial events

Miriam Garcia-Oliva*, Slobodan Djordjević, Gavin Tabor
College of Engineering, Mathematics and Physical Sciences, University of Exeter
North Park Road, Exeter, EX4 4QF, United Kingdom

Summary: This study investigates how tidal farms interact with coastal and fluvial flooding events in estuaries. A numerical model of the Solway Firth has been developed to identify the changes in the maximum water levels. Two different farm layouts have been introduced in order to compare their effects and extracted power. As a conclusion, the results are positive in terms of the flood risk in both cases while the parallel layout turns out to give a better performance in relation to the energy extraction.

Introduction

Estuaries represent a high resource of tidal energy in the UK and they also benefit of being more accessible for the installation of tidal farms than offshore locations. On the other hand, being a transition between the rivers and the open sea, their hydrodynamic behaviour is highly complex. Besides, there is a probability of extreme events happening in these areas with damages to the associated assets and environment. This study aims to give a better understanding of the interaction that large groups of tidal turbines could have in estuaries under the combination of coastal and fluvial flooding events.

Methods

The Solway Firth estuary, located between Cumbria and Dumfries and Galloway, was selected as a real case study from a group of estuaries with a high resource of tidal energy in the UK. There is a high current speed (up to 2 m/s) at some locations and there is significant risk of flooding.

A numerical model (Mike 21 by DHI) was used to reproduce the hydrodynamic conditions in the Solway Firth under the extreme events. A more detailed description of the software can be found in DHI, 2005 [1]. A summary of the main features of the model is presented in Figure 1. A broader description of the parameters involved, the calibration of the model and the data sources can be found in Garcia-Oliva et al., 2014 [2].

The boundary conditions in the model were mainly defined by the water levels at the open sea and the discharge from the rivers flowing into the estuary. Three different scenarios were used to cover a combination of events under normal and extreme conditions. In the first scenario, boundary conditions consisted of the 200-year return period event happening at the open sea, formed by storm surge and the highest astronomical tide, and the average discharges of the rivers, as explained in Garcia-Oliva et al., 2014 [2]. In the second scenario, boundary conditions at the open sea consisted of the tidal elevations, given by the Global Tide Model by means of the Mike 21 toolbox for the prediction of tidal heights. The river discharges were related to the values for the 200-year return period event provided by the CEH (Centre for Ecology and Hydrology) according to the procedures in Morris, 2003 [3]. Finally, the third scenario was a combination of the aforementioned cases.

A tidal farm consisting of 32x32 turbines was introduced in the model at the area with highest current velocities and a suitable depth. Turbines are defined by a drag force component directly included in the governing equations. The turbine dimensions are based on the MRL design (Momentum Reversal Lift), described by Gebreslassie et al., 2013 [4]. This design can be installed in shallow estuaries because the diameter is smaller than the one in axial flow designs. A description of the turbine parameters in the model can be found in Garcia-Oliva et al., 2014 [2]. Two different layouts, parallel and staggered, were used to analyse the effects that the geometry of the farm could have on the hydrodynamics and the extracted power. The spacing between the turbines is the same in both configurations, namely lateral spacing of 85.8 m and longitudinal distance of 124.8 m. The numerical mesh was refined in the area of the tidal farm with the use of rectangular elements including each turbine. (Figure 4)

* Corresponding author.
Email address: mg391@exeter.ac.uk

Results

Only the results for the third scenario are provided in this document as it represents the worst situation. Figure 2 shows the main values for the differences between the maximum water levels in the situation with and without tidal farms (Δh_M) and the total mean and peak extracted power by each tidal farm. A statistical analysis tool in Mike21 provided the maximum values of the water levels. The mean extracted power was obtained as the sum of the results (product of drag force and incident flow speed) from all turbines and time steps and averaged over the period of the simulation (14 hours), being the peak power the maximum value for the farm from all time steps.

Conclusions

The effects of both configurations in the maximum water levels are very similar, resulting in a decrease of the order of cm at the inner part of the estuary and an increase of the order of mm in the rest of the estuary, as can be seen from Figure 3. On the other hand, the parallel layout would imply a higher extracted power than the staggered layout. However, it would be necessary to undertake further research regarding the use of different spacing in the farm and a drag coefficient obtained through experimental testing of the MRL turbine.

Acknowledgements:

This research was conducted as part of the '*Optimal Design of Very Large Tidal Stream Farms: for Shallow Estuarine Applications*' project commissioned and funded by grant EP/J010138/1 from the UK Engineering and Physical Sciences Research Council (EPSRC). The authors would also like to acknowledge the support and software licence provided by DHI.

References:

[1] DHI (2005). MIKE 21 & MIKE 3 FLOW MODEL Hydrodynamic Module Scientific Documentation. *Demark: DHI Water & Environment*.

[2] Garcia-Oliva, M., Tabor, G., & Djordjevic, S. (2014) Modelling the impact of tidal farms on flood risk in the Solway Firth estuary. In: Proc. 2nd *International Conference on Environmental Interactions of Marine Renewable Energy Technologies*, Stornoway, Isle of Lewis, Outer Hebrides, Scotland

[3] Morris, D. G. (2003). Automation and appraisal of the FEH statistical procedures for flood frequency estimation. *Final Report to Defra*.

[4] Gebreslassie, M. G., Tabor, G. R., & Belmont, M. R. (2013). Numerical simulation of a new type of cross flow tidal turbine using OpenFOAM–Part I: Calibration of energy extraction. *Renewable Energy*, *50*, 994-1004.

Simulation Period	100 h
Time step	900 seconds
Number of elements	14266 (parallel), 15910 (staggered)
Maximum mesh Size	1 km^2
Bed roughness (1/n)	22 $m^{1/3}/s$
Smagorinsky's coeff.	0.28

Figure 1. Model features

Results		*Scenario c*	
		Parallel	*Staggered*
Δh_M (m)	**Max. Increase**	0.004	0.004
	Max. Decrease	0.064	0.063
Mean Extracted Power (MW)		58.39	57.49
Peak Extracted Power (MW)		179.00	176.49

Figure 2. Model results for the worst case scenario

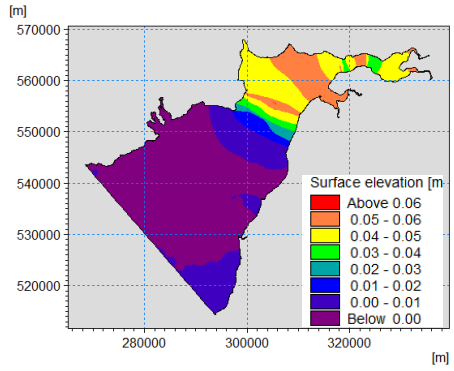

Figure 3. Difference in maximum water levels

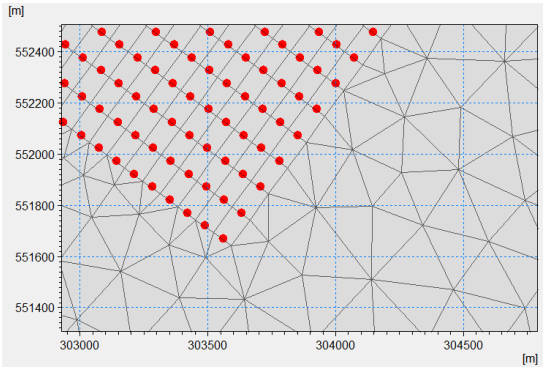

Figure 4. Computational grid refinement

Moving Meshes and Virtual Porpoise

Thomas Lake*, Ian Masters and T. Nick Croft

College of Engineering, Swansea University, Singleton Park

Summary: Individual Based Models (IBMs) provide a way of taking simple rules and principles and simulating the movement and interaction of living creatures with each other and/or the environment around them. This includes simulating potential impacts of marine energy devices on local marine mammals.
This model uses the mesh and tidal flow data from an openTELEMAC model to define a virtual environment in which porpoise can be simulated, with behaviours based on food availability, flow speed, water depth and noise levels in the local environment. A shallow water avoidance behaviour has been implemented in the code, and is illustrated here alongside some of the complications when working with a time varying mesh.

Individual Based Modelling

Individual Based Models (IBMs) are a class of computer model which use a selection of simple rules and principles to simulate the movement and interaction of living creatures with each other and/or the environment around them. These models have been used to investigate habitat use and movements of a variety of animals, including both marine and terrestrial mammals, fish and birds, over a range of timescales and degrees of sophistication. These models have been applied to a variety of species, from panthers and seabirds to larvae, fish and cetaceans. Within the context of marine energy developments, individual based models may be able to feed into the Environmental Impact Assessment (EIA) of projects going through the consenting process[1]. In this instance, the simulated animals will be designed to mimic Harbour Porpoise (*Phocoena Phocoena*) - a small cetacean species commonly found in UK coastal waters and protected under the EU Habitats Directive[2].

Defining a marine environment

The environment in which the virtual porpoise will be placed is defined by the output of an openTELEMAC model. The results of the openTELEMAC model provide both the details of the tidal flows in the area and a mesh defining the physical extent and bathymetry of the simulated habitat. These meshes can cover a very large area (a mesh used for testing is bounded by a 488km $\times$ 368km box), but have a much smaller depth (A 90m range in the same example). The mesh output by openTELEMAC is formed from stacked layers of a triangular 2D mesh (see figure 1), and is bounded vertically by the seabed and the free surface of the water. The mesh moves vertically to represent the rising and falling water levels caused by the tides, compressing and expanding the depth (in z) of the elements as required - this can lead to elements with no measurable depth. For the openTELEMAC results used in testing, the input data is available at one hour intervals for the duration of the simulation. This is interpolated linearly to provide shorter simulation timesteps, typically between 4 and 10 seconds in length.

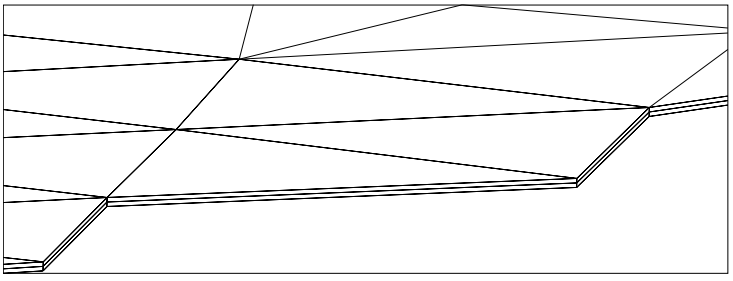

Figure 1: Slice through an example mesh, showing how the 2D triangular mesh forms layers of prisms in 3D

*Corresponding Author
Email: 527562@swansea.ac.uk

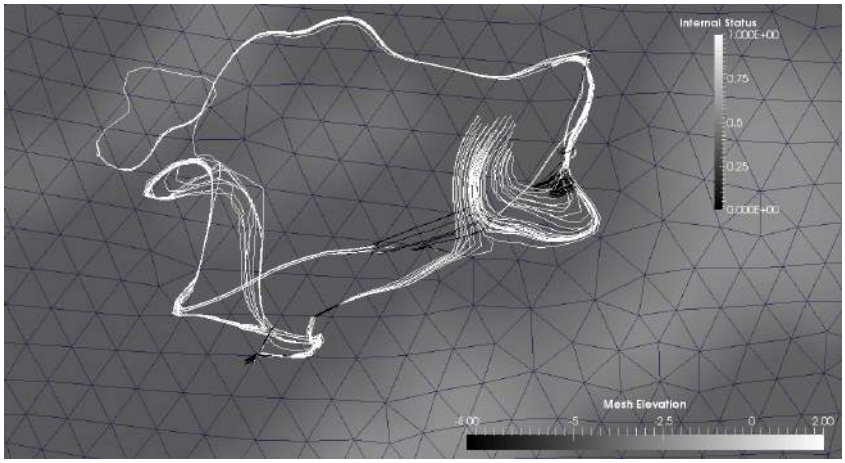

Figure 2: Example output, showing paths taken by virtual porpoise in shallow water

Shallow water behaviour

The vertical movement of the mesh, and the existence of zero height elements within it, can cause problems if not explicitly handled within the model. The vertical movement of the mesh can result in a previously valid location suddenly being outside the domain - any simulated porpoise at these locations are then stranded outside the simulation.

The IBM can be outlined as an iterative process, with the basic process being outlined as follows:

1. Load mesh
2. Find enclosing element for each porpoise
3. Move porpoise according to behaviour rules
4. Update mesh for next timestep
5. Check enclosing element for each porpoise remains valid
   If enclosing element is no longer valid:
   - Check if porpoise is now within another element.
     If so: update porpoise properties and continue
   - Move porpoise vertically based on change in water depth, to attempt to keep it within the domain.
     If no valid position is found: Ignore porpoise for remainder of simulation
     Otherwise: Update porpoise properties and continue
6. Move porpoise according to behaviour rules
7. Continue from 4 for each simulation timestep.

This basic process ensures that only validly located porpoise are simulated, and prevents porpoise being simulated in midair or over land, but doesn't reflect any aspect of the behaviour of real Harbour Porpoise. Real Harbour Porpoise are more likely to be found in depths between 20m and 200m, with one study suggesting a preference for depths >60m and avoidance of depths <10m[3]. Consistent with this, a behavioural rule was implemented that takes precedence over other rules and directs the virtual porpoise towards deeper water if the depth at the current location is less than 10m. The simulation was then seeded with 40 porpoise in a shallow area of the simulation. The results are shown in figure 2, with white paths showing porpoise trying to find deeper water and black paths representing porpoise following their remaining behaviour rules. These rules include food seeking and noise avoidance behaviours, and remain under development.

References

[1] T. Lake, T. N. Croft, and I. Masters, "Methods for Individual Based Modelling of Harbour Porpoise," in *Proceedings of the 10th European Wave and Tidal Energy Conference*, 2013.

[2] P. Berggren, P. Wade, J. Carlström, and A. Read, "Potential limits to anthropogenic mortality for harbour porpoises in the Baltic region," *Biological Conservation*, vol. 103, no. 3, pp. 313 – 322, 2002.

[3] S. Isojunno, J. Matthiopoulos, and P. G. H. Evans, "Harbour porpoise habitat preferences: robust spatio-temporal inferences from opportunistic data," *Marine Ecology Progress Series*, vol. 448, pp. 155–170, 2012.

4^{th} Oxford Tidal Energy Workshop
23-24 March 2015, Oxford, UK

Analytical model for tidal farm design with free-surface deformation effect

Vikrant Gupta*, Anna Young
[1]*Whittle Laboratory, Department of Engineering, University of Cambridge, UK.*

Summary: An analytical model is developed to account for the effects of free-surface deformation, i.e. drop in water level in the downstream region of turbines, in tidal farm arrays. The free-surface deformation is found to be higher in tidal arrays with higher local blockages and small number of turbines. Consequently, the effects of free-surface deformation increase the local blockage that is required for the optimal performance of a tidal array.

Introduction

When a turbine or an array of turbines is introduced in a tidal channel/experimental-flume the water level drops in the wake. This drop in the water level causes an increase in the turbine performance as compared to its performance in a case where water-level is not allowed to drop. More importantly, this effect can change the design of turbines and the array arrangement that are required for the optimal performance.

Analytical Model

A two-scale-dynamics analytical model, as developed in Ref. [1], is coupled with the model developed in Ref. [2], which accounts for the free-surface deformation. The model gives a set of nonlinear algebraic equations, which are solved by using "fzero" and "fsolve" in matlab.

Results and Discussion

Figure 1 presents the results for the maximum global power coefficient (Cpg_{max}) and the corresponding optimal induction factors (a_{opt}) as functions of the local blockage ratio (Bl). The free-surface deformation effects are insignificant in the $Bg = 0.001$ case (top), but are clearly visible in the $Bg = 0.3$ case (bottom). These effects increase the power coefficient (Cpg_{max}) and the corresponding optimal induction factors (a_{opt}) as also predicted in Ref. [2]. Although it is not clear from this figure, a more important effect of free-surface deformation is the increase in the optimal Bl at which the Cpg_{max} is maximised. The right side plots are not smooth because of the lack of resolution in the induction factor 'a' and local blockage 'Bl'.

Figure 2 presents the optimal global power coefficient normalised by the corresponding optimal power coefficient in the case with no free-surface deformation ($Cpg_{max}|_{ratio}$) for (a) $Bg = 0.1$ and (b) $Bg = 0.3$. The increment in the power coefficient because of the free-surface deformation effects is higher in the cases with higher local blockage (Bl) even when the Bg is constant. Physically, this is because when the Bl is higher the flow through the turbines decreases (also seen in figure 4(b) of Ref. [1]). Consequently the flow in the outside region and along the free-surface increases. By applying Bernoulli's equation a higher drop in water-level, and therefore higher free-surface deformation effects as well, are predicted for the higher Bl cases. The free-surface deformation effects are also usually higher in small tidal arrays as compared to in large tidal arrays. This is because a_{opt} is higher in smaller tidal arrays (figure 1), which again reduces the flow rate through the turbines.

Conclusion

It is seen that free-surface deformation effects are high only in the cases with high Bg and Fr. In realistic tidal farm designs both the Bg and Fr are relatively low. In laboratory scale experimental flumes and CFD calculations, however, both the Bg and Fr are usually significantly higher. An important consequence of the present study is then to understand the extrapolation of results from the experimental flumes/CFD to the realistic tidal farm designs.

References:
[1] Nishino, T. and Willden, R. H. J. (2013). *Two-scale dynamics of flow past a partial cross-stream array of tidal turbines*. J. Fluid Mech. **(730)** 220–244.
[2] Whelan, J. I., Graham, J. M. R. and Peiro, J. (2009). *A free-surface and blockage correction for tidal turbines*. J. Fluid Mech. **(624)** 281–291.

*Corresponding author.
Email address: vg277@cam.ac.uk

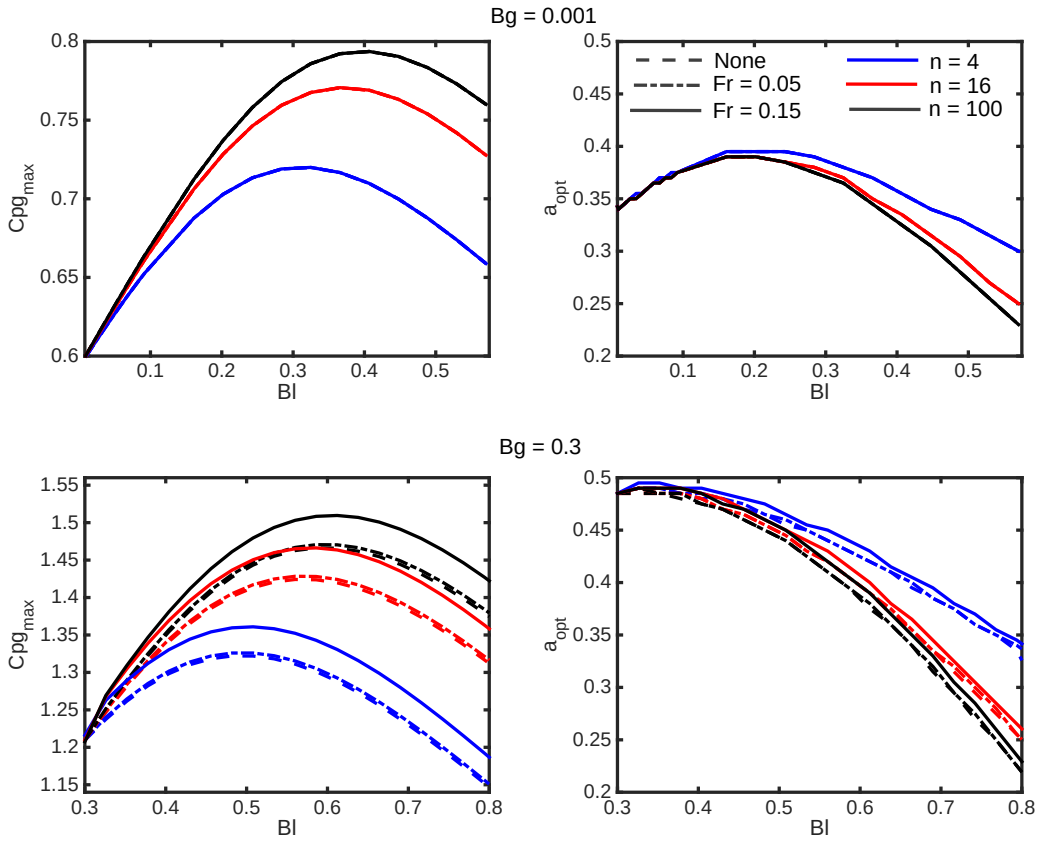

Figure 1: The left and right plots present the results for the maximum global power coefficient Cpg_{max} and the corresponding optimal induction factors (a_{opt}), respectively, as functions of the local blockage ratio Bl. The top plots are for a low blockage case $Bg = 0.001$, and the bottom plots are for a high blockage case $Bg = 0.3$. The results are presented for farms with different number of turbines and Froude number as shown by the markers in the top right plot. As expected the free-surface deformation effects are not observable in the $Bg = 0.001$ case, and in the $Bg = 0.3$ case these effects increase with the Froude number. Cpg_{max} increases with the increase in Bg and Fr. Bl and a_{opt} corresponding to the maximum in Cpg_{max} also increase slightly with Fr.

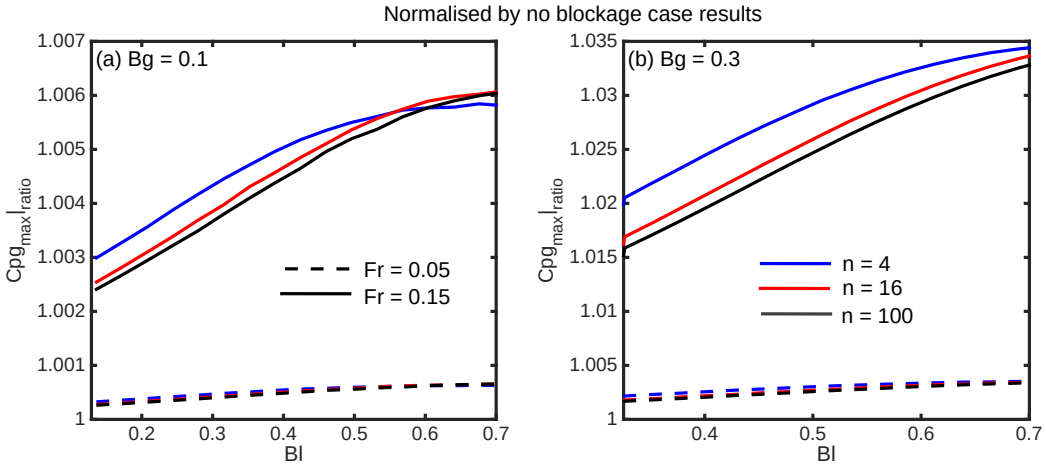

Figure 2: The optimal global power coefficient normalised by the corresponding optimal power coefficient in the cases with no free-surface deformation ($Cpg_{max}|_{ratio}$) are presented for (a) $Bg = 0.1$ and (b) $Bg = 0.3$. It is seen that the increment in the power coefficient caused by the free-surface deformation effects increase with Bl, and that this increment is usually higher in the farms with a fewer number of turbines.

Characterising the tidal energy resource of Pembrokeshire

Sophie L. Ward[*1], M. Reza Hashemi[2], Simon P. Neill[1]
[1]*School of Ocean Sciences, Bangor University, UK*
[2]*Department of Ocean Engineering and Graduate School of Oceanography, University of Rhode Island*

Summary: There is considerable interest in marine renewable energy development in the Pembrokeshire region of south Wales (UK). Pembrokeshire is an attractive region for marine renewable energy due to the significant wave resource and, in particular, the strong tidal streams in the area, in combination with good grid connections, and good port facilities. When considering the resource potential of a tidal stream energy site, in addition to considering the magnitude of the tidal stream, it is important to consider local variations in tidal asymmetry and turbulence. Here, we consider simulated and observed tidal currents in areas of potential (and existing) tidal stream energy extraction in Pembrokeshire, as well as showing how tidal asymmetry and turbulence vary across the region. We show that along with complex bathymetry in the area, there is significant variation in the tidal dynamics, at both semi-diurnal and spring-neap timescales.

Introduction

When considering the resource potential of a tidal stream energy site, it is important to consider hydrodynamics of the area, and not simply the magnitude of the tidal stream. For example, Neill et al. [1] and Robins et al. [2] showed that it is important to consider local variations in the ebb and flood phases of the tide (i.e. tidal asymmetry) when quantifying the tidal stream resource of a site, since tidal asymmetry can significantly affect the net power output of a location. Further, turbulence affects power production and turbine operation and efficiency through turbulent kinetic energy and coherent turbulent kinetic energy. Here, we use a high resolution three-dimensional (3D) ROMS tidal model of the Pembrokeshire region to assess the variability in tidal current speeds, tidal asymmetry, and estimated power output off the Pembrokeshire coast. This study builds upon previous lower resolution, two-dimensional, modelling studies, and has the potential to contribute significantly to preliminary resource assessment for tidal stream developments in the region.

Methods

The focus of the study was on a 3D tidal model of the Pembrokeshire region (5.70°W to 4.85°W and 51.35°N to 52.10°N), with a spatial resolution of approximately ~110 x 110 m, and with 10 vertical (sigma) levels. This high resolution ROMS (Regional Ocean Modeling System) model was forced by the amplitudes of the tidal elevation and current velocities of the principal semi-diurnal and diurnal tidal constituents of the region (M_2, S_2, N_2, K_1, O_1, Q_1), generated by a lower resolution outer ROMS model (750 x 750 m) for the southern Irish Sea. The lower resolution model was forced at the boundaries using tidal elevations and tidal currents from the FES2012 product (1/16°globally). Allowing for model spin-up, the last 30 days of the 32-day model simulations were output for subsequent analysis. When compared with nine coastal tide gauges (www.ntslf.org), the simulated M_2 and S_2 tidal elevations were found to have a root mean square error (RMSE) of <6 cm in amplitude and <5°in phase. The simulated depth-averaged M_2 and S_2 tidal currents had an RMSE of <3 cm s^{-1} and <2° in amplitude and phase respectively, when compared with published data from eight off-shore current meter stations [3]. Future work will include developing a tidal model of Ramsey Sound and St Davids Head, at a resolution of around 50 x 50 m, and will incorporate extensive new multibeam bathymetry data for the region.

To assess the observed current properties at potential tidal energy sites, an acoustic Doppler current profiler (ADCP) was deployed north of St Davids Head, throughout October and November 2014. The ADCP was set up to collect data every 2 seconds (0.5 Hz), with 1 m depth bins. The observed tidal current speeds were compared with the simulated tidal currents at the ADCP location for the time of the data recovery. Mean peak tidal current velocities were considered, as well as considering the variation in the tidal stream during spring and neap tides. Using the model simulations, the potential power output was estimated across the region for both depth-averaged tidal currents speeds, and for a range of example typical hub heights, based on the published power curve for the 1.2 MW Strangford Narrows SeaGen S deployment [4]. The spatial variability in the estimated 'capacity factor' was also calculated, which indicates to developers and policy makers the expected annual power output of an installed turbine, relative to the rated capacity, and is used here as a simple characterisation of the resource.

[*] Corresponding author.
Email address: sophie.ward@bangor.ac.uk

Results

The 3D tidal model enabled quantification of the variability in the vertical velocity profiles in the region, which can be compared with the observed tidal currents collected via a bottom-mounted ADCP. Model outputs of depth-averaged current speeds have been used to calculate the percent time over which the example cut-in speed of 1 m s^{-1} is exceeded in potential tidal stream sites in northern Pembrokeshire (Fig. 1). Owing to the combination of complex bathymetry, headlands and fast tidal streams in the area, there is significant tidal asymmetry and variation in turbulent kinetic energy around St Davids Head. The simulated tidal currents have been used to calculate the variability in the tidal currents over a spring-neap cycle. A larger difference between spring and neap tidal current speeds is less desirable for optimising energy generation, since it results in less continuous extractable energy.

Conclusions

Fast tidal streams, existing grid connectivity and good port facilities make Pembrokeshire an attractive region for tidal stream developments. Here, we use a high resolution, 3D ROMS tidal model of the region to calculate the tidal stream energy resource in the north Pembrokeshire region. The tidal model, along with observed current data allow for vertical variations in the velocity structure to be considered. We show that there is considerable variation in tidal asymmetry, both across the region and during the lunar cycle. Further, we demonstrate the importance of using 3D models for site characterisation since vertical variations in tidal turbulence is an important consideration for turbine developers.

Acknowledgements:
The author acknowledges modelling support from Peter Robins and Matthew Lewis, and data collection by SEACAMS technicians and Marco Piano. This work was undertaken as part of the SEACAMS project, which is part-funded by the European Union's Convergence European Regional Development Fund, administered by the Welsh Government. The model simulations were made on High Performance Computing (HPC) Wales, a collaboration between Welsh universities, the Welsh Government and Fujitsu.

References:

[1] Neill, S. P., Hashemi, M. R. and Lewis, M. J., (2014). Optimal phasing of the European tidal stream resource using the greedy algorithm with penalty function. *Energy* 73, 997-1006.
[2] Robins, P. E., Lewis, M. J., Neill, S. P. and Ward, S. L., (*in press*). Characterising the temporal and spatial variability of the European tidal-stream energy resource. *Applied Energy*.
[3] Jones, J., 1983. Charts of O_1, K_1, N_2, M_2 and S_2 Tides in the Celtic Sea including M_2 and S_2 Tidal Currents. Institute of Oceanographic Sciences, Natural Environment Research Council. Report No. 169.
[4] Macenri J, Thiringer T and Reed M. (2012). Power quality and flicker performance of the tidal energy converter, SeaGen. In: *44th International Conference on Large High Voltage Electric Systems 2012*, Paris, 26-31 August 2012.

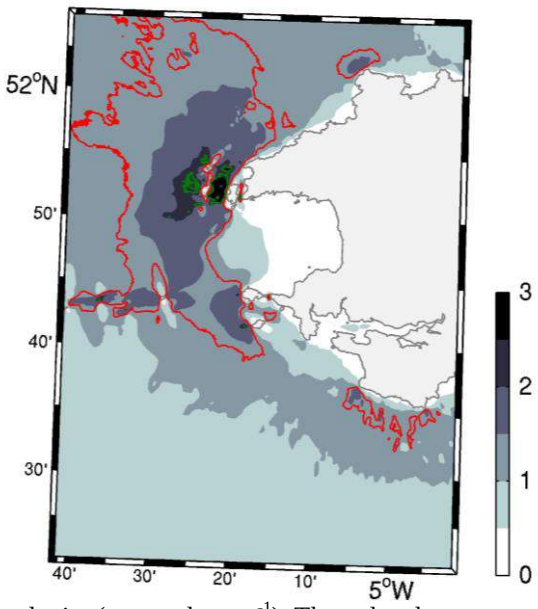

Fig. 1. Peak mean spring velocity (grayscale, m s^{-1}). The red and green contour lines indicate where a 1 m s^{-1} cut-in speed is exceeded 20% and 40% of the time, respectively.

A Numerical Study of Vertical Axis Tidal Turbines' Performance Improvement by Active Pitch Control

Pierre-Luc Delafin *
Centre for Offshore Renewable Energy Engineering, Cranfield University, UK

François Deniset, Jacques-André Astolfi
BCRM Brest, Ecole navale, IRENav, CC 600, 29240 Brest cedex 9, France

Summary: The power coefficient of Vertical Axis Tidal Turbines (VATT's) is usually limited due to the inherent variation of the blades' angle of attack, i.e. the blades cannot always work at their optimal angle of attack. The aim of this study is to use an active pitch control to modify the angle of attack of the blades during their rotation. 3 pitching laws are tested so as to decrease the angle of attack in the upstream half of the turbine. This leads to a decrease of the blades' loading in the upstream half. The flow velocity at the centre of the turbine is then higher and more energy is available for the blades in the downstream half. The average power coefficient is increased by 35% with the best pitching law.

Introduction

The Power Coefficient (CP) of Vertical Axis Tidal Turbines (VATT) is limited by the inherent variation of the blades' angle of attack, given by Eq. (1):

$$\alpha = \arctan\left(\frac{\sin\theta}{\lambda + \cos\theta}\right), \text{ with } \theta \text{ the azimuth angle and } \lambda \text{ the tip speed ratio} \quad (1)$$

Depending on the tip speed ratio (λ = ω R / U_∞), the maximum angle of attack can reach high (>20°) or low (<10°) values. The blades may then undergo dynamic stall or low loadings. Staelens et al. [1] used DMST (Double Multiple Streamtubes) calculations to show that limiting the blades' angle of attack just below the static stall angle increases the CP of the turbine. Hwang et al. [2] used CFD calculations (on a coarse grid) and a genetic algorithm to find an optimal pitching law. Their results show an increase of 25% of the power coefficient by reducing the angle of attack in the upstream half of the turbine. Paillard [3] showed, through CFD calculations, that decreasing the angle of attack in the upstream half of the turbine thanks to sinusoidal pitching laws, increases its CP. Based on these results, this paper aims at studying the effect of the blades' angle of attack decrease in the upstream half of the turbine on its power coefficient. The turbine used in this study (SHIVA) is a straight bladed VATT (3 blades), currently under construction at the French Naval Academy Research Institute [1]. A subsidiary motor is mounted on top of each blade to make possible the pitch variation during the rotation.

Methods

Two-dimensional CFD calculations are used in this study. The computational domain is divided in 3 parts (Fig. 1, left): one rotating ring containing the 3 blades and two stators (inner and outer). The GGI method is used for the two rotor / stator interfaces. The grid uses a maximum y^+ value of 1 on the blades to have a y^+ independent solution, according to Maître et al. [4]. A verification study has been carried out to ensure that the solution does not depend on the computational domain size (square of side 60 D). Time step ($\Delta\theta = 1°$) and grid convergences have also been studied. Deforming mesh is used inside the rotating ring to take into account blades' pitching. The grid quality remains good for all pitch angles.

The pitching laws used in this study consist in limiting the angle of attack of the blades to a given value, at the optimal tip speed ratio of the turbine ($\lambda = 3$). Three Pitching Laws are defined (Fig. 1, right), limiting the angle of attack to 6° (PL1), 8° (PL2) and 10° (PL3). Cubic spline interpolations are used out of the "limitation area" to ensure $\alpha = 0°$ at $\theta = 0°$ and $\theta = 180°$ as well as the continuity of the complete law.

*Corresponding author. Email address: p.p.delafin@cranfield.ac.uk
[1]This study was conducted during the PhD of the corresponding author at the French Naval Academy Research Institute.

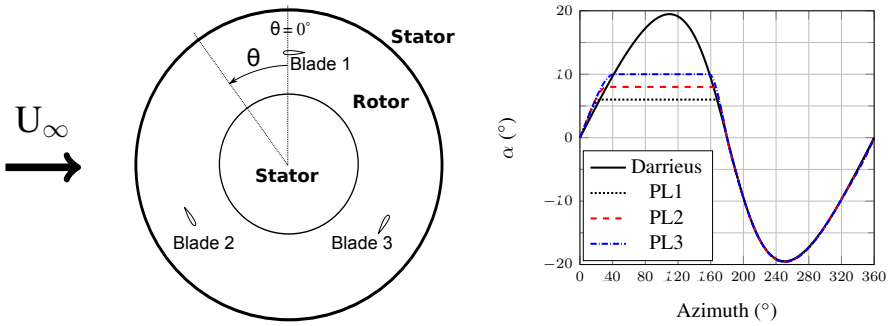

Figure 1: Close view of the computational domain (left) and blades' angle of attack (α) resulting from the pitching laws (right).

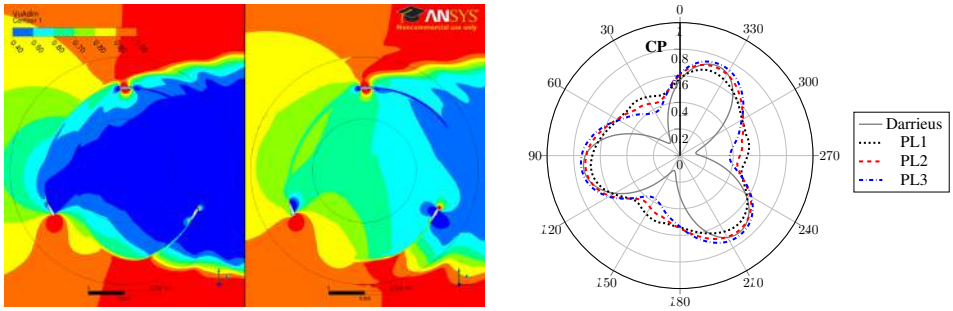

Figure 2: Left: visualisation of axial velocity (U_x / U_∞) in the vicinity of the rotor: left = Darrieus and right = PL2. Right: polar plot of the power coefficient CP.

Results

Decreasing the angle of attack in the upstream half leads to an increase of the axial velocity at the centre of the turbine (Fig. 2, left). The energy available for the downstream half is then higher than in the Darrieus case. Though not presented in this paper, the blades' tangential force is decreased in the upstream half of the turbine and significantly increased in the downstream half. Variable pitch then leads to a smoother distribution of the CP during one revolution (Fig. 2, right) and to an increase of the average power coefficient up to 35% for the PL2 law. This can be explained by the higher lift to drag ratio at which the blades operate when using variable pitch.

Conclusions

The use of variable pitch for VATT leads to a significant increase of the turbine power coefficient. An interesting feature is that the torque ripple is significantly reduced as well, thanks to the better balance between the blades' upstream and downstream contributions to the torque. Further studies should focus on the coupling between the upstream and downstream pitching laws.

References:

[1] Y. Staelens, F. Saeed, and I. Paraschivoiu. A straight-bladed variable-pitch VAWT concept for improved power generation. In *Proceedings of the 22nd ASME Wind Energy Symposium held in Conjunction with the 41st Aerospace Sciences Meeting & Exhibit*, pages 146–154, 2003.

[2] I.S. Hwang, Y.H. Lee, and S.J. Kim. Optimization of cycloidal water turbine and the performance improvement by individual blade control. *Applied Energy*, 86(9):1532–1540, 2009.

[3] B. Paillard. *Simulation numérique et optimisation d'une hydrolienne à axe transverse*. PhD thesis, Institut de Recherche de l'Ecole Navale, December 2011.

[4] T. Maître, E. Amet, and C. Pellone. Modeling of the flow in a Darrieus water turbine: Wall grid refinement analysis and comparison with experiments. *Renewable Energy*, 51(0):497–512, 2013.

Power Shedding from Stall and Pitch Controlled Tidal Stream Turbines

Matt Edmunds*, Alison J. Williams, Ian Masters, T. Nick Croft.
MERG, College of Engineering, Swansea University, UK

Summary: The ability to capture and understand the flow characteristics of a Horizontal Axis Tidal Turbine (HATT) poses challenges. CFD simulation is one of many useful tools for deriving the required information. Previous research focusses on the use of Blade Element Momentum Theory (BEMT) and Blade Element Momentum CFD (BEM-CFD). The advantage of the BEM-CFD method is the prediction of a time averaged downstream velocity field, and thus the turbine wake. In this work the performance of HATT's in power limiting mode, i.e. in stall or pitch control, is studied. The two techniques for power limiting are compared with respect to C_P, C_T, and wake characteristics. Pitch control power limiting generates less thrust than stall control, and thus allows greater flow through the rotor. Also differences in turbulence intensity in the near wake region are observed. The net effect of these characteristics are reflected in the wake recovery rate, i.e. the wake recovers more quickly for pitch control power limiting.

Introduction

To meet the growing requirements of the tidal stream renewable energy sector, investment in improving current tidal stream power extraction knowledge and technology is necessary. This can be achieved through the study of practical experiment [2], or numerical and analytical modelling [3]. In this work the performance of HATT's in power limiting mode, i.e. in stall or pitch control, is studied using the rotor geometries from [2]. The two techniques for power limiting are compared with respect to C_P, C_T, and wake characteristics. Previous work looked at the effects of wake size at differing flow velocities [1]. This work studies the effect of stall and pitch control to understand the characteristics of power shedding on the structure of the wake.

Results

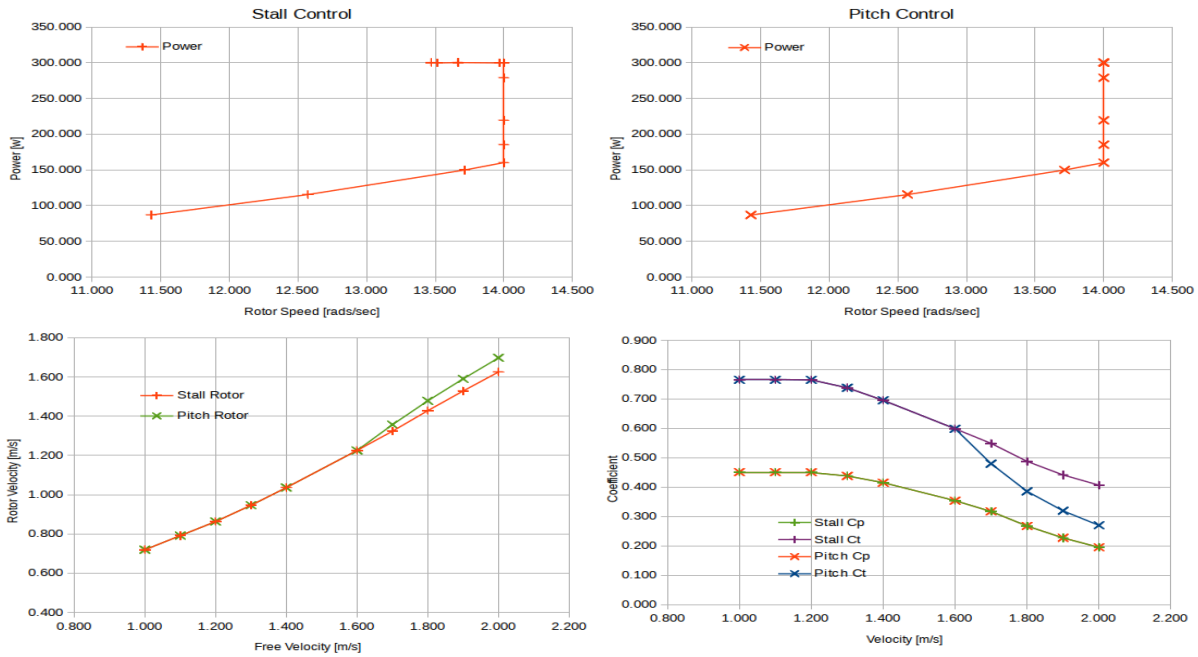

Figure 1: From top left to bottom right; stall control, pitch control, free velocity plotted against disc averaged rotor velocity, coefficient of power C_P and thrust C_T plotted against free velocity.

Generally speaking torque and pitch control algorithms all attempt to follow peak C_P for a range of operating speeds. Outside the specified range, the rotor either becomes stationary (when under-speed is reached), or when over-speed/max power rating is reached a pitch control algorithm will maintain the current rotor speed/max power by adjusting the blade pitch towards zero lift. A torque control algorithm will follow a curve of maximum rated

*Corresponding author.
Email address: m.edmunds@swansea.ac.uk

power slowing the rotational speed of the turbine to achieve this. Pitch control power limiting generates less thrust than stall control, and thus allows greater flow through the rotor. Also differences in turbulence intensity in the near wake region are observed. The net effect of these characteristics are reflected in the wake recovery rate, i.e. the wake recovers more quickly for pitch control power limiting.

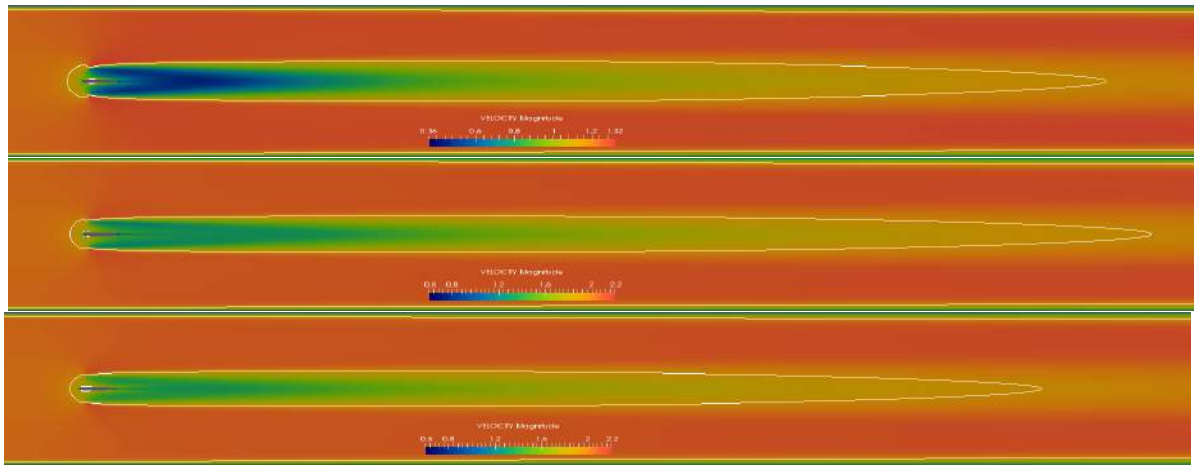

Figure 2: Wake velocity top to bottom; 1.2m/s TSR 4, 2.0m/s Stall control, 2.0m/s Pitch control. Isoline at 95 % free velocity. The colour map (blue to red) is in the range 0.3% to 1.1% of free velocity for all images, i.e. 0.36m/s to 1.32m/s for the top image, and in the range 0.6m/s to 2.2m/s for the remainder.

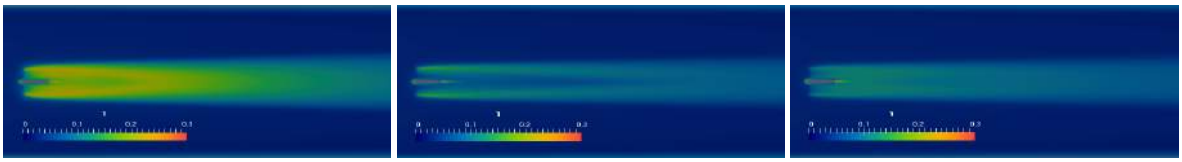

Figure 3: Wake turbulence Ti left to right: 1.2m/s TSR 4, 2.0m/s Stall control, 2.0m/s Pitch control. The colour map (blue to red) is in the range 0 to 0.3.

Conclusions

Application of an optimum control curve for a torque or pitch control system applied to a turbine within the BEM-CFD model, will better represent the wake dynamics and interactions across a turbine site. This will provide a more realistic assessment of energy yield maximisation. We demonstrate the effectiveness of this automated approach on a range of simulations, studying not only power yield but also the turbine wake at differing operating conditions. Evaluation of the results provides valuable insight into the effectiveness of our approach, and usefulness to the tidal turbine site design engineer.

Acknowledgements:
This work is undertaken as part of the Low Carbon Research Institute Marine Consortium (www.lcrimarine.org). The authors wish to acknowledge the financial support of the Welsh Assembly Government, the Higher Education Funding Council for Wales, the Welsh European Funding Office, and the European Regional Development Fund Convergence Programme.

References:

[1] Rami Malki, Ian Masters, Alison J Williams, and T Nick Croft. Planning tidal stream turbine array layouts using a coupled blade element momentum–computational fluid dynamics model. *Renewable Energy*, 63:46–54, 2014.

[2] Paul Mycek, Benoît Gaurier, Grégory Germain, Grégory Pinon, and Elie Rivoalen. Experimental study of the turbulence intensity effects on marine current turbines behaviour. part i: One single turbine. *Renewable Energy*, 66(0):729 – 746, 2014.

[3] Takafumi Nishino and Richard HJ Willden. Two-scale dynamics of flow past a partial cross-stream array of tidal turbines. *Journal of Fluid Mechanics*, 730:220–244, 2013.

Investigation on H-shape Vertical Axis Turbine with Flexible Blade

Wendi Liu and Qing Xiao*
Department of Naval Architecture, Ocean and Marine Engineering, University of Strathclyde, UK

Summary: A fully passive three-dimensional Vertical Axis Turbine with flexible bend and twist blades has been numerically investigated. Realistic model of internal structures are designed to obtain a certain degree of flexibility for the turbine blades. A sinusoidal displacement and the twist of turbine blades are presented with the simulation results. Also, a better power extraction efficiency of the turbine with flexible blades has been indicated from the simulation.

Introduction

With the increasing of the severe pollution generated by traditional fossil fuel, nowadays, people have been researching tremendously into renewable energies due to its clean and sustainable properties. The present study is conducted with the H-shaped lift force driven Vertical Axis Turbine (VAT), due to its simplicity in blade design, the ability can working in variable current flow directions and the non-sensitivity with water depth [1], when comparing with horizontal axis turbine or drag force driven turbine, as shown in Fig. 1(a).

In recent years, many studies and researches have been taken in the use of composite materials to potentially improve the fluid dynamic and structural performance of VATs. Passive control on the deformation of a turbine blade under its external exerted forces can be achieved by implementing advanced composite materials into the blade structure via taking advantages of the material directionality of anisotropic features. An anisotropic structure has shown its various levels of elasticity, which also relies on the blade's angle of attack [2]. This type of behaviour is defined as a potential means to reduce the loads on the blade and thus can control the blade dynamic stall effectively [3].

In this study, a fully coupled fluid-structure-dynamics of a three-dimensional Vertical Axis Turbines with flexible bend and twist blades is studied: the Reynolds number is chosen as 10^5; the ratio between the turbine chord (c) and the turbine radius (R) is 0.125; the tip speed ratio (λ) is fixed at 5.5. The classic NACA0018 foil is adopted for the 3-D blade cross-section and realistic internal structures are designed to achieve the flexibility for turbine blades, as shown in Fig. 1(b). The structure effective stiffness Π in this study is 3.19×10^3. The span length (H) is ten times of chord length and the holding arms are located at H/3 and 2H/3, as shown in Fig. 1(c). With the acting of fluid forces and centrifugal forces on the structure, the turbine blade tends to bend and twist during the cycle of rotation.

Methods

In this study, our in-house code has been developed which applies a fluid-structure interaction model by coupling unsteady Navier-Stokes solver with a linear structural model. High computational efficiency has been achieved by applying an implicit dual-time multi-grid method on the simulation of the flow and a model analysis approach for the structural part. The fluid-structure coupling is simulated by sub-iterations. In the fluid solver, a cell centred finite-volume method has been applied, with the enhanced numerical stability by residual smoothing. A k-ω turbulence model has been applied to model the high Re of VAT. A grid-deformation algorithm (TFI) has been developed to interpolate the deformation of the structural boundaries onto the flow grid. Also, the rigid turbine calculated by using the in-house code has been validated and achieves a good agreement with both experimental and numerical data which are presented by Ponta and Jacovkis 2001[4], as shown in Fig. 2(a).

Results

Fig. 1 and 2 have presented the preliminary results. The pressure distribution along the 3-D turbine blade is a key parameter that can represent the dynamic loads applied on the blades. From the contour plot, it shows that the pressure varies significantly within one rotational period. The low-pressure distribution has occurred at two time instants of t/T=2/8 and 6/8, and the high-pressure distribution has appeared at the instants of t/T=3/8 and 7/8, respectively. A detailed pressure coefficients contour at t/T=5/8 and different span locations are shown in Fig. 2(b), which shows that the lower pressure load occurs when using flexible blades. The non-dimensional blade

* Corresponding author.
Email address: qing.xiao@strath.ac.uk

deformation (D_{isp}/c) at various span wise directions (H/c) at different instantaneous time is presented in Fig. 2(c). It can be seen obviously that the blade deformation exhibits a sinusoidal motion profile. At the blade tip, a maximum displacement has been reached at 0.75c while it is only 0.02c when at the middle of the blade (i.e. H/c=5). Also, a quicker deformation can be observed at the blade tip than at the centre of the blade. As the deformation is induced by a combined effect from fluid load and non-inertial centrifugal force, a positive D_{isp}/c (bending outwards) has been presented at most of the time instants during one period. The maximum twist angles are 1^0 and 0.2^0 at blade tip and the centre of blade, respectively. The blade tip deformation can lead to an enhanced normal force applied on the blade. In addition, the time-mean C_{op} for a rigid turbine is 0.40 and it becomes 0.56 when using a flexible blade turbine.

Conclusions

A fully passive three-dimensional Vertical Axis Turbine with flexible bend and twist blades has been numerically investigated. Realistic model of internal structures are designed to obtain a certain degree of flexibility for the turbine blades. A sinusoidal displacement and the twist of turbine blades are presented with the simulation results. Also, a better power extraction efficiency of the turbine with flexible blades has been indicated from the simulation.

Acknowledgements:

Results were obtained using the EPSRC funded ARCHIE-WeSt High Performance Computer (www.archie-west.ac.uk). EPSRC grant no. EP/K000586/1.

References:

[1] Khalid, S. S., Liang, Z., & Shah, N. (2012). Harnessing tidal energy using vertical axis tidal turbine. Research Journal of Applied Sciences, Engineering and Technology, 5(1), 239-252

[2] Nicholls-Lee, R. F., & Turnock, S. R. (2007, June). Enhancing performance of a horizontal axis tidal turbine using adaptive blades. In OCEANS 2007-Europe (pp. 1-6). IEEE.

[3] Lachenal, X., Daynes, S., & Weaver, P. M. (2013). Review of morphing concepts and materials for wind turbine blade applications. Wind Energy, 16(2), 283-307.

[4] Ponta, F. L., & Jacovkis, P. M. (2001). A vortex model for Darrieus turbine using finite element techniques. Renewable Energy, 24(1), 1-18.

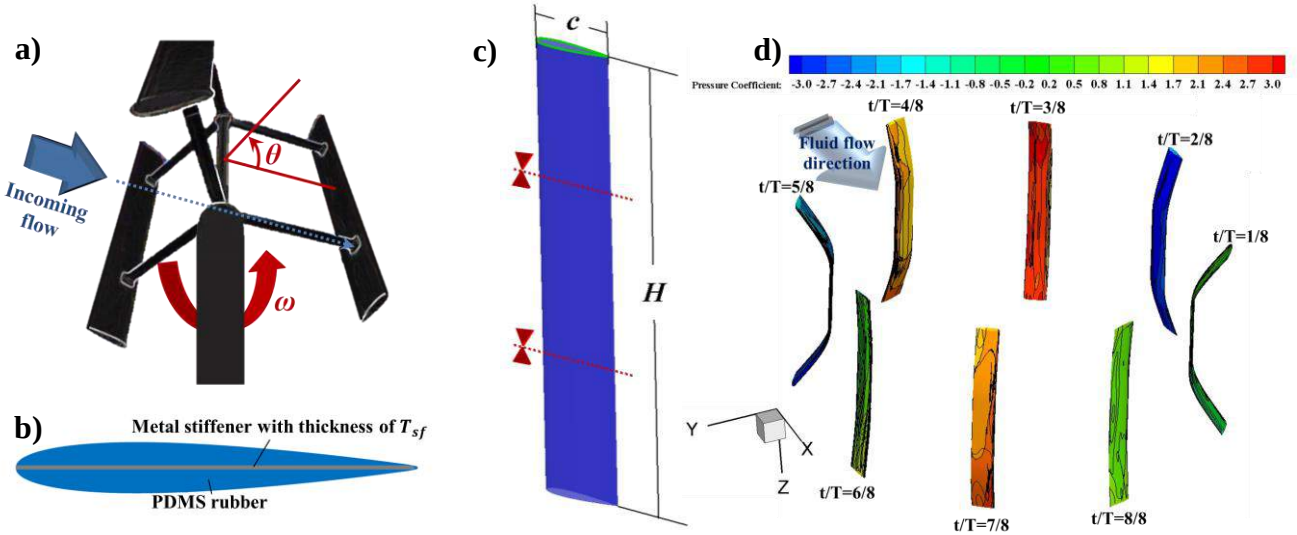

Fig. 1. Simulation model (a and b) and pressure coefficient distribution on blade surface at each instant (c)

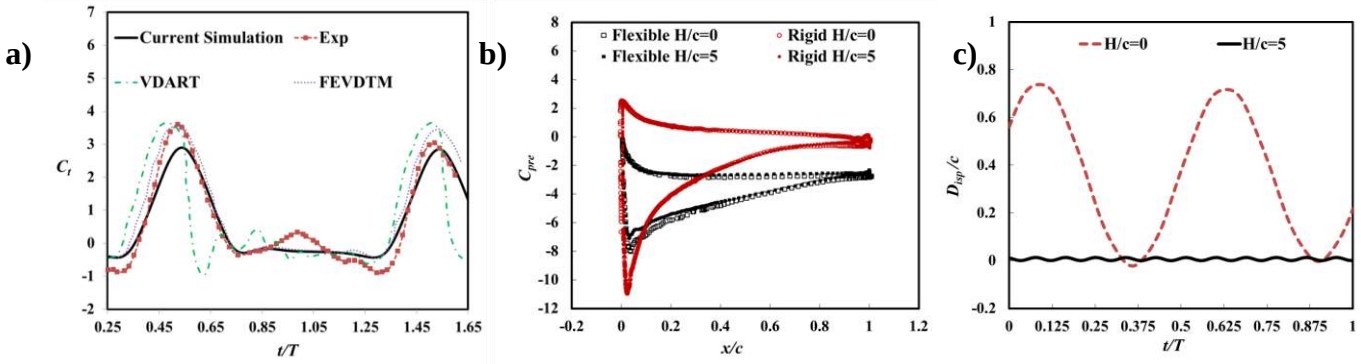

Fig. 2. Structure results for the vertical axis turbine blade and corresponding validation.

Oxford Tidal Energy Workshop 2015 - Participants

McNaughton, James	Alstom
Vigars, Paul	Alstom
Goward Brown, Alice	Bangor University
Lewis, Matthew	Bangor University
Neill, Simon	Bangor University
Robins, Peter	Bangor University
Ward, Sophie	Bangor University
Evans, Paul	Cardiff University
Delafin, Pierre-Luc	Cranfield University
Nishino, Takafumi	Cranfield University
Chen, Bing	Dalian University of Technology
Liu, Chongqi	Dalian University of Technology
Ning, Dezhi	Dalian University of Technology
Yu, Haipeng	Dalian University of Technology
Zhang, Huan	Dalian University of Technology
Gunn, Kester	E.On
Stock-Williams, Clym	E.On
Swatton, Stewart	ETI
Hieatt, Matthew	Flow HD
Sheng, Qihu	Harbin Engineering University
Sun, Ke	Harbin Engineering University
Wang, Xiaohang	Harbin Engineering University
Carlier, Clément	IFREMER
Culley, David	Imperial College
du Feu, Roan	Imperial College
Mulligan, Ryan	Queen's University
Shuker, Robert	Shuker & Sons
Edmunds, Matthew	Swansea University
Fairley, Iain	Swansea University
Lake, Thomas	Swansea University
Masters, Ian	Swansea University
Togneri, Michael	Swansea University
Wang, Ji	Swansea University
Pinon, Grégory	Université du Havre
Fraser, Shaun	University of Aberdeen
Farman, Judith	University of Cambridge
Gupta, Vikrant	University of Cambridge
Sequeira, Carl	University of Cambridge
Young, Anna	University of Cambridge
Allsop, Steve	University of Edinburgh
Arredondo Galeana, Abdel	University of Edinburgh
Bonar, Paul	University of Edinburgh

Clayton, Robert	University of Edinburgh
Crossley, George	University of Edinburgh
Harrold, Magnus	University of Edinburgh
Haverson, David	University of Edinburgh
Inman, Tsutomu	University of Edinburgh
Kreitmair, Monika	University of Edinburgh
Muir, Rowan	University of Edinburgh
Pérez-Ortiz, Alberto	University of Edinburgh
Reynolds, Simon	University of Edinburgh
Shah, Sunny	University of Edinburgh
Tulley, Susan	University of Edinburgh
Viola, Ignazio Maria	University of Edinburgh
García, Mariam	University of Exeter
Hardwick, Jonathan	University of Exeter
Smith, Helen	University of Exeter
Bruce, Esther	University of Hull
Ahmed, Umair	University of Manchester
Feng, Tong	University of Manchester
Hachmann, Christoph	University of Manchester
Olczak, Alexander	University of Manchester
Stallard, Timothy	University of Manchester
Sudall, David	University of Manchester
Zhang, Yuquan	University of Manchester
Adcock, Thomas	University of Oxford
Byrne, Byron	University of Oxford
Cooke, Susannah	University of Oxford
Gao, Chanshu	University of Oxford
Houlsby, Guy	University of Oxford
Houlston, Peter	University of Oxford
Hu, Jianxin	University of Oxford
Hunter, William	University of Oxford
Joseph, Trevon	University of Oxford
Muchala, Subhash	University of Oxford
Papamaximou, Dani	University of Oxford
Vogel, Christopher	University of Oxford
Whyte, Scott	University of Oxford
Willden, Richard	University of Oxford
Wimshurst, Aidan	University of Oxford
Liu, Wendi	University of Strathclyde
Xiao, Qing	University of Strathclyde